

LEACHING IMPACT ON COMPRESSIBILITY OF UNTREATED AND CEMENT-TREATED CHAMPLAIN SEA CLAY

by

Ali Ahmad

BASc., Herat University, 2011

Herat, Afghanistan

A thesis

presented to Ryerson University

in partial fulfillment of the

requirements for the degree of

Master of Applied Science

in the program of

Civil Engineering

Toronto, Ontario, Canada, 2018

© Ali Ahmad, 2018

AUTHOR'S DECLARATION

I hereby declare that I am the sole author of this thesis. This is a true copy of the thesis, including any required final revisions, as accepted by my examiners.

I authorize Ryerson University to lend this thesis to other institutions or individuals for scholarly research.

I further authorize Ryerson University to reproduce this thesis by photocopying or by other means, in total or in part, at the request of other institutions or individuals for scholarly research.

I understand that my thesis may be made electronically available to the public.

Leaching Impact on Compressibility of Untreated and Cement-Treated Champlain Sea Clay

Master of Applied Science, 2018

Ali Ahmad

Department of Civil Engineering

Ryerson University

ABSTRACT

The pore fluid salinity level of undisturbed Champlain Sea clay samples were reduced from 19.81 to 0.79 g/L using a leaching apparatus designed for this experimental study. Then the impact of leaching on the compressibility characteristics of the undisturbed, remoulded, and cement-treated clay samples were investigated through constant rate of strain tests. It was found that the compressibility of Champlain Sea clay was affected by the level of salinity in its pore fluid. The reduction of salinity to 0.79 g/L in this study impacted the compressibility of both remoulded and cement-treated clay but did not affect on the compressibility of undisturbed clay. A higher compressibility was recorded from remoulded leached sample compared to the remoulded unleached sample. In cement-treated samples, an improvement in the compressibility characteristics was observed from the leached samples treated with 50 kg/m³ GU cement compared to that of their corresponding treated unleached samples.

ACKNOWLEDGEMENTS

First, I would like to express my most profound appreciation to my supervisor, Dr. Jinyuan Liu, whose expertise, generous guidance, patience, in timely feedback, and support made it possible for me to complete this thesis. Dr. Liu also provided me with invaluable advice to pass through difficulties in life and to become a better version of myself. I enjoyed the opportunity to work with Dr. Liu, a good friend and supervisor.

Next, I would like to thank Mr. Naresh Gurpersaud of the Keller Foundation Ltd and the members of my thesis committee: Dr. Tareq Salloum, Dr. Laifa Cao, and Dr. Elsayed Elbeshbishi for generously offering their time, support and guidance for preparation and review of this document. I would also like to thank NSERC, OPG, and Keller Foundation Ltd for the financial support of this research.

Finally, I would like to thank my parents for their lifetime supports and my fiancée, Marzia Ebrahimi, for her patience and understanding during this demanding period.

CONTENTS

AUTHOR’S DECLARATION	ii
ABSTRACT	iii
ACKNOWLEDGEMENTS	iv
LIST OF TABLES	viii
LIST OF FIGURES	ix
LIST OF APPENDICES	ix
1. INTRODUCTION	1
1.1 General Background	1
1.2 Scope of Research and Objective	1
1.3 Research Methodology	2
1.4 Thesis Organization	2
2. LITERATURE REVIEW	4
2.1 Champlain Sea Clay	4
2.1.1 The Behavior of Sensitive Clays	6
2.1.2 Shear Strength Measurement of Sensitive Clay	10
2.1.3 Compressibility of Champlain Sea Clay	11
2.1.4 Atterberg Limits Variation Due to Leaching	16
2.2 Deep Mixing Method for Ground Improvement	18
2.2.1 Deep Mixing Method	19
2.2.2 Factors Affecting Strength Improvement in DMM	19
2.2.3 Mechanism of Clay-Cement Stabilization	21
2.2.4 Deep Mixing Applications on Sensitive Clay	22
2.2.5 Improvement of Compressibility of Sensitive Clay by DMM	23
2.3 Summary	25
3. SOIL PROPERTIES AND EXPERMENTAL PROGRAM DESIGN	26
3.1 Introduction	26
3.1.1 Atterberg Limits	26

3.1.2	Grain Size Distribution	26
3.1.3	Specific Gravity	30
3.1.4	Pore-Fluid Salinity	30
3.1.5	Mineralogical Compounds.....	31
3.1.6	Sensitivity	32
3.2	Experimental Devices Developed and Used	33
3.2.1	Constant Rate of Strain Testing Device.....	33
3.2.2	Cutting Machine Designed for the Tests	34
3.2.3	Sample Extruder.....	35
3.2.4	Humidity Chamber Designed to Cure the Samples	36
3.2.5	Leaching Apparatus Designed for the Study	37
3.3	Sample Preparation Procedures	39
3.3.1	Reducing Pore Fluid Salinity Level.....	39
3.3.2	Samples Tags and Experiment Numbering.....	42
3.3.3	Undisturbed CRS Samples.....	42
3.3.4	Remoulded CRS Samples	43
3.4	Experimental Parameters.....	43
3.4.1	Cement-Treated CRS Samples	43
3.4.2	Binder Dosage Selection.....	44
3.4.3	Sample Mixing Method and Procedures.....	44
3.4.4	Sample Curing	44
3.5	Testing Method and Procedures	45
3.5.1	Compressibility Tests by CRS Testing Device.....	45
3.6	Data Processing and Calculations.....	47
3.6.1	Determination of the Initial Void Ratio	49
3.6.2	Determination of Pre-Consolidation Pressure	50
3.7	Summary	52
4.	RESULT AND ANALYSIS OF CRS TESTS	53
4.1	Impact of Leaching on Undisturbed Champlain Sea Clay.....	53
4.2	Impact of Leaching on Remoulded Champlain Sea Clay.....	61
4.3	Compressibility of Cement-Treated Champlain Sea Clay	69

4.4	Impact of Cement Treatment on Champlain Sea Clay at Different Salinity Levels .	
	73
4.5	Summary	82
5.	SUMMARY AND CONCLUSION	84
5.1	Introduction	84
5.2	Main Conclusions	84
5.3	Recommendation for Future Work.....	86
	APPENDICES	87
	REFERENCES.....	93

LIST OF TABLES

Table 2-1: Quantitative mineralogical analyses results from clay in eastern Canada (Locat, Lefebvre, Ballivy, & Ballivy, 1984).....	5
Table 2-2: Chemical compounds in percentages (Locat et al., 1984).....	5
Table 2-3: Classification of sensitivity according to CFEM (CGS, 2006).....	6
Table 2-4: Depositional and post-depositional factors that affect the sensitivity (Torrance, 1984)8	
Table 2-5: Factors affect the strength improvement (Terashi, 1997)	20
Table 3-1: Summary of XRD Analysis (OPG internal report, 2016)	31
Table 3-2: Consolidation stages and strain rates.....	47
Table 4-1: List of CRS tests conducted on various soil condition of Champlain Sea clay samples	83

LIST OF FIGURES

Figure 2-1: Concentration of cation in the pore water from Treadwell, Ontario (Torrance, 1979)..	9
Figure 2-2: Fabric of marine clay at different stages of consolidation (Quigley & Thompson, 1966)	11
Figure 2-3: Sensitive Clay typical e-log p curve (Nagaraj et al., 1990)	12
Figure 2-4: Compressibility of marine clay due to leaching (Bjerrum, 1967).....	13
Figure 2-5: Void ratio vs. time for leached and unleached remoulded marine clay (Torrance, 1974)	14
Figure 2-6: Effect of leaching on over-consolidated marine clay (Torrance, 1974)	15
Figure 2-7: Compression curves of reconstituted clays with and without pore salt (Song et al., 2017).....	16
Figure 2-8: Some Norwegian clays activity (Bjerrum, 1954).....	17
Figure 2-9: Effect of Porewater salinity on Atterberg limits (Torrance, 1974)	18
Figure 2-10: Unconfined compressive strength vs. total water to cement ratio (Bruce et al., 2013)	21
Figure 2-11: Mechanism of clay-cement stabilization (Kitazume & Terashi, 2013)	22
Figure 2-12: Binder dosage vs. strength improvement ratio (Li, 2017)	23
Figure 2-13: One-dimensional compression curves of untreated and cement treated soft Bangkok clay (Lorenzo & Bergado, 2006).....	24
Figure 2-14: e-log P curve of natural and cement treated Champlain Sea clay (Li, 2017)	25
Figure 3-1: Sample of clay at plastic limit.....	27
Figure 3-2: Atterberg limits distribution (Liu, Shi, Afroz, & Kirstein, 2017).....	28
Figure 3-3: Plasticity chart of Champlain Sea clay near to the Waba dam (Liu et al., 2017)	29

Figure 3-4: Grain size distribution of clay samples used in this study	30
Figure 3-5: Mini vane shear tests on leached (left) and natural (right) Champlain Sea clay	32
Figure 3-6: Undrained shear strength measured at different salinity levels of Champlain Sea clay	33
Figure 3-7: Schematic of the CRS machine (Trautwein, 2001).....	34
Figure 3-8: View of the cutting machine (right), & a clay sample halfway inserted into the leaching mould (left)	35
Figure 3-9: View of the sample extruder	36
Figure 3-10: Schematics of the curing chamber	36
Figure 3-11: View of inside and outside of the curing chamber.....	37
Figure 3-12: Leaching apparatus	38
Figure 3-13: Leaching mould.....	39
Figure 3-14: Decrease in percentage of salinity level in the collected leachate during the leaching process	40
Figure 3-15: Collected mass of salt over time	41
Figure 3-16: Inserting leached samples into CRS rings.....	42
Figure 3-17: Sealed cement-treated samples before placing in the curing chamber	45
Figure 3-18: Silva's construction to determine pre-consolidation pressure (<i>Clementino, 2005</i>) .	51
Figure 4-1: Pore pressure vs. effective stress UU samples at different strain rates.....	54
Figure 4-2: Pore pressure vs. effective stress UL samples at different strain rates	54
Figure 4-3: Influence of leaching on e-log p curve of undisturbed Sample 1	56
Figure 4-4: Influence of leaching on the permeability of undisturbed Sample 1	57
Figure 4-5: Influence of leaching on the coefficient of volume change of undisturbed Sample 1	58

Figure 4-6: Influence of leaching on the coefficient of consolidation of undisturbed Sample 1..	58
Figure 4-7: Influence of leaching on e-log p curve of undisturbed Sample 2	59
Figure 4-8: Influence of leaching on the permeability of undisturbed Sample 2	59
Figure 4-9: Influence of leaching on the coefficient of volume change of undisturbed Sample 2...	60
Figure 4-10: Influence of leaching on the coefficient of consolidation of undisturbed Sample 2....	61
Figure 4-11: e-log p curves of RL and RU samples of Champlain Sea clay	62
Figure 4-12: e-log p curves of UL and RL samples of Champlain Sea clay	63
Figure 4-13: Variation of hydraulic conductivity versus change in void ratio of RL and RU samples	64
Figure 4-14: Variation in hydraulic conductivity versus change in void ratio of UU and RU samples	65
Figure 4-15: Variation of M_v versus log effective stress of RL and RU samples.....	66
Figure 4-16: Variation of M_v versus log effective stress of UL and RL samples	67
Figure 4-17: Variation of C_v versus log effective stress of RL and RU samples.....	68
Figure 4-18: Variation of C_v versus log effective stress of UU and RU samples	68
Figure 4-19: e-log p curve of UU and TU samples	70
Figure 4-20: Hydraulic conductivity of cement-treated and remoulded clay	71
Figure 4-21: Variation of M_v versus log effective stress of UU and the TU sample	71
Figure 4-22: Variation of C_v versus log effective stress of UU and TU samples	72
Figure 4-23: Variation of the e-log p curve of treated leached (TL) samples due to curing	74
Figure 4-24: e-log p curve of TU samples due to curing period.....	74
Figure 4-25: Change in e-log k curves of TL samples.....	77

Figure 4-26: Change in e - $\log k$ curves of TU samples	77
Figure 4-27: Change in pore pressure ratio vs total effective stress of TL samples.....	78
Figure 4-28: Change in pore pressure ratio against the total effective stress of TU samples	78
Figure 4-29: Variation of M_v vs effective stress of TL samples.....	79
Figure 4-30: Variation of M_v vs effective stress of TU samples	80
Figure 4-31: Trend of M_v change vs effective stress from 2 day-cured TU sample	80
Figure 4-32: Variation of C_v - $\log p$ curves of TL samples.....	81
Figure 4-33: Change of C_v - $\log p$ curves of TU samples	82

LIST OF APPENDICES

Appendix A: Sample of CRS test record sheet and void ratio calculation	88
Appendix B: Sample of mix design sheet from cement treated samples.....	91

1. INTRODUCTION

1.1 GENERAL BACKGROUND

Champlain Sea clay in Eastern Canada is an unusual soil like the Scandinavia clay. The soil is highly compressible under load with a brittle and sensitive structure that transforms into a liquid mass when disturbed. Post-depositional changes in pore fluid chemistry can also affect the behaviour of sensitive clay. In Norway, the salt-leaching theory seems to be a key reason behind sensitivity of clay but so far, no correlation is found between salt content and the sensitivity of Champlain Sea clay (Crawford, 1968). The fabric of sensitive clay may become metastable due to the changing pore solutions (Torrance, 1979).

The deep mixing method (DMM) is a soil treatment method that is typically referred to as a condition that binders like cement, lime, or a mix of both are blended in-situ with the soil. The binders enhance the native soil properties such as its strength and compressibility. However, DMM has rarely used in Canada and investigation of DMM of Champlain Sea clay is scarce. The strength improvement of soil by DMM is influenced by many factors due to direct relation of strength improvement and chemical reaction of soil and binder. According to Terashi et al. (1997), pore water of soil can affect the strength improvement. However, no effect of salinity level of pore fluid of sensitive clay and strength improvement with cement has ever been investigated. Thus, it is necessary to determine the impact that salinity level can play on the compressibility behaviours of undisturbed and cement treated Champlain Sea clay.

1.2 SCOPE OF RESEARCH AND OBJECTIVE

The scope of this research is to investigate the effect of leaching of salts on the undisturbed, remoulded, and cement-treated Champlain Sea clay. First, a device will be built to leach the undisturbed Champlain Sea clay to a desired level.

To directly measure any effect of leaching, a series of mechanical tests will be performed:

- 1) Obtain and compare the index properties of undisturbed leached (UL) and undisturbed unleached (UU) samples, including Atterberg limits, sensitivity, and shear strength by mini vane
- 2) Obtain and compare the impact of leaching on the compressibility of UL, UU, remoulded leached (RL), remoulded unleached (RU), cement-treated leached (TL) and cement-treated unleached (TU) samples of the clay by the constant rate of strain (CRS) tests.

1.3 RESEARCH METHODOLOGY

A series of geotechnical tests will be performed in this investigation. First, the salinity level of undisturbed Champlain Sea clay will be lowered from its initial level of 12.68 g/kg (19.81 g/L of salt mass per pore water) to a value about 0.5g/kg (0.79 g/L) of salt mass to dry soil mass. Then two series of CRS tests will be conducted. The first series is to investigate the effect of salinity on undisturbed and remoulded Champlain Sea clay. Thus, undisturbed and remoulded samples with the initial salinity and the reduced salinity will be obtained. The second series is to observe the effect of salinity on the cement-treated samples with both the initial and reduced pore fluid salinity levels. General use Portland cement will be used to treat the sample at a dosage of 50 kg/m³ per total volume of the mix and samples will be cured for 2-day, 7-day, and 28-day.

1.4 THESIS ORGANIZATION

This thesis is organized into five chapters with the intention of conveying a complete and thorough picture of the conducted research and recorded results.

Chapter 1 presents the general background information, scope and objectives, and methodology of this research.

Chapter 2 presents the history of behaviour, shear strength, compressibility, and Atterberg limits of Champlain Sea clay

Chapter 3 explains the experimental lab program, parameters obtained from experiments, experimental devices developed for this study, and the testing machine used. The sample preparation procedure, testing method and procedures, data processing and calculations are also presented in this chapter.

Chapter 4 discusses all the results and analyzes of CRS tests and impact of leaching on the compressibility of undisturbed, remoulded, and cement-treated samples.

Chapter 5 summarizes the results and conclusions of this study and notes all the recommendations for future studies.

2. LITERATURE REVIEW

2.1 CHAMPLAIN SEA CLAY

The continental ice sheet during the Pleistocene depressed the crust of the earth in the eastern part of Canada. The area was overrun about 8,000-12,000 years ago by an arm of Champlain Sea when the ice melted (Gillott, 1969). The oldest sedimentation took place in the south region, and the youngest deposition occurred in the north. Sediments are known as Champlain Sea clay or Leda clay deposited from detritus of streams, erosion of shorelines, and ice melting which are now commonly found along the St. Lawrence Lowlands region in Ontario and Quebec (Penner, 1965).

Moreover, an ice front at the north-west boundary of the Champlain Sea formed and experienced cycles of freezing and thawing near the boundaries that resulted in the deposition of clay till in those areas. These sediments are also referred by geotechnical engineers as “quick clay” or “sensitive clay”. The primary minerals of Champlain Sea’s sediments mainly come from the Canadian Shield that is consist of quartz, feldspar, mica, smectite, amphibole, and glacial amorphous material (Gillott, 1970; Moore, Brown, & Rashid, 1977; Penner, 1965; Quigley et al., 1983). Canadian sensitive clay contains all of these minerals but depending on the location, their percentage varies (Rasmussen, 2012). The most well-known feature of quick clay is its transformation from a relatively brittle material to liquid when it is disturbed (Crawford, 1968).

Canadian sensitive clay has been found to contain minerals according to Table 2-1 and a chemical compound according to

Table 2-2. Depending on the location of the clay, the amount of each mineral may vary.

Table 2-1: Quantitative mineralogical analyses results from clay in eastern Canada (Locat, Lefebvre, Ballivy, & Ballivy, 1984)

Site No.	Site	N	P _L (%)	Q _Z (%)	Microcline (%)	Hornblende (%)	Dolomite (%)	Calcite (%)	P (%)	Illite (%)
1a	Grande-Baleine	4	41.3 (39–46)	15.3 (14–16)	13.5 (13–14)	12.7 (11–15)	1.0 (0–2)	0.3 (0–0.5)	15.9	7.5
1b	Grande-Baleine	5	47.9 (41–57)	13.9 (13–16)	13.8 (12–16)	11.8 (11–13)	3.5 (1–5)	0.6 (0.3–0.9)	8.5	7.2
1c	Grande-Baleine	5	40.4 (37–48)	16.8 (13–20)	14.5 (13–16)	11.0 (9–14)	1.9 (1–3)	0.4 (0.2–0.6)	15.0	5.7
2a	Olga	6	29.1 (22–34)	11.4 (10–13)	9.6 (8–11)	9.4 (7–10)	3.7 (0–5)	2.3 (1.5–2.7)	34.5	10.2
2c	Olga	3	33.1 (31–36)	13.0 (11–15)	10.8 (8–13)	8.6 (7–9)	2.5 (2–3)	0.7 (0.5–0.9)	31.3	9.4
3a	St. Marcel	3	35.6 (35–36)	11.0 (11)	8.9 (8–10)	11.4 (9–14)	5.2 (3–8)	1.2 (1.0–1.6)	26.7	9.2
3b	St. Marcel	3	33.7 (34)	13.9 (13–14)	9.8 (8–11)	11.1 (9–12)	5.0 (5–6)	1.6 (1.5–1.7)	24.9	8.9
4	St. Léon	15	36.3 (27–45)	11.8 (10–13)	13.4 (11–16)	12.6 (10–16)	3.6 (2–5)	0.1 (0–0.4)	32.2	11.1
5	St. Alban	19	25.1 (22–33)	20.5 (17–24)	9.5 (8–13)	9.5 (5–14)	1.5 (0–5)	0.7 (0–1.2)	33.2	11.2
6	St. Barnabé	3	37.0 (33–40)	12.2 (11–13)	14.4 (12–16)	13.3 (12–15)	3.5 (3–5)	0.2 (0.2–0.3)	19.4	6.9
7	Shawinigan	5	36.8 (32–42)	19.6 (17–24)	15.0 (14–16)	13.4 (12–17)	2.4 (0–4)	—	12.8	9.4
8	Chicoutimi	8	41.1 (35–44)	19.8 (17–23)	13.2 (12–16)	9.7 (7–13)	1.5 (0–3)	0.7 (0.4–1.0)	14.0	2.7

Table 2-2: Chemical compounds in percentages (Locat et al., 1984)

Compound	Site No.							
	Grande-Baleine (1b)	Olga (2a)	St. Marcel (3a)	St. Léon (4)	St. Alban (5)	St. Barnabé (6)	Shawinigan (7)	Chicoutimi (8)
SiO ₂	59.33	52.83	53.36	55.36	59.79	58.26	61.87	62.43
TiO ₂	0.77	0.61	0.72	0.92	0.89	0.97	0.87	0.80
Al ₂ O ₃	16.10	17.05	16.42	16.38	15.28	16.15	15.55	16.37
CaO	2.90	4.41	4.26	3.60	3.73	3.51	3.62	5.40
K ₂ O	3.59	3.72	3.19	3.51	3.40	3.71	3.32	2.38
Na ₂ O	4.10	2.47	2.88	3.89	2.60	3.98	3.63	3.74
MgO	3.78	4.06	4.75	3.95	2.88	3.23	2.70	2.06
Fe (total)	4.22	4.72	5.16	5.19	4.46	4.86	4.32	3.07
FeO	3.25	2.99	4.11	3.19	2.92	3.85	3.58	2.52
Fe ₂ O ₃	2.42	3.42	2.80	3.87	3.13	2.66	2.19	1.58
P ₂ O ₅	0.25	0.20	0.18	0.29	0.27	0.34	0.32	0.22
CO ₂	0.48	3.74	3.96	2.13	1.50	0.72	0.43	1.06
H ₂ O (total)	2.24	4.15	3.51	3.03	2.32	1.84	1.12	0.83
MnO	0.09	0.08	0.11	0.12	0.10	0.11	0.11	0.08

Due to de-structuration of its natural in-situ fabric, the behaviour of sensitive clay may change from solid form to fluid. Destruction of the fabric of clay may be due to induced stress or

remoulding of the clay. For sensitive clay, the weak particle bonds and high water content is the reason behind its change state to fluid (Quigley, 1980). The ratio between undisturbed shear strength and remoulded shear strength of sensitive clay is called “sensitivity”. Sensitive clays are categorized based on their sensitivities in geotechnical engineering. Skempton & Northey (1952) first proposed to classify the clay as Insensitive, Low sensitive, Medium sensitive, Sensitive, Extra sensitive, and Quick clay. Other researchers also proposed many other classifications. The following classification system, shown in Table 2-3, is adopted in the 4th edition of the Canadian Foundation Engineering Manual (CGS, 2006).

Champlain Sea clay can have a sensitivity higher than 20. Often the remoulded strength is hundred times lower than undisturbed strength and thus leads to the difficulty of measuring the shear strength of remoulded clay (Crawford, 1968; Penner & Burn, 1978).

Table 2-3: Classification of sensitivity according to CFEM (CGS, 2006)

Sensitivity	Definition
<2	Low sensitivity
2-4	Medium sensitivity
4-8	Extra (high) sensitivity
>16	Quick

2.1.1 The Behavior of Sensitive Clays

In the middle of the 20th century, researchers started to investigate the mechanism of quick clays. Rosenqvist (1946) proposed a theory that leaching of salt from marine clays is the reason for this. Champlain Sea clays were deposited in saline water. However, their saline pore water changed when the glacial retreat caused geostatic uplift and resulted in the infiltration of freshwater through sand and silt lenses. Generally, three different types of leaching or the combination of them may occur: rainwater infiltration through the deposits, water seeping upward due to artesian pressure, and moving of salt towards zones with lower ion concentration due to diffusion of salts (Rankka et al., 2004). Moreover, seeping fresh water can also remove the salt from the layered clay through diffusion (Torrance, 1974).

After Rosenqvist, the importance of leaching salt from marine clay has also been investigated by many other researchers (Kim & Do, 2010; Moore et al., 1977; Nabil, 1993; Yong, Elmonayeri, & Chong, 1985)

These further studies have shown that reduction of salt content is not always enough to make a clay sensitive. One important reason for this is the existence of many marine clays with low salt content and no sensitivity. Two clays can have similar fabric but different properties due to various forces between particles. Sensitive clays may not be different from clay with low sensitivity in term of composition, grain size but due to the chemical environment, they can behave differently. It should bear in mind that in everyday language, the term 'salt' is used to mean sodium chloride (NaCl), while salt in the context of chemistry refers to compounds that are consist of anions and cations. These compounds are free ions in solution, for instance, Ca^{2+} , Na^+ , Cl^- , but make salts when they are dried.

Torrance (1979) investigated the pore water chemistry of four sites in Ottawa. He observed that leaching has occurred in all the sites because of downward infiltration of rainfall. The evidence includes channels and terraces that contain marine remains but have fresh water passing through them. The marine contents of these deposits can be evidence for the initial properties of the deposition and its environment. Zones with high salinity clay exhibited low sensitivity, while variable sensitivities were obtained from the leached zones. The pore fluids in the leached zones with high sensitivities usually have a low concentration of Ca, Mg, and K and a high amount of Na, while in the places that the sensitivity is low the higher concentrations of Ca and Mg and a low proportion of Na can be found (Torrance, 1979).

Chemical conditions in the depositional environment and post-depositional changes of pore fluid chemistry can affect the behaviour of the sensitive clay. To understand the magnitude of chemical changes of pore fluid after deposition of the clay, the estimation of initial conditions is necessary. The depositional and post-depositional environments features, as shown in Table 2-4, are also believed to be important factors to produce quick clay.

Table 2-4: Depositional and post-depositional factors that affect the sensitivity (Torrance, 1984)

Factors producing a high undisturbed strength	
Depositional	Post-depositional
Flocculation <ul style="list-style-type: none"> • Salinity • Divalent cation adsorption • High suspension concentration 	Cementation bonds <ul style="list-style-type: none"> • Rapidly developed • Slowly developed Slow load increase <ul style="list-style-type: none"> • Time for cementation • Thixotropic process
Factors producing a low remoulded strength	
Depositional	Post-depositional
Material properties <ul style="list-style-type: none"> • Low-activity minerals dominate 	Minimal Consolidation Leaching <ul style="list-style-type: none"> • Decrease in $W_L >$ Decrease in W_C Dispersants <ul style="list-style-type: none"> • Decrease in $W_L >$ Decrease in W_C

A condition which individual particles of clay precipitate into a fragile formation in the presence of another substance like salt water is called flocculation. Salt flocculation of the clay in the marine environment may have influences on the sensitivity of clay. However, originated clay in freshwater can also become sensitive (Desautniers and & Cherry, 1989). In Norway, the salt-leaching theory seemed to be a key reason behind sensitivity of clay, but no correlation is found between salt content of pore fluid of Champlain Sea clay of Canada or the Bootlegger Cove clays of Alaska. The chemistry of pore-water from four sites in the Ottawa region, including Treadwell, Touraine, Chelsea, and Angers, was previously studied by Torrance (1979). In the Treadwell, the concentrations of the potassium, sodium, calcium, and magnesium are low in the upper zone but increasing with the depth of 75 meters (Figure 2-1). Similarly, the remoulded shear strength of the clay follows the same pattern with smaller values in the upper zones. Besides the lower salt level in the upper zones, the higher water content of the clay may also contribute to the lower remoulded

shear strengths. The maximum salinity in the Ottawa area is measured about 21‰ of its pore water. However, the remaining of fossils that were found in the clay suppose a higher concentration of actual salinity in the past. All the clay investigated in the Touraine, Chelsea, and Angers experienced weathering and have low pore-water salinities due to leaching (Torrance, 1979). The soils in the three leached areas have a low sensitivity that may be due to desiccation and oxidation (Moum & Rosenqvist, 1961). Although the reduced pore-water salinities is one of the requirements for the development of high sensitivity of the marine clays, the existence of low salinity pore water does not guarantee that high sensitivity will be observed (Torrance, 1979). There are many other factors that influence on the sensitivity of clay (Eden & Crawford, 1957; Leroueil, Tavenas, Samson, & Morin, 1983; Penner, 1965; Song, Zeng, & Hong, 2017; Yong, Sethi, & Larochelle, 1979).

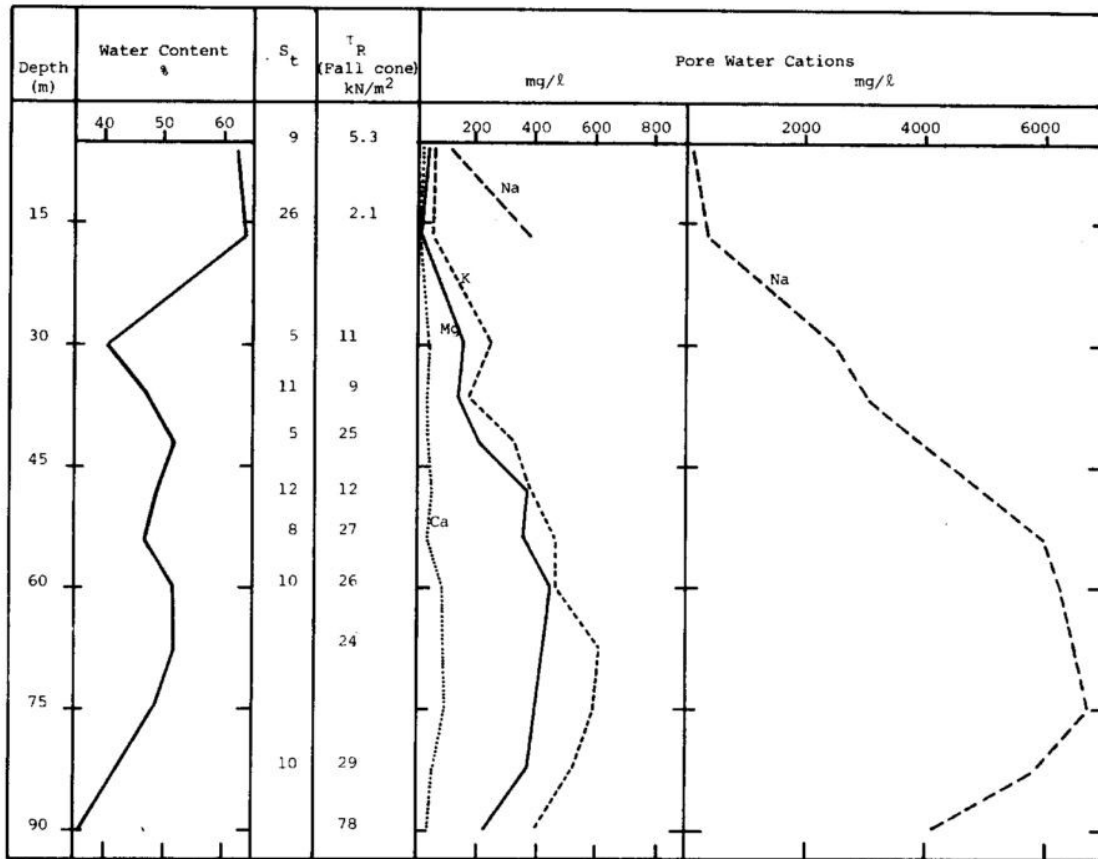


Figure 2-1: Concentration of cation in the pore water from Treadwell, Ontario (Torrance, 1979)

Skempton & Northey (1952) gradually leached and reduced the salt content of undisturbed samples of marine clay from salt content of 12.6 g/liter to 2.2 g/liter. They observed a small increase in sensitivity although the salt content was reduced significantly.

Effect of removing cementing agents from sensitive clay is investigated by Loiselle et al. (1970). He concluded that cementing agents can be reduced by introducing a solution of the disodium salt of ethylenediaminetetraacetic acid (EDTA) and 35 g/l of NaCl solution. However, this results in slight changes in the stiffness of the clay structure and no substantial changes in strength except under very small consolidation pressure.

A relationship between the sensitivity of clay and its electro-kinetic potential was found in an investigation conducted by Penner (1965). The electrokinetic potential defines the thickness of the double layer between particles. Thus, the higher the number of electrolytes results in a thinner double layer which means lower repulsive forces and lower sensitivities. However, the sensitivity of Champlain Sea clay does not necessarily just depend on its salt content (Penner, 1965). The composition of pore fluid and the ion composition is apart from leaching whereby the ion may or may not be released from the particle to the pore water. It depends on the possible weathering of the clay mineral (Penner, 1965).

In physicochemical hypotheses, it is argued that the open fabric has become metastable due to the environmental changes since deposition. According to one of the well-known theories, this fabric of the clay became metastable because of changing pore solutions/ reduction of salt content by diffusion or leaching to the freshwater when the marine deposits emerged above the sea level (Hendershot & Carson, 1978; Penner, 1965; Rosenqvist, 1966; Torrance, 1979). Other theories include the formation of dispersing agents (Penner & Burn, 1978; Soderblom, 1966), dissolution of cemented junctions (Bentley & Smalley, 1979) and exchange of ion because of leaching or weathering (Moum & Rosenqvist, 1961). None of the present theories are universally valid to explain the behaviour and fabric change of sensitive clay (Gillott, 1979).

2.1.2 Shear Strength Measurement of Sensitive Clay

The undrained shear strength of soft clays is an essential parameter in geotechnical design, particularly for the design of foundations and embankments on soft clay. Some common methods to estimate the shear strength of clay is using correlations with cone penetration test data, direct

measurement with field or laboratory vane shear testing device and unconfined compression strength test (UCS). The sensitive of clay is the ratio of undisturbed and remoulded shear strength of clay. Vane shear test and UCS test are more widely used to measure the sensitivity of clay. It is likely that the vane test replaces the UCS test because the remoulded strength of some disturbed clay is too low to form UCS specimens (Gao & Ge, 2016). Thus, the vane test is more often used instead of UCS for measuring the sensitivity of soft soil in field and laboratory.

Leaching affects the forces between the soil particles and this affects the ability of particles to re-flocculate after remoulding. In another word, the clay is built up from deposits of large aggregates joined by a system of links in sea water. If the salt is leached and the clay is remoulded, they cannot come together and connect into large aggregate again (Rankka et al., 2004).

Since compressibility, shear strength, and permeability of clay soil is related to the water retention of soil mass, the ability of soil mass to remain its state is severely depended on a) factors that produced the initial structural state of soil, b) chemistry of pore-water solution, c) local boundary conditions, and d) time (Yong et al., 1985).

2.1.3 Compressibility of Champlain Sea Clay

The structure of Champlain Sea clay is “card-house” type that when consolidated it will experience a noticeable reorientation (Quigley & Thompson, 1966). Reorientation of the clay flakes happens in a perpendicular plane to a major principle of consolidation pressures σ_1 and σ_3 , as shown in Figure 2-2.

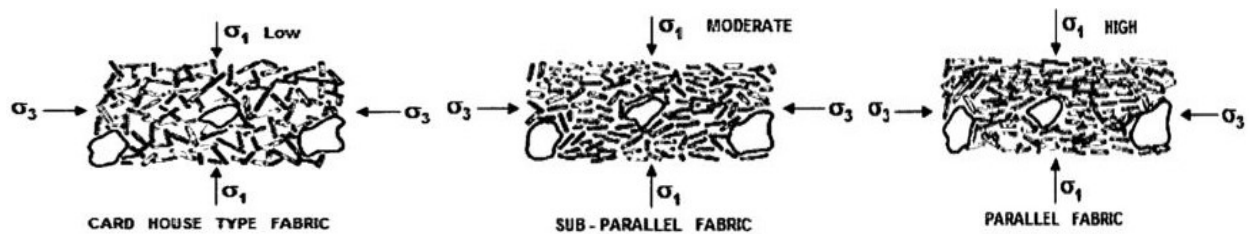


Figure 2-2: Fabric of marine clay at different stages of consolidation (Quigley & Thompson, 1966)

For obtaining the amount of settlement of clay, it is necessary to plot the void ratio versus consolidation pressure (e - $\log p$) which can be obtained from oedometric tests on undisturbed

samples. The usual e -log p curve of an undisturbed sensitive clay compared to its remoulded condition is seen in Figure 2-3. In general, the curve is divided into three zones; zone one from start to preconsolidation pressure (σ_c), zone two from σ_c to transition stress σ_t , and zone three beyond σ_t . In zone one the soil response is almost rigid because of inherent cementation bonds, in zone two the soil tends to reach the remoulded state due to a gradual breakdown of bonds, in zone three the soil behaves as in the remoulded state because all the bonds are completely broken (Nagaraj, Murthy, Vatsala, & Joshi, 1990). The sudden decrease of void ratio after σ_c has been associated with the cementation bonds failure (Mitchell, 1970). Technically, the response of soil in the three zones can be explained consequently as nonparticulate, transitional, and particulate.

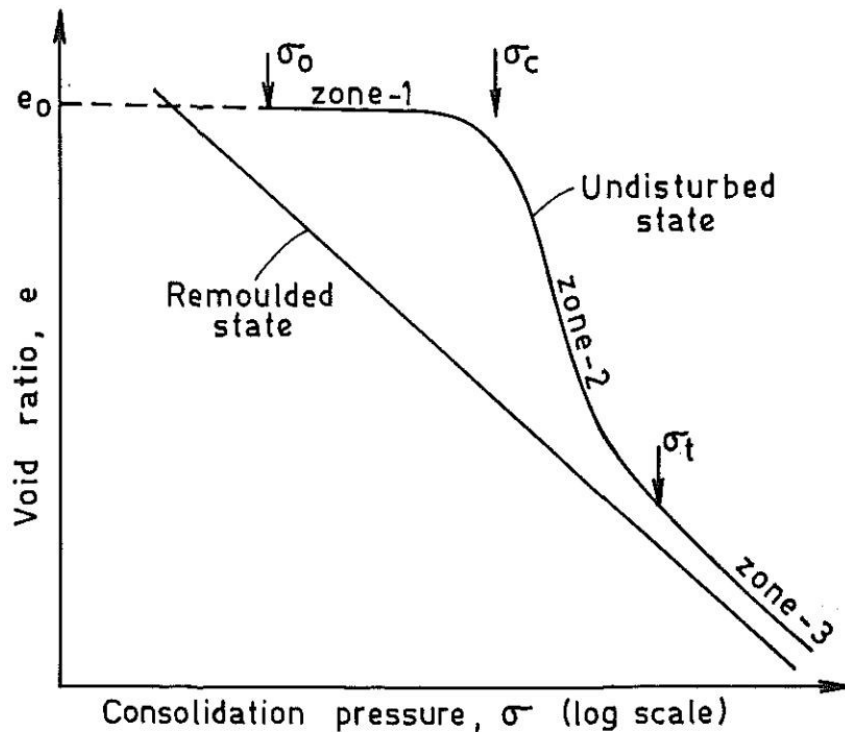


Figure 2-3: Sensitive Clay typical e -log p curve (Nagaraj et al., 1990)

Brand & Brenner (1981) reported that leaching could reduce shear strength and increase the compressibility of the clay. In addition to salt leaching, there is evidence that organic and inorganic dispersing agents may cause the development of quick clay (Casey, 2014; Moore et al., 1977; Soderblom, 1966; Taha, 2010; Torrance, 1975). Moore et al. (1977) investigated the effects of leaching organic and inorganic constituents on the compressibility and shear strength of a shallow

depth of marine clay. In their studies, chemical substances were used as dispersing agents to leach the clay. They introduced acetic acid to remove the inorganic cations, sodium hydroxide to remove organic matter, and artificial seawater to observe the hydraulic effects of leaching process. The results of consolidation tests on samples after leaching revealed that there is a high degree of similarity in the results, except higher compressibility observed from the samples that sodium hydroxide was introduced to them. They strongly suggested that the effective cohesion of sediments is primarily due to bonding forces. Sodium hydroxide affects on the structure of the clay and bonding forces by removing organic and inorganic compounds. The dispersing agents are important in the cases where the clay contains more than 5 % organic content and may not affect the clay with lesser than 0.5 % organic matter (Torrance, 1974).

The results of the investigation conducted by Bjerrum (1967) on the samples with reduced pore fluid salt concentration from 21 g/liter to 1 g/liter showed an increase in compressibility when compared with the compressibility of unleached samples (Figure 2-4).

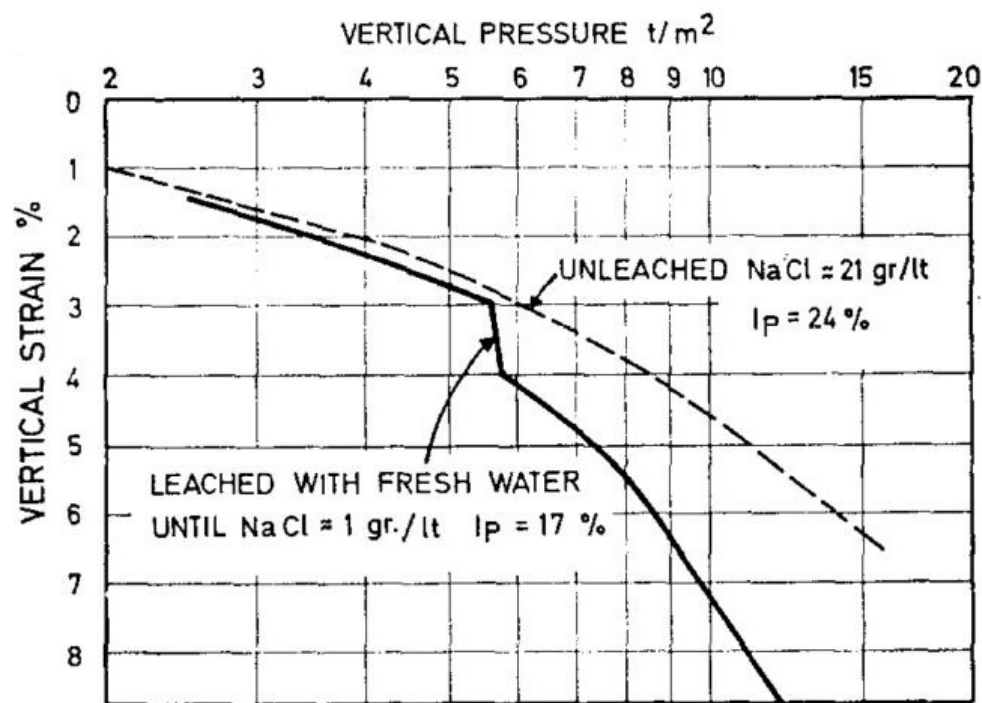


Figure 2-4: Compressibility of marine clay due to leaching (Bjerrum, 1967)

A series of consolidation tests were performed by Torrance (1974) to investigate the effect of leaching on consolidation behaviour of remoulded and undisturbed marine clay. In his investigation, leaching process was achieved by diffusion process with distilled water and for some tests aqueous solution with a desired ionic composition of the marine clay. The fluid was flushing through each porous stone on top and bottom 2 cm thick oedometer samples. The result of experiments (Figure 2-5 & Figure 2-6) illustrates that the quasi-preconsolidation pressure of the samples reduces when the salt is leached from undisturbed and disturbed marine clay samples. Because of a reduction in preconsolidation pressure, leached clay experienced a spontaneous settlement.

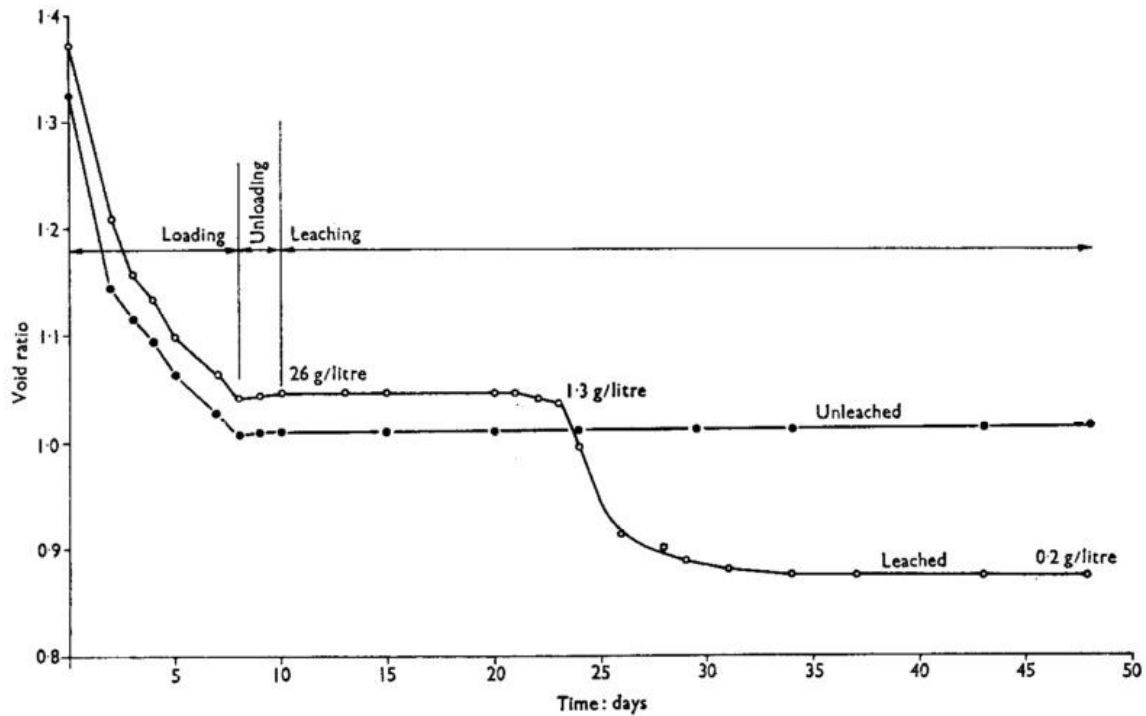


Figure 2-5: Void ratio vs. time for leached and unleached remoulded marine clay (Torrance, 1974)

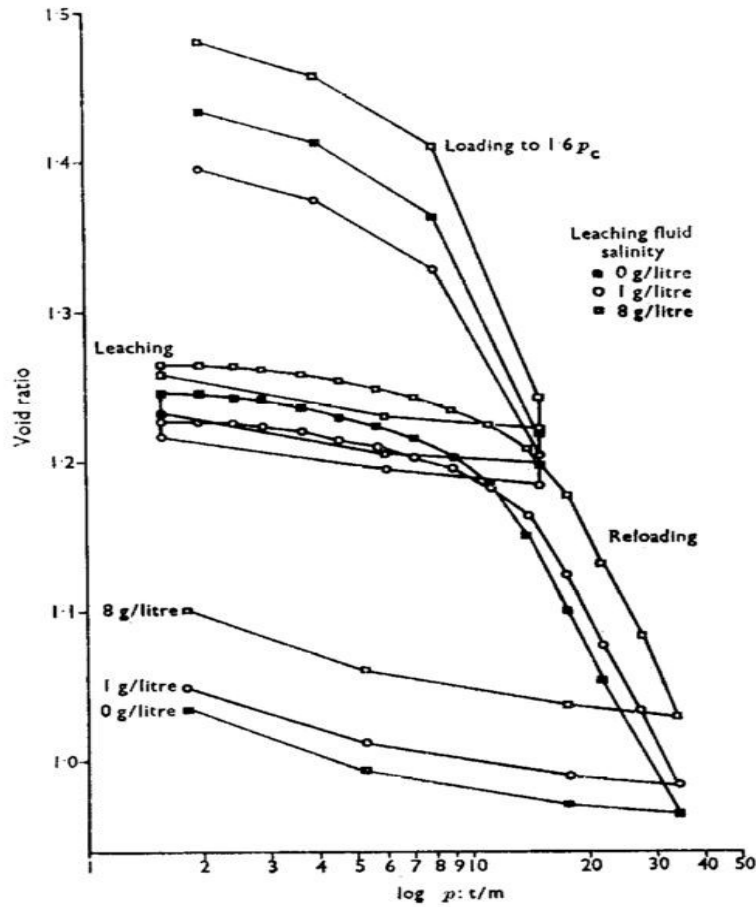


Figure 2-6: Effect of leaching on over-consolidated marine clay (Torrance, 1974)

Recently, Song et al. (2017) investigated the effect of pore fluid salinity on the consolidation of reconstituted marine clay using an oedometer. They found salt leaching increases the compressibility of the illite-dominant reconstructed marine clays (Figure 2-7) and the change is attributed to the decrease in the void ratio at the liquid limit.

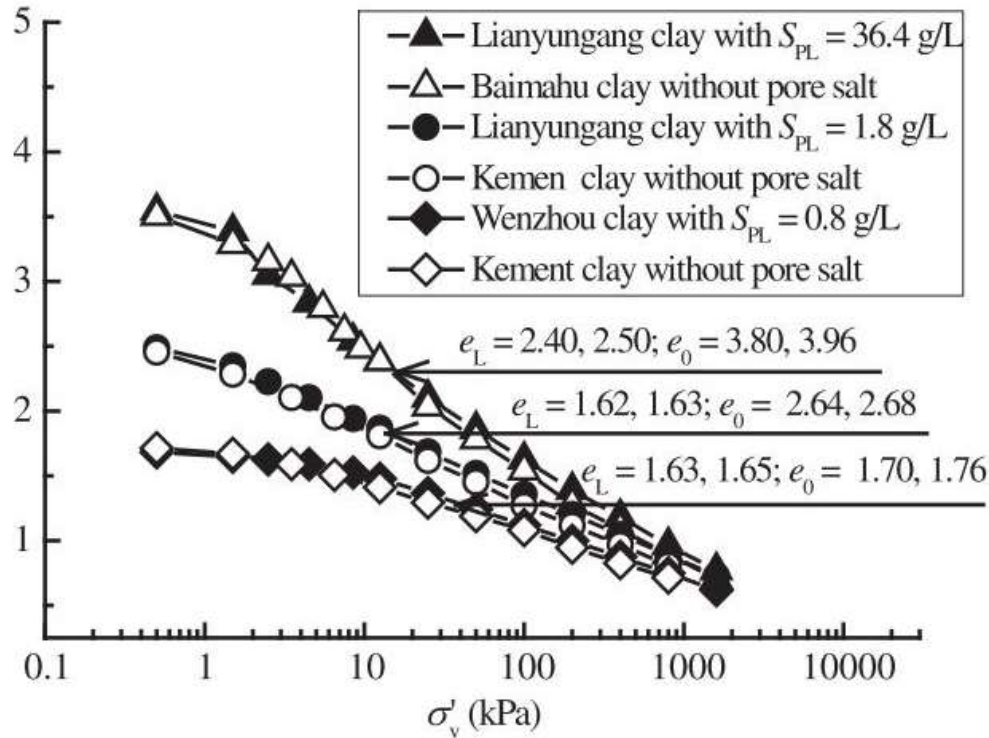


Figure 2-7: Compression curves of reconstituted clays with and without pore salt (Song et al., 2017)

2.1.4 Atterberg Limits Variation Due to Leaching

The liquid limit and plastic limit (and the shrinkage limit in some references) of soil are collectively referred to as the Atterberg limits. The role of pore water salinity and its influence on the Atterberg limits is an important factor (Torrance, 1975). Sensitive clays may have liquid limits lower than their natural water content. If such clay is remoulded after the salt is leached; the clay particle cannot connect in large aggregates again. Thereby, the water holding capacity of the clay is reduced and reflected the liquid limit. Torrance (1974, 1984) recorded similar water content from the clay with high and low salt content, but the liquid limit of leached clay was recorded sufficiently lower. Bjerrum (1954) noted that there is a relation between Atterberg limits and pore fluid salinity in Norwegian marine clays. Constant liquid limits were obtained from the clay with original pore water salinity within the range of 26 g/liter to 10 g/liter. Once the salinity was lower than 10 g/liter, the liquid limit gradually decreased. Low liquid limits like the values for the quick clay conditions were obtained when salinity was below 5 g/liter. For the plastic limit, a similar but

less dramatic effect was observed. The value of the salt concentration in the pore fluid of some Norwegian clays (Figure 2-8) also well confirmed the effect of salt concentration of pore fluid on the plasticity index of the clay. In another investigation, Torrance (1974) also concluded a similar finding that salt leaching causes a substantial decrease in the liquid limit but having a small effect on the plastic limit of Norwegian marine clays. The results are illustrated in Figure 2-9 against the pore water salinity. Sridharan and Prakash (1999) concluded that the decrease in the liquid limit by salt leaching is due to the increase in the interparticle repulsive forces in reconstituted non-swelling clays that illite and kaolinite are their primary minerals.

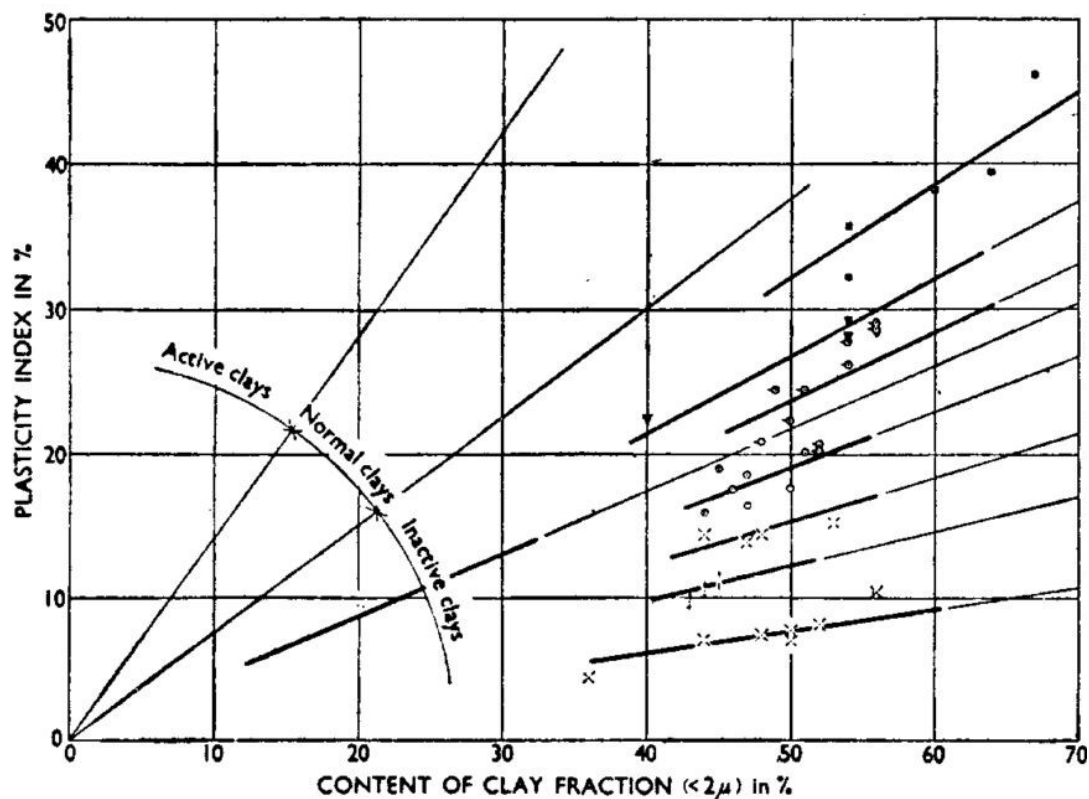


Figure 2-8: Some Norwegian clays activity (Bjerrum, 1954)

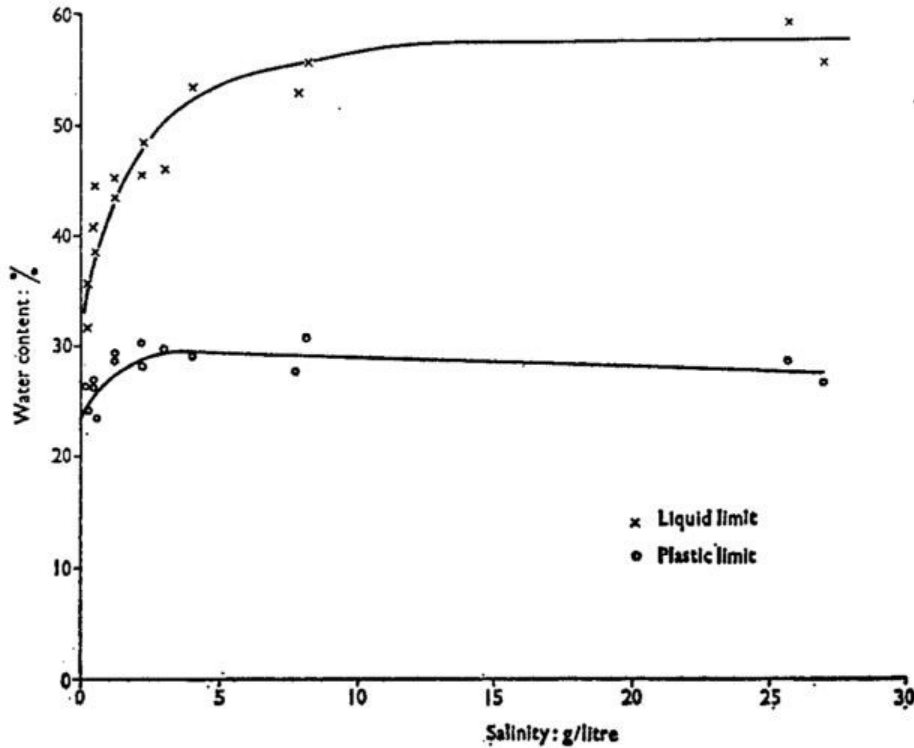


Figure 2-9: Effect of Porewater salinity on Atterberg limits (Torrance, 1974)

2.2 DEEP MIXING METHOD FOR GROUND IMPROVEMENT

When a structure is to be constructed over compressible marine clays, excess deformation or stability issues would be expected. According to Kitazume & Terashi (2013), it is necessary to take some countermeasures as following: a) alter the type of foundation or structure, b) replace the soil with a better one, c) improve the properties of soft soil or d) add some reinforcing material to the soil. The measures b, c, and d mentioned above are covered by “Ground Improvement” in soft soil to obtain an excellent performance of the structure. The classification of ground improvement is based on their working principles some of the methods including, admixture stabilization, solidification by admixture, replacement, densification, consolidation, grouting, thermal stabilization, etc. (Kitazume & Terashi, 2013). Moreover, the admixture stabilization is further divided into categories of shallow mixing and deep mixing.

2.2.1 Deep Mixing Method

The deep mixing method (DMM), also called deep soil mixing, cement soil mixing, etc., is a soil treatment method in the field that the cementitious material, typically referred to as binders, are blended with the soil. DMM was first invented in the United States in 1954. However, until the end of the 1980s, DMM has been used and practiced only in Japan and Nordic countries. In 1996 in Tokyo the first international specialty conference on DMM was co-organized by the Japanese Geotechnical Society (Kitazume & Terashi, 2013).

The treated soil with the binder compared to the native soil has enhanced properties such as higher strength, lower permeability, and reduced compressibility. Cohesive soil with high-water content, loose, and fine granular soils are best suited for DMM applications. However, ground with obstructions like boulders or cobbles, dense soil, and stiff material are not feasible to be treated with DMM. Depending on the methods to add the binders, DMM is divided into two types: wet mixing and dry mixing. In the wet mixing method, the binder in the slurry form and primarily single auger, multi auger, or cutter based mixing procedure is used (Bruce et al., 2013). The dry mixing method is usually used for the soil with a high water content which the binder in powder form (dry) treats the soil and reacts with water in the soil for the hydration process. For the dry mixing method, the single-auger dry mixing process is used.

2.2.2 Factors Affecting Strength Improvement in DMM

The strength improvement of soil by DMM is influenced by many factors because the mechanism behind the strength improvement is closely related to the chemical reaction between the binder and soil. Terashi et al. (1997) divided the factors into four categories: I) characteristics of a hardening agent, II) characteristics and conditions of soil, III) mixing conditions, and IV) curing conditions as illustrated in Table 2-5.

Table 2-5: Factors affect the strength improvement (Terashi, 1997)

I.	Characteristics of hardening agent <ul style="list-style-type: none"> a. Type of hardening agent b. Quality c. Mixing water and additives
II.	Characteristics and conditions of soil <ul style="list-style-type: none"> a. physical, chemical and mineralogical properties of soil b. organic content c. pH of pore water d. water content
III.	Mixing conditions <ul style="list-style-type: none"> a. degree of mixing b. timing of mixing c. quantity of hardening agent
IV.	Curing conditions <ul style="list-style-type: none"> a. temperature b. curing time c. humidity d. wetting and drying/freezing and thawing, etc.

In conventional design of DMM, the controlling parameter is just the binder content at a defined curing time (Lorenzo & Bergado, 2006). However, the effect of initial moisture content of soft and sensitive clays on engineering behaviour of treated soil is brought into attention by Lorenzo & Bergado (2004), Miura et al. (2002) and Bruce et al. (2013). Furthermore, these studies defined a new parameter as the ratio of total soil moisture content to binder content. The effect of total water content on strength improvement of samples from different studies is illustrated in Figure 2-10.

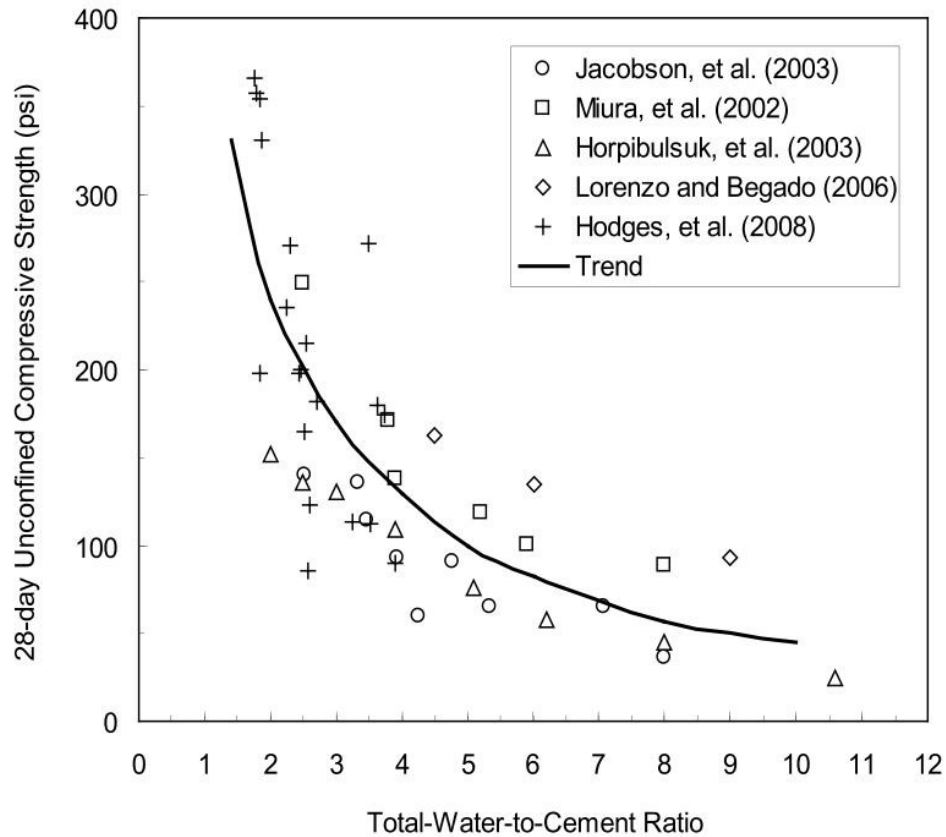


Figure 2-10: Unconfined compressive strength vs. total water to cement ratio (Bruce et al., 2013)

2.2.3 Mechanism of Clay-Cement Stabilization

According to Kitazume & Terashi (2013), the mechanism behind DMM stabilization consists of four stages: hydration of binder, reaction due to ion exchange, generation of gel or hydration product, and generation of pozzolanic product (Figure 2-11). These four stages can be further divided into short-term and long-term phases. The strength increase in the soil binder mixture is mostly due to the formation of cement hydration products and pozzolanic products. Portland cement type I is usually used to stabilize soft clays. There are four compounds: tricalcium silicate (C_3S), dicalcium silicate (C_2S), tricalcium aluminate (C_3A), and tetra calcium alumni ferrite (C_4AF) in the Portland cement. The hydration process occurs when the pore water of soil encounters with the compounds. Major hydration (cementitious) productions are hydrated calcium silicates (C_2SH_x , $C_3S_2H_x$), hydrated calcium aluminates (C_3AH_x , C_4AH_x) and hydrated lime $Ca(OH)_2$.

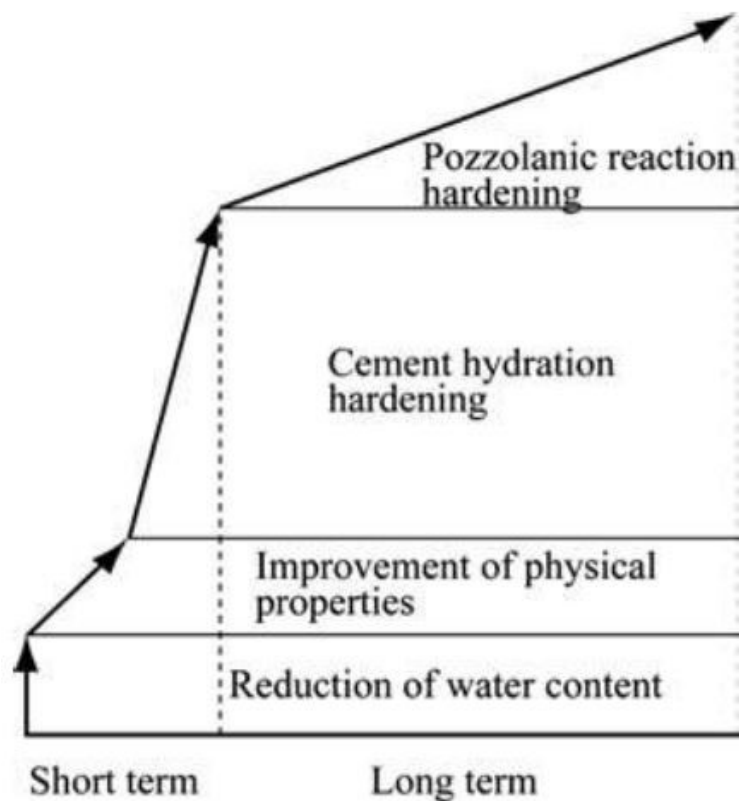


Figure 2-11: Mechanism of clay-cement stabilization (Kitazume & Terashi, 2013)

2.2.4 Deep Mixing Applications on Sensitive Clay

DMM is a suitable ground improvement method when dealing with sensitive clay. The method can be used to increase bearing capacity, minimize settlement, prevent slope stability failure, lower seepage of soft ground (Bouassida & Porbaha, 2004).

Currently, there are a few research studies on admixture stabilization of sensitive clay including Champlain Sea clay. Choquette et al. (1987) concluded that mineralogy and surface properties of sensitive clays are responsible for the gain of strength when treated with lime and the clay minerals seem to be the main target for chemical attack. Locate et al. (1990) has found that 10% of quicklime by mass can significantly improve the undrained shear strength of sensitive clays. Shen, Han, & Du (2008) conducted field tests to evaluate the effect of deep mixed columns on properties of surrounding sensitive Ariake marine clay. Their test results confirmed that there is an influential

zone in neighbouring clay around the deep mixed column that properties the clay within the zone are effected by the installation of the column. Initially, the undrained shear strength of clay in the influential zone is decreased but regained after approximately seven days.

Recently, Li (2017) conducted a laboratory investigation of the feasibility of using cement, slag/cement, and lime binder to treat Champlain Sea clay. Among his findings, a 25-time strength improvement was recorded when clay was treated with cement at a dosage of 103 kg/m³ per native soil volume. Proportionally higher strength improvements can be seen with higher cement dosages among his findings (Figure 2-12).

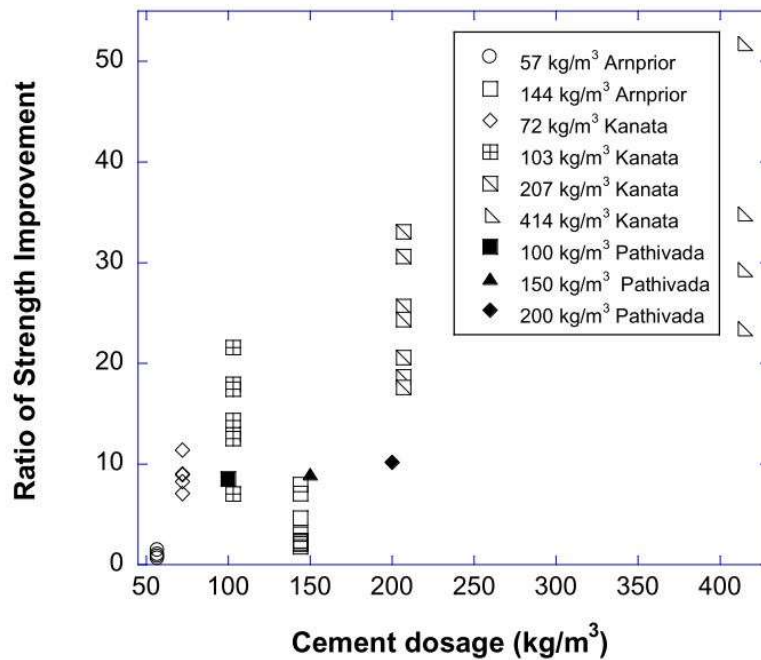


Figure 2-12: Binder dosage vs. strength improvement ratio (Li, 2017)

2.2.5 Improvement of Compressibility of Sensitive Clay by DMM

Previous studies (Bruce, Dimillio, & Ellen, 1998; Filz, Hodges, Weatherby, & Marr, 2005; Lorenzo & Bergado, 2006; Puppala, Nazarian, Yuan, & Hoyos, 2007) have reported that DMM significantly decreases the compressibility of soft clay and reduces its permeability.

Lorenzo & Bergado (2006) have conducted one-dimensional oedometer tests on natural soft Bangkok clay, and treated samples of the clay with 10 and 15% cement per volume of the clay. They have reported significantly higher yield stress and lower compression indexes due to cement treatment (Figure 2-13).

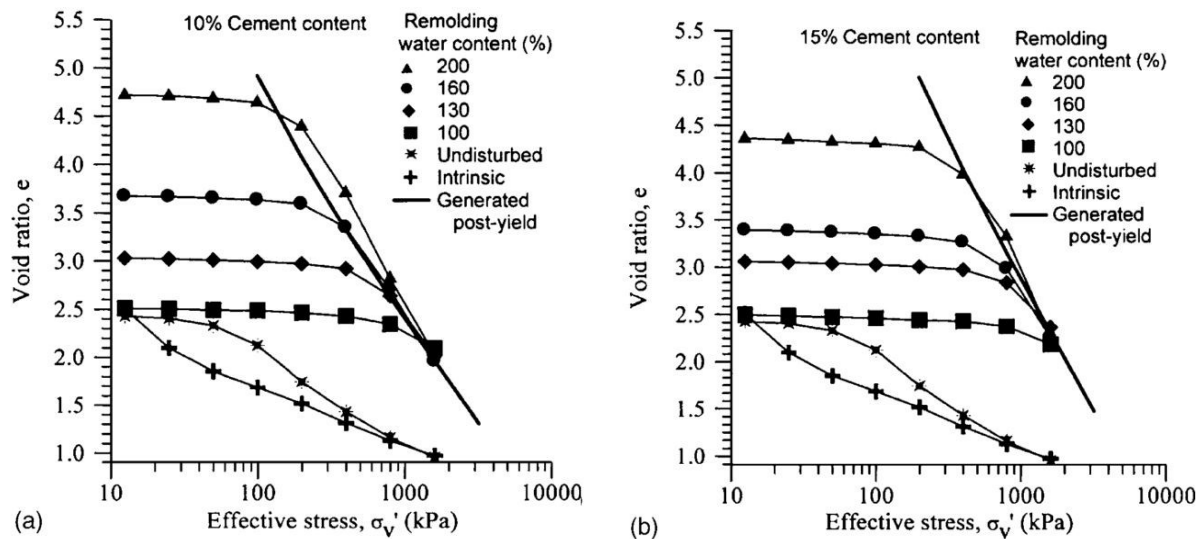


Figure 2-13: One-dimensional compression curves of untreated and cement treated soft Bangkok clay (Lorenzo & Bergado, 2006)

Similarly, lower compressibility, a higher preconsolidation pressure, and a smaller change of void ratio were reported by Li (2017) when the Champlain Sea clay was treated with cement (Figure 2-14).

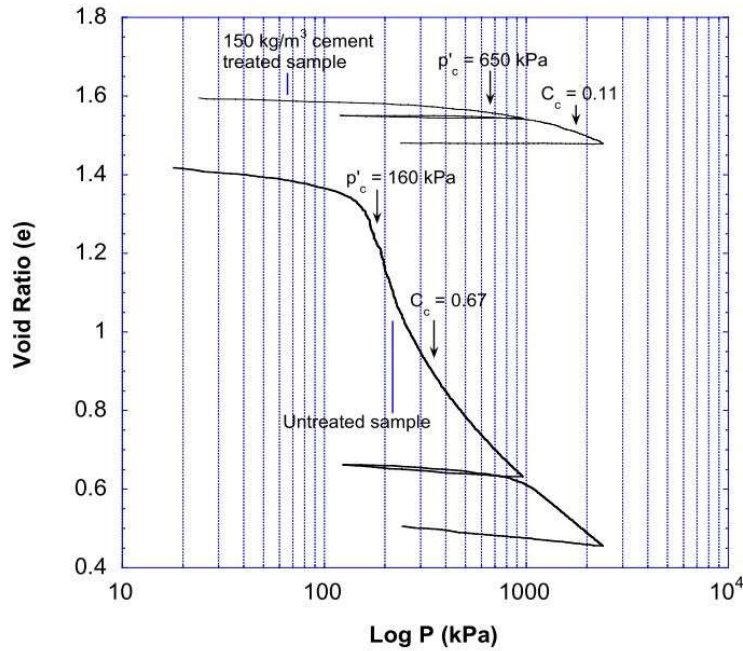


Figure 2-14: e-log P curve of natural and cement treated Champlain Sea clay (Li, 2017)

2.3 SUMMARY

This chapter introduced the mineral composition of Champlain Sea clay. The sensitivity of the clay and some possible effects of leaching on the strength behaviour of marine clay were addressed. Moreover, the potential of deep mixing method (DMM) as the field treatment method for Champlain Sea clay was reviewed.

3. SOIL PROPERTIES AND EXPERIMENTAL PROGRAM DESIGN

3.1 INTRODUCTION

This chapter first presents some index properties, mineralogical compound, and the sensitivity of the Champlain Sea clay sample used in this study. Next, information about the used and developed devices in this study will be given. In addition, the procedures for sample preparation and reducing the pore fluid of undisturbed clay will be discussed. Finally, the formula and the parameters used to process the data and test results will be explained.

3.2 PHYSICAL PROPERTIES OF SOIL SAMPLES

The soil used in this study was recovered with Laval sampler from foundation clay of Waba Dam which is located east of the Madawaska River, approximately 65 km to the west of Ottawa.

3.1.1 Atterberg Limits

The liquid limits and plastic limits according to ASTM D 4318 (ASTM, 2017) were performed on clay samples before and after leaching (Figure 3-1). The tests are conducted to evaluate any significant changes in Atterberg limits due to leaching. Liquid limit and plastic limit of natural clay recorded at 44.7 and 25.7 consecutively while 48.3 and 23.4 were obtained from undisturbed leached clay. The results show a slight reduction of plastic limit and increase of liquid limit after the salt level is reduced by the leaching process. More tests are needed to confirm the results.

The Atterberg limits obtained from the undisturbed unleached sample are similar to the results at the same depth reported by Liu et al. (2017) as seen in Figure 3-3.

3.1.2 Grain Size Distribution

The soil used in this study was obtained from 38.8 meters below the berm of Waba dam. Sieve analysis was performed on clay of the same location but from slightly lower depth (39.48 m). The grain size distribution of the clay is seen in Figure 3-4. ASTM D 6913 is to obtain the grain size distribution of clay. However, with this method, more soil was retained on sand fraction. Thus, the

sieve analysis was performed with slight modifications. In the modified method, the sample of soil was oven dried, ground with a pestle and then placed in a dispersion cup with water to form a slurry. The slurry was then mechanically mixed for a complete separation of clay particles. To conform with the ASTM D422, the slurry was passed from No. 10 Sieve before the hydrometer test was performed.



Figure 3-1: Sample of clay at plastic limit

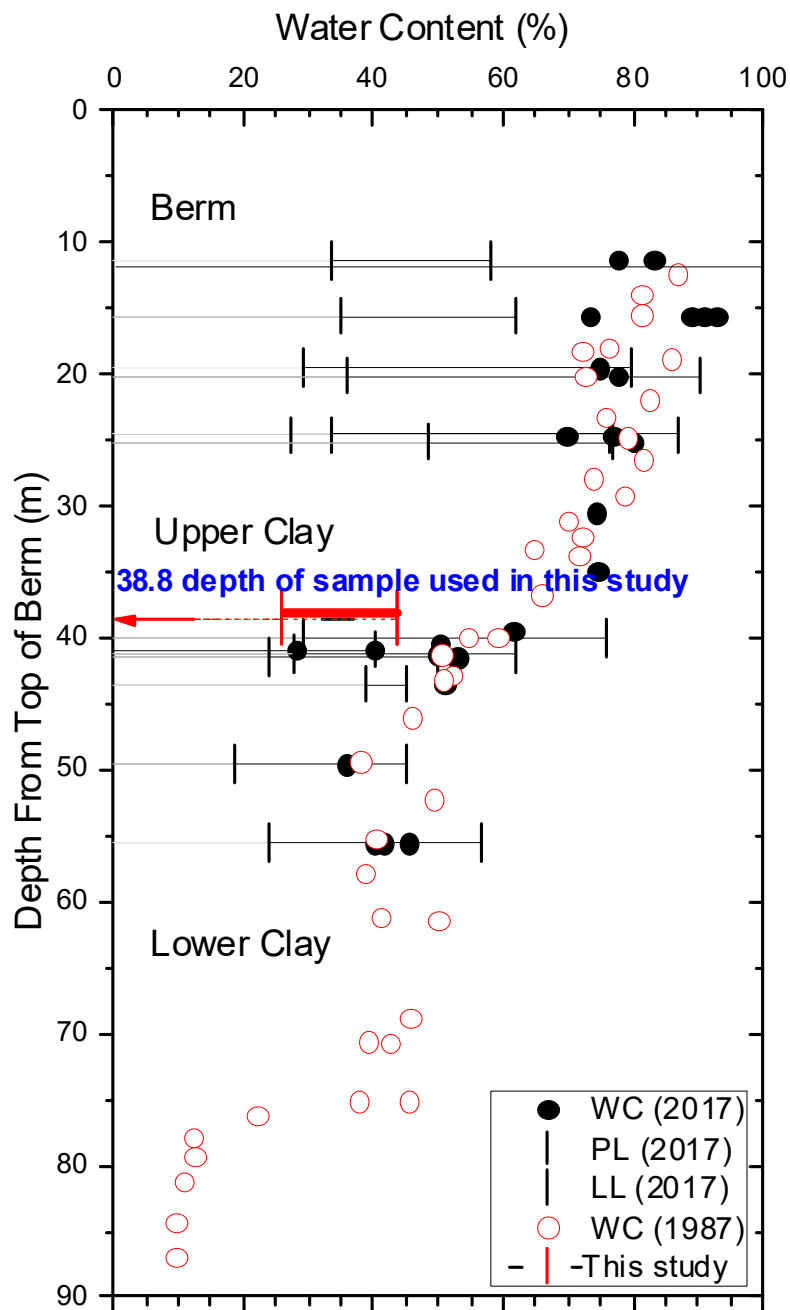


Figure 3-2: Atterberg limits distribution (Liu, Shi, Afroz, & Kirstein, 2017)

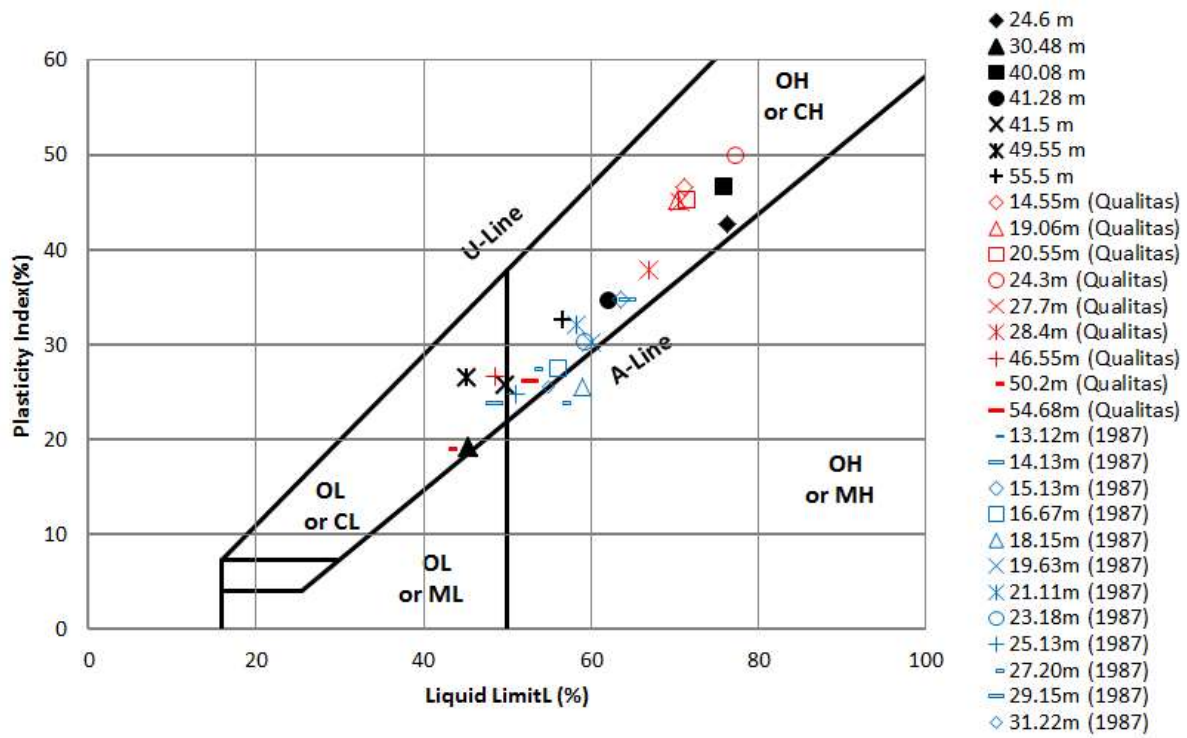


Figure 3-3: Plasticity chart of Champlain Sea clay near to the Waba dam (Liu et al., 2017)

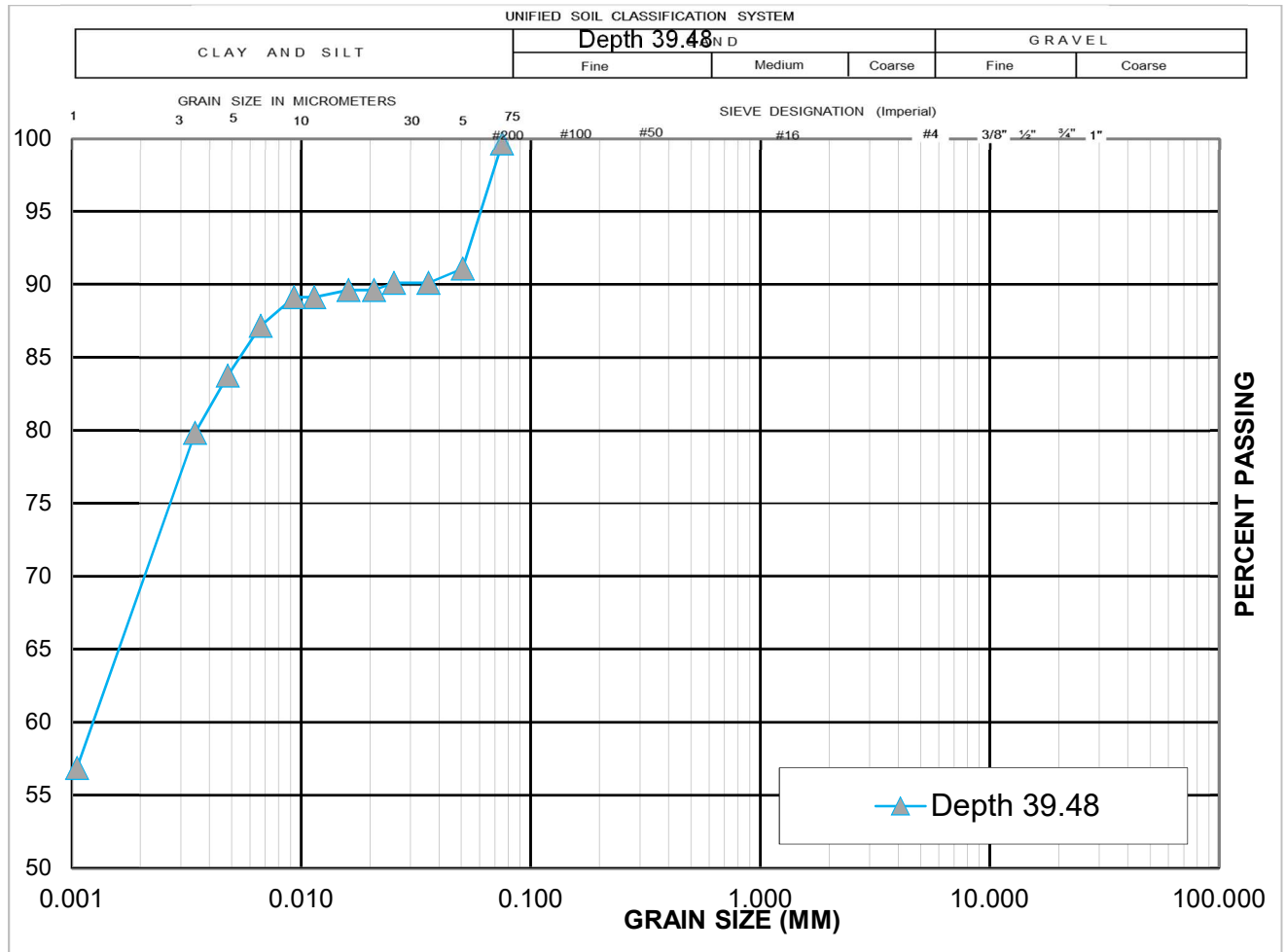


Figure 3-4: Grain size distribution of clay samples used in this study

3.1.3 Specific Gravity

The specific gravity of the clay was determined 2.7 from the tests performed according to ASTM D854.

3.1.4 Pore-Fluid Salinity

The salinity of clay was measured by the diluted fluid method. For obtaining the salinity level of natural clay, a sample of clay was oven dried. Then a known mass of the dried clay was dissolved into a known volume of distilled water, and the salinity level was recorded using Horiba ES-5

portable conductivity/salinity meter. The initial salinity of soil was recorded 19.81 g/L of salt mass per pore water (12.68 g/kg of salt mass to dry soil mass).

3.1.5 Mineralogical Compounds

Mineralogical compounds of a few samples of Champlain Sea clay used in this study were analyzed by Ontario Power Generation (OPG) in 2016. The test results from the three clay samples that were obtained from different depth are borrowed from that investigation report.

The clay X-ray Diffraction (XRD) outcomes (Table 3-1) show that the clay portion consists largely of illite (77% to 87%), with minor quantities of chlorite (5% to 10%), kaolinite (3% to 6%), hornblende (2%), quartz (1% to 2%), potassium (1% to 2%) and plagioclase (1% to 2%) feldspar.

The examinations show that these clay specimens consist mainly of clastic elements illite clays, chlorite clays and possible mica sized particles, quartz, kaolinite clay, hornblende, plagioclase and potassium feldspar and lesser amounts of pyrite (diagenetic minerals or detrital mineral). Hornblende and probably the pyrite are possible mafic minerals within this highly weathered and transported clastic mudstone. The abundance of illite clays in the samples suggests they are highly ductile to external stress. The total lack of smectite clays indicates that clay would not swell significantly in the presence of freshwater.

Table 3-1: Summary of XRD Analysis (OPG internal report, 2016)

Sample ID.	Type of Analysis	Weight (%)	Quartz	Plagioclase Feldspar	Potassic Feldspar	Calcite	Dolomite	Anhydrite	Pyrite	Marcasite	Hornblende	Siderite	Clays					Total Clay
													Kaolinite	Chlorite	Illite	Corrensite	Smectite	
TM-13B 1 18.49-18.71 m	Bulk Fraction:	49.85	12	14	7	0	0	0	3	0	8	0	3	5	48	0	0	56
	Clay Fraction:	50.15	1	1	0	0	0	0	1	0	2	0	3	5	87	0	0	95
	Bulk and Clay	100	7	7	3	0	0	0	2	0	5	0	3	5	68	0	0	76
TM-23A 2 24.27-24.49 m	Bulk Fraction:	50.00	20	13	5	0	0	0	4	0	7	0	3	10	38	0	0	51
	Clay Fraction:	50.00	1	1	1	0	0	0	0	0	2	0	5	10	80	0	0	95
	Bulk and Clay	100	10	7	3	0	0	0	2	0	5	0	4	10	59	0	0	73
TM-42B 3 35.99-36.21 m	Bulk Fraction:	42.46	16	15	5	0	0	0	4	0	7	0	6	6	41	0	0	53
	Clay Fraction:	57.54	2	2	1	0	0	0	1	0	2	0	6	10	77	0	0	93
	Bulk and Clay	100	8	8	3	0	0	0	2	0	4	0	6	8	61	0	0	75

3.1.6 Sensitivity

The undrained shear strengths of samples were performed by the mini vane shear testing device according to ASTM D4648 as seen in Figure 3-5. These tests were performed to observe any changes in shear strength and sensitivity of the clay before and after leaching. For avoiding any loss in water content, machine remoulded test was performed according to ASTM D4648M (ASTM, 2016) on failed specimens. This procedure is to remould the sample like remoulded field tests by rapidly rotating the vane with ten revolutions. The result from machine remoulded strength is typically higher than hand remoulded strength and, thus, produces lower sensitivities (ASTM, 2016). The sensitivity of samples was then determined by dividing the undisturbed shear strength by the remoulded shear strength as shown in Figure 3-6. Both undisturbed and disturbed shear strength obtained from a leached sample are significantly lowered than the result obtained from the unleached sample. It should be kept in mind that the reduced shear strength may be because of weathering effect on the sample at the time of leaching process. More tests are required to confirm the results.



Figure 3-5: Mini vane shear tests on leached (left) and natural (right) Champlain Sea clay

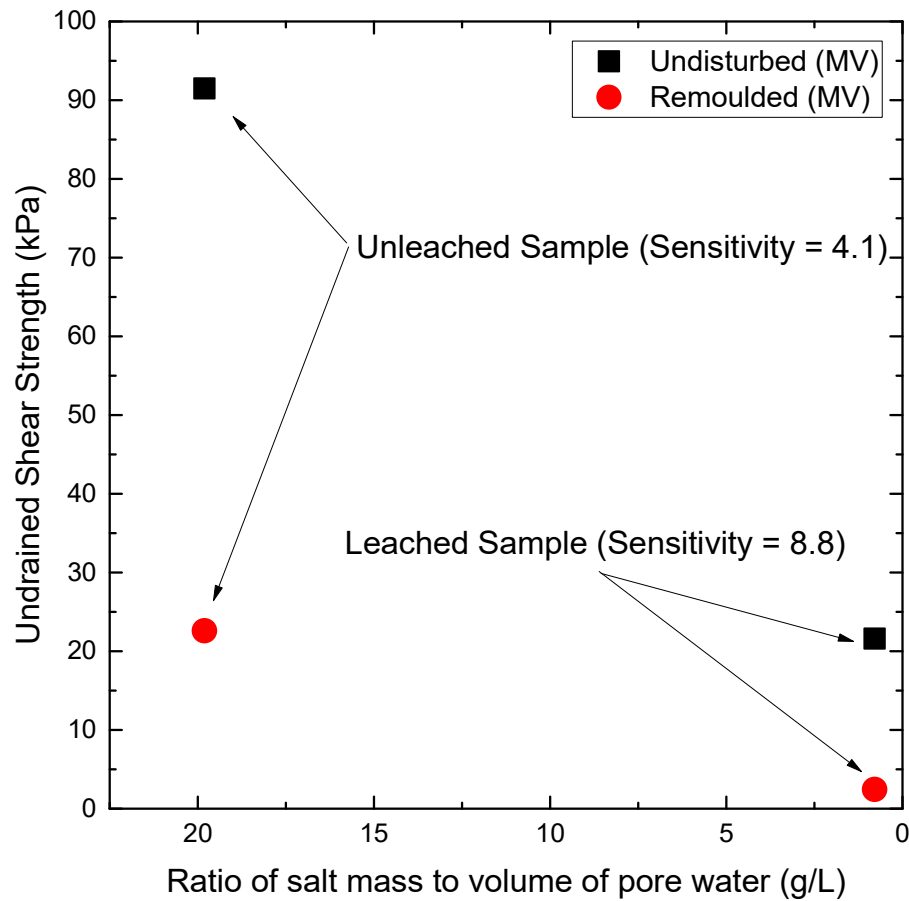


Figure 3-6: Undrained shear strength measured at different salinity levels of Champlain Sea clay

3.2 EXPERIMENTAL DEVICES DEVELOPED AND USED

This section describes the testing equipment used in this laboratory investigation program.

3.2.1 Constant Rate of Strain Testing Device

The constant rate of strain (CRS) testing machine used in this experiment is an automated consolidation system designed particularly for geotechnical laboratories by GEOTAC. Figure 3-7 shows the schematic of the CRS machine. The machine is the result of extensive development and research effort which has made the automated testing more affordable than ever. Advantages of this testing device include its capability to perform deformation; load/pressure controlled testing (Trautwein, 2001). Moreover, the instant machine feedback by real-time plots allows the

practitioner to take critical decisions and adjustments at the time of testing. The machine backbone system is GeoTAC's Test Net system. The system duty is to provide automation via data acquisition and control. The new concept, Distributed Data Acquisition and Control (DDAC), is employed by the TestNet which offers significant advantages comparing conventional methods (Trautwein, 2001). With the DDAC system, data conversion hardware is located near to the location of sensors where analog signals are converted to digital signals. Then, the digital signals can efficiently transmit long distances and reach to the computer.

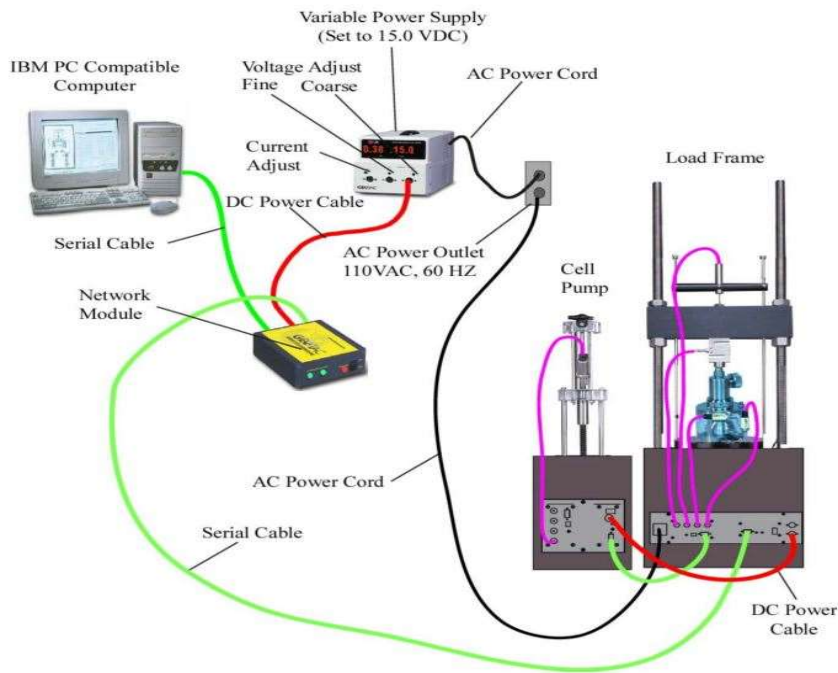


Figure 3-7: Schematic of the CRS machine (Trautwein, 2001)

3.2.2 Cutting Machine Designed for the Tests

A clay cutting apparatus is designed and developed for this study. This machine was built to precisely cut and trim a Champlain Sea clay sample and insert it into a 12 cm height and 15 cm diameter leaching mould. The device is adjustable to trim any size of clay with a diameter between the range of 2 to 40 cm. The following parts as seen in Figure 3-8 are the main components of the

machine, 1) scraper, 2) mould holder, 3) rotary plate, 4) adjustable edge to change the size of cutting.

For inserting an undisturbed sample into a leaching mould, the clay sample was first trimmed with a wire saw, and then its surface was smoothened by the scraper attached to the machine. Each time about 5 mm of the sample was pushed into the mould slowly after the top of the sample was scaped, and clay with a 2 mm bigger diameter than the mould was obtained near the edge of the mould. This procedure was repeated until about 120 mm of the clay was inserted into the mould. During the sample insertion, the mould was kept plump on top of the sample by the mould holder to prevent any tilting and sample disturbance during the sample insertion.



Figure 3-8: View of the cutting machine (right), & a clay sample halfway inserted into the leaching mould (left)

3.2.3 Sample Extruder

A sample extruder was designed and built for this investigation to extract the samples with minimal disturbance from the leaching mould after the completion of the leaching process. The main parts of the tool consist of a hydraulic jack, a platform, and a ring holder as seen in Figure 3-9.

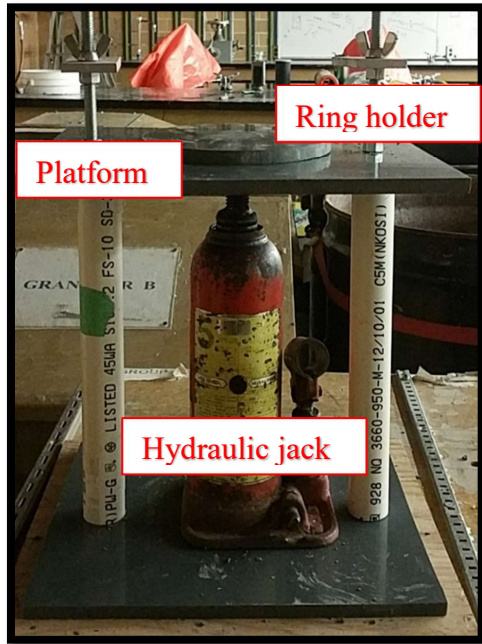


Figure 3-9: View of the sample extruder

3.2.4 Humidity Chamber Designed to Cure the Samples

A curing chamber to cure DMM specimens of this investigation at a relative humidity of 95-100 percent and a temperature of 22-25°C was designed and built. The main components of the curing chamber are a pond mister to produce humid, an aquarium heater, and a plastic chamber as shown in Figure 3-10 and Figure 3-11.

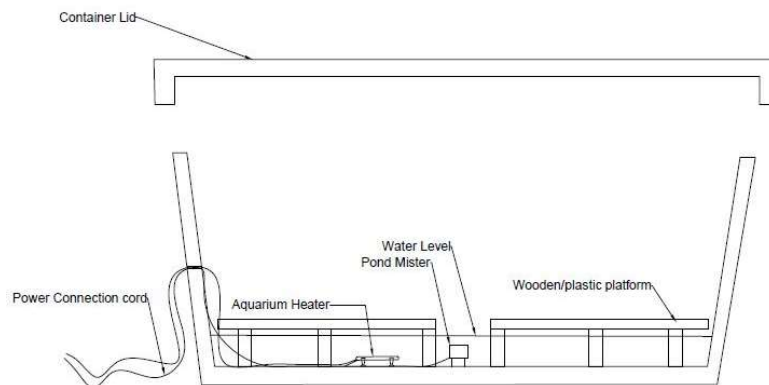


Figure 3-10: Schematics of the curing chamber



Figure 3-11: View of inside and outside of the curing chamber

3.2.5 Leaching Apparatus Designed for the Study

First, a sample was inserted into a leaching mould as described in Section 3.2.2. To lower the salt level of the undisturbed Champlain Sea clay, an apparatus was built and used to pass distilled de-aired water (DDW) through the clay samples. DDW was pumped into the system from a reservoir then the water pressure was adjusted to 100 kPa with a pressure regulator and guided to the top of the clay in the mould through pipes. The water pressure was chosen that it is lower than preconsolidation of the sample to avoid any consolidation during the leaching process and is also high enough to generate a constant seepage flow through the low permeability clay sample.

The main components of the apparatus as seen in Figure 3-12 are 1) distilled water reservoir, 2) pump, 3) solenoid valve & pressure gauge, 4) pressure switch, 5) pressure tank, 6) pressure regulator, 7) pressure gauge, 8) leaching mould.

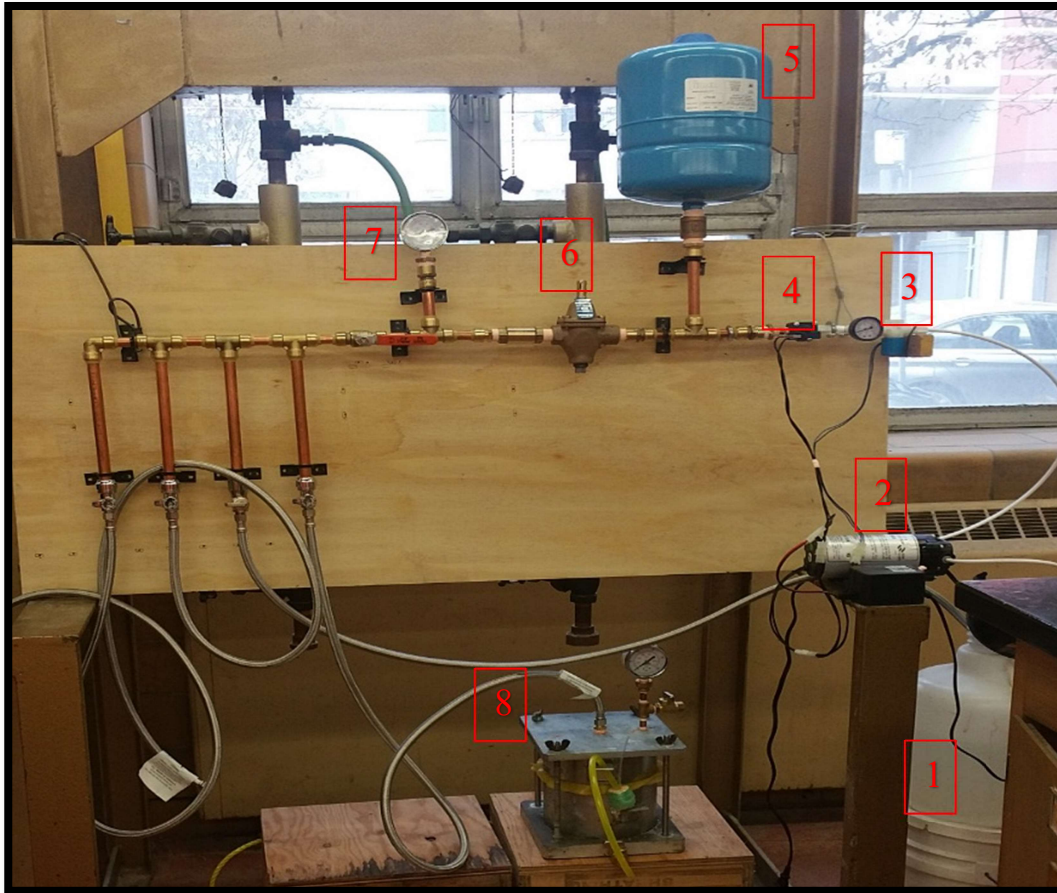


Figure 3-12: Leaching apparatus

Moulds from permeability test were modified as in Figure 3-13 and used as the leaching mould. The water pressure on the sample within the mould was one-dimensional and passed through the sample until it reached to the bottom and was collected in the leachate collection beaker. A filter paper and pore stone were placed on the top and bottom of the sample in the mould to distribute and homogenize the pressure on the sample.

This test set-up was designed to have a large sample size to accommodate more tests, including index properties, compressibility and shear strength on the same sample of leached clay. In addition, the leaching condition can be better controlled in this set-up, and it is more feasible

compared to a situation when an expensive testing machine like CRS and triaxial system is used for a prolonged time to leach a sample of clay.

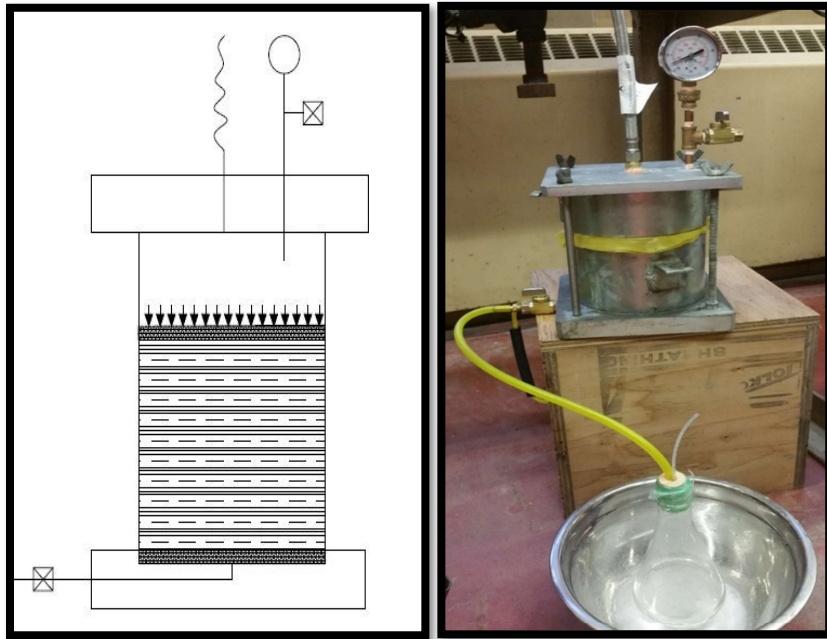


Figure 3-13: Leaching mould

3.3 SAMPLE PREPARATION PROCEDURES

3.3.1 Reducing Pore Fluid Salinity Level

The objective of this investigation is to determine the effect of leaching on compressibility Champlain Sea clay with or without DMM treatment. A sample of clay was leached with DDW to reduce the salinity level of pore water. The leachate was collected in a glass beaker, and the salinity level was recorded using Horiba ES-5 portable conductivity/salinity meter within 24 to 48 hours from the accumulated leachate in the beaker as seen in Figure 3-13. Each time, after the proper recording of the salinity, the beaker was replaced with another clean beaker and the procedure repeated until the salinity level of the clay was reduced from 19.81 g/L of salt mass per pore water (12.68 g/kg of salt mass to dry soil mass) to 0.79 g/L (0.505 g/kg). A total of 8032 ml of leachate and total of 11.93 g of salt was collected from the sample in 83 days, the total period of the leaching process. It should be mentioned that the amount of leachate collected from the sample was not

equal each time due to different collection time and this is the reason behind the fluctuation of salt level in 3-15 a. Variation of the salinity level of if the clay is shown in Figure 3-14. The leaching period can be divided into two stages. In stage one, the salt level was drastically decreased from high salinity level to low values. The reason for this is the replacement of the existing pore fluid in the sample by fresh water. Stage two that was started right after stage one with a small change in the salinity level in a period of 65-day leaching process. The small variation of salinity at stage two may be due to leaching of salts from the double-layer around the clay particles by diffusion.

At the end of the leaching process, the uniformity of salinity level in the sample was confirmed by testing three specimens retrieved from the top, middle and bottom parts of the leached sample.

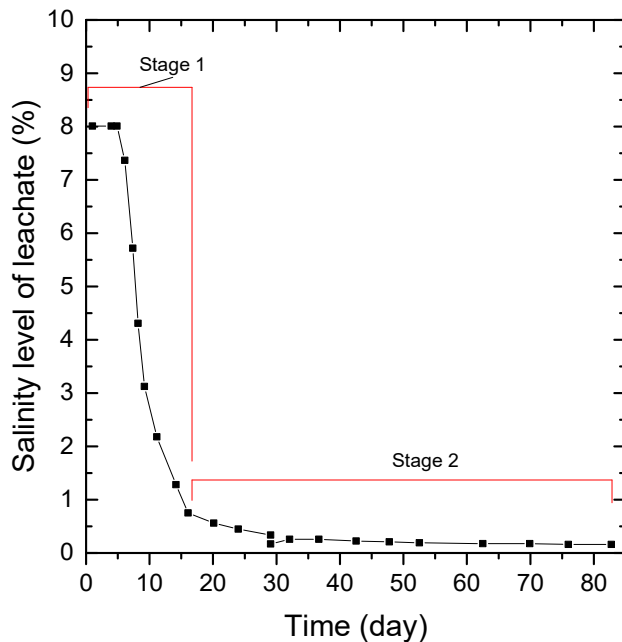
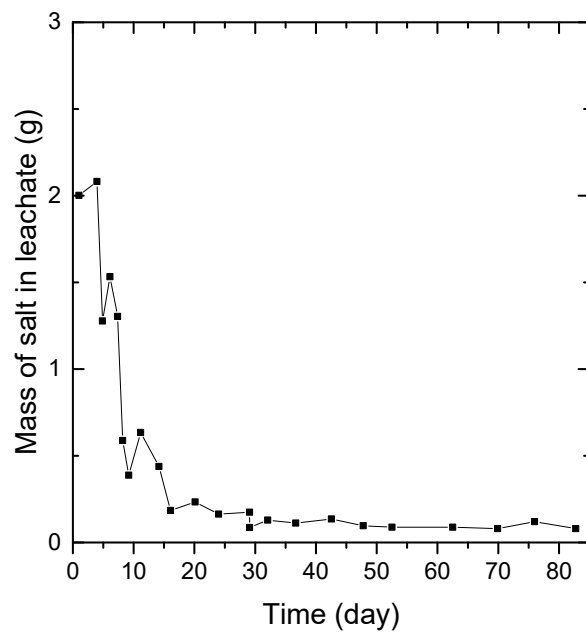
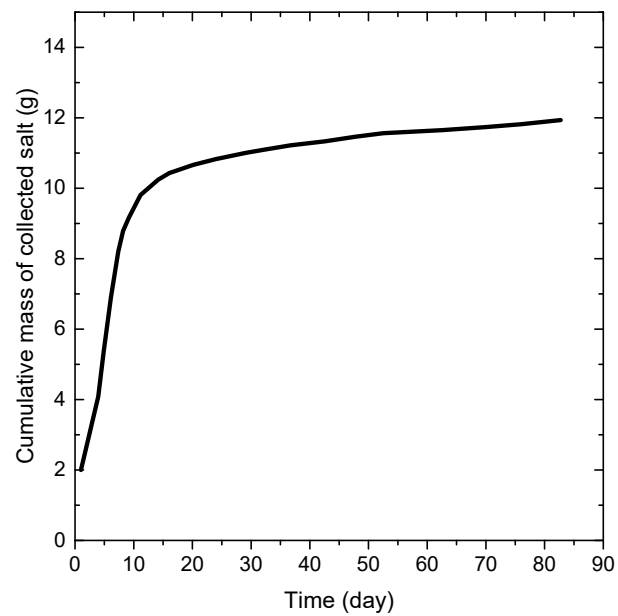


Figure 3-14: Decrease in percentage of salinity level in the collected leachate during the leaching process



a) Daily collection of leachate



b) Cumulative amount of leachate

Figure 3-15: Collected mass of salt over time

3.3.2 Samples Tags and Experiment Numbering

Each CRS test is designated with a tag that is an abbreviated form of the sample conditions. The first three letters are consistent in all the tests. The first letter shows the sample is undisturbed (U), remoulded (R), or cement treated (T). The second letter shows whether the sample is leached (L) or unleached (U). The third letter indicates the soil sample number: S1 represents the soil from the depth of 38.8 meters as described earlier. For samples treated with cement, the cement dosage and curing period are shown as following: 50C means the sample is treated with 50 kg/m³ of the total wet volume of the mix after mixing and 28D indicates the curing period of 28 days. As an example, TLS1-50C-2D is representing a treated (T) leached (L) sample from a depth of 38.8 meters (S1) that was treated with 50 kg/m³ cement (50C) and cured for two days (2D).

3.3.3 Undisturbed CRS Samples

A total of four (4) CRS tests were performed on undisturbed samples to evaluate the effect of leaching on undisturbed Champlain Sea clay. Both leached and unleached undisturbed samples were inserted carefully into a CRS ring to minimize disturbance. First, the sample was extruded slowly from the leaching mould using the sample extruder. Then, the CRS ring was placed on the top of the clay, as shown in Figure 3-16. The clay was trimmed carefully with a spatula to about 1 mm bigger diameter than the diameter of the ring, and then the ring was pushed into the clay while maintaining the ring plump.



Figure 3-16: Inserting leached samples into CRS rings

3.3.4 Remoulded CRS Samples

To investigate the effect of salt level on electro-kinetic potential and the thickness of the double layer between particles, two remoulded samples (RLS1-28D & RUS1-28D) were tested: one was provided from leached and the other from unleached clay samples. First, remoulded clay was inserted into the CRS ring on top of a flat surface piece of glass. Then the bottom of the ring was slowly hit by ten strokes to the ground while it was attached on the glass. This was done to remove any trapped air pockets from the samples. After the sample was inserted into the ring, its top was smoothened with a wire saw, and the sample was wrapped by plastic nylons and placed for curing into the curing bath. The reason for the curing was to allow the clay particles to come together and form layers under the effect of existing charges between particles. Each sample was cured for 28 days inside the curing chamber. It should be noted that after the completion of the curing period, the specimens in the rings were observed a little smaller in diameter and height. They were also stiffer samples than fresh remoulded clay. A small amount of bleeding water was also found after unwrapping the samples. It is believed that the reason for this is that the clay particles were moved closer to each other due to existing forces between particles. Since the cured samples were smaller in size, the gapes in the CRS rings were filled with the same clay samples before placing them under the test.

3.4 EXPERIMENTAL PARAMETERS

Based on the previous studies on cement-treated soil, the final strength of the treated soil may vary due to the influence of many factors, including soil type, binder type, binder content, curing condition. In this study, the effect of salinity level and curing condition on the strength of soil was investigated.

3.4.1 Cement-Treated CRS Samples

Samples of cement-treated leached and unleached clay were tested under CRS test to investigate the effect of leaching on cement-treating of Champlain Sea clay.

3.4.2 Binder Dosage Selection

A dosage of cement, 50 kg/m³ of the total volume of the mix (soil + binder) was selected for this study. The relatively low binder dosage was selected because of the load capability limitation of the CRS machine. All procedures recommended in Federal Highway Administration (FHWA) design manual (Bruce et al., 2013) were followed for mix design, and the total water/cement (Wt/C) ratio was controlled and kept constant in all the mixes.

3.4.3 Sample Mixing Method and Procedures

The wet mixing method was used in this study since the inherent moisture content of clay samples was close to 60%. The wet mixing method is recommended by Kitazume and Terashi (2013) when the water content of the soil is lower than 65 %.

First, wet cement slurry was prepared with 0.7:1 water to cement ratio. The binder slurry was added to the clay, and the specimen was then manually mixed for 5 minutes by two spatulas. Then, the required amount of sample was placed into each CRS ring and compacted with ten strokes by small wooden compaction pestle.

3.4.4 Sample Curing

At the final stage, each sample was wrapped by soft nylons, as shown in Figure 3-17, and kept sealed in the curing chamber with 95-100 % relative humidity for curing. The curing of samples took 2, 7, and 28 days for this study.



Figure 3-17: Sealed cement-treated samples before placing in the curing chamber

3.5 TESTING METHOD AND PROCEDURES

3.5.1 Compressibility Tests by CRS Testing Device

It has been confirmed that the actual field settlement can be detected from the stress-strain relationship of CRS test results when the clay deposit in the field is improved by the vertical drain (Jia, 2010). There are two methods of testing to determine the consolidation of soil: namely consolidation by incremental loading (IL), and constant rate of strain (CRS). Comparing the two methods, the CRS test method has several merits on measuring of soil consolidation parameters such as controlling the sample drainage conditions, measuring the pore water pressure, measuring the hydraulic conductivity of the specimen, using back pressure to saturate the sample and simulating field condition, controlling of loading, minimizing the vibration effects and testing time. Despite many advantageous of CRS test, developing transient water flow conditions upon loading stage is one of its disadvantages. Although many solutions to deal with it, the most applicable one is to use slow strain rates to limit the range of generated excess pore pressures. So soil with a low hydraulic conductivity must be tested with a low strain rate. The specimen under the CRS test is drained from the top side, and the developed excess pore pressure is measured from the bottom side.

After the proper curing time, each sample was trimmed with a wire saw for removing any extra part of the specimen and obtaining flat surfaces of the specimen in the ring. All the air was flushed out of the CRS base porous stone and ports with water. The testing sample was carefully placed on the platform. In each test, the CRS machine was turned on at least half an hour before the test as the requirement per its manual (Trautwein, 2001). Two filter papers were used, one on the top and the other on the bottom side of the specimen with a porous stone placed on top of the specimen to keep the top drainage open. Once the specimen was mounted, the cell was assembled, and the piston was locked on top of the specimen. In the next stage, the load cell and the piston were unlocked and lowered to contact with the specimen. The option of ‘Target Strain and Maintain Height’ was selected and target stress of 6.13 kPa (128 psf) was applied to promote sealing any gap between the specimen, porous stone, piston and the bottom of the cell. Once the target stress was achieved, the cell was filled with water, and the pressure sensors were saturated by loosening the bleed port set screw.

DDW was used to fill the CRS cell for all the leached samples while the salinity level of saline water collected from the leaching process was adjusted to the salt level of the unleached testing samples and used to fill the CRS cell. The different cell water was used to avoid any alteration salt level in unleached samples by the effect of diffusion on the cell water during the saturation stage.

Then, a back pressure of 350 kPa was applied for 24 hours to saturate the specimen before the start of consolidation. During the saturation time, the bottom valve was kept open to having the same back pressure applied on the top and the base of the specimen. In the next day, the bottom valve was closed for measuring the pore pressure development before the consolidation stage was initiated.

The strain rates according to Table 3-2 was used for all the tests except for two tests: UUS1CRS2 and ULS1CRS2 which slightly lower strain rate, 0.8 %/hr for loading stage and 0.2 %/hr for unloading stage were used to evaluate the effect of strain rate on test results. The low strain rates in all the tests kept the pore water pressure to mean effective stress ratio (u_b/σ') within the range of the recommended value of 3-15% as per ASTM D4186 (ASTM, 2012).

Table 3-2: Consolidation stages and strain rates

Loading Stages	Strain Rate, ϵ_r (%/hr)	Limit Stress (kPa)
1-Loading	1	2394 (50000 psf)
2-Unloading	0.25	96 (2000 psf)

3.6 DATA PROCESSING AND CALCULATIONS

The CRS machine outputs are load (lbs), displacement (in), pore pressure (psi), cell pressure (psi), and pump pressure (psi). These outputs were first converted to engineering values using the user's manual (Trautwein, 2001). Then the following formulas per ASTM D4186 (ASTM, 2012) were used to calculate the required parameters.

$$P = \frac{CF \cdot (V_s - V_0)}{V_e} \quad \text{Equation 3-1}$$

Where:

P = Physical input (e.g. load, displacement,...) (unit of the physical input)

CF = Calibration factor (unit/volt/volt)

V_s = Sensor output voltage (volts)

V_0 = Sensor voltage when zero stress is applied (volts)

V_e = Sensor excitation voltage (volts)

Using steady state equation, the axial stress is computed:

$$\sigma_{a_i} = \frac{P_i}{A} * 1000 \quad \text{Equation 3-2}$$

Where:

P_i = load (N)

A = specimen cross section area (mm^2)

Axial strain in percentage at any given time:

$$\epsilon_i = \frac{H_0 - H_i}{H_0} * 100 \quad \text{Equation 3-3}$$

Where:

H_i = initial height of sample (mm)

H_0 = current height of sample (mm)

100 = conversion of strain into percentage

$$e_i = e_0 - \frac{\epsilon_i}{100} * (1 + e_0) \quad \text{Equation 3-4}$$

Where:

e_0 = initial void ratio

The excess pore water pressure (kPa) at any time is calculated:

$$\Delta u_i = u_i - u_0 \quad \text{Equation 3-5}$$

Where:

u_i = current base pore pressure (kPa)

u_0 = initial base pore pressure (kPa)

The effective stress at any time calculated as:

$$\sigma_{i'} = \sigma_{a_i} - \frac{2}{3} \Delta u_i \quad \text{Equation 3-6}$$

Hydraulic conductivity (m/s) at any given time is calculated:

$$K_i = (\epsilon_i H_i H_0 \gamma_w) / 2 \Delta u_i \quad \text{Equation 3-7}$$

Pore pressure ratio at any given point:

$$R_i = \Delta u_i / \sigma_{a_i} \quad \text{Equation 3-8}$$

Coefficient of volume compressibility (m^2/KN) at any given time is calculated:

$$M_{v,i} = \frac{\epsilon_{i+1} - \epsilon_{i-1}}{\sigma_{i'+1} - \sigma_{i'-1}} * 1/100 \quad \text{Equation 3-9}$$

Coefficient of consolidation (m^2/s) at any given time step is calculated as:

$$C_{v,i} = \frac{K_i}{M_{v,i} * \gamma_w} \quad \text{Equation 3-10}$$

3.6.1 Determination of the Initial Void Ratio

After the completion of the CRS test and retrieving the specimen from the cell, the change in height and change in mass of the sample were recorded for each sample. Then the sample was placed in the oven for obtaining the after-test water content. In this study, it was found that using the after-test water content mass of the sample resulted in the most accurate calculation of void ratio for the CRS samples. In this method, the air phase in the sample can be ignored due to the saturation stage of the test that saturates the sample.

Following equations and parameters used to calculate the initial void ratio for each sample.

Mass of solid (M_s)

$$M_s = \frac{M_2}{(1 + \frac{\omega_{ii}}{100})} \quad \text{Equation 3-11}$$

Where:

M_2 = mass of sample after the test (g)

ω_{ii} = water content after test (%)

Mass of water exist in the sample after the test

$$M_w = M_2 - M_s \quad \text{Equation 3-12}$$

Change in height (Δ_H) (assumed to be equal to the height of water squeezed from the sample during consolidation)

$$\Delta_H = H_1 - H_2 \quad \text{Equation 3-13}$$

Where:

H_1 = height of sample before test (cm)

H_2 = height of sample after test (cm)

Total volume of the sample after test (cm^3)

$$V_T = 3.14 * R^2 * H_2 \quad \text{Equation 3-14}$$

Where:

R = Radius of CRS ring (cm)

Volume of water after the test (cm³)

$$V_w = \frac{M_w}{0.9982} \quad \text{Equation 3-15}$$

Where:

0.9982 = density of water at 22 degrees Celsius

Volume of solid after the test (cm³)

$$V_s = V_T - V_w \quad \text{Equation 3-16}$$

Height of solid (cm)

$$H_s = \frac{V_s}{A} \quad \text{Equation 3-17}$$

Where:

A= area of the CRS ring (cm²)

Height of water (cm)

$$H_w = \frac{V_w}{A} + \frac{\Delta H}{10} \quad \text{Equation 3-18}$$

The initial void ratio is estimated as

$$e_i = \frac{H_w}{H_s} \quad \text{Equation 3-19}$$

3.6.2 Determination of Pre-Consolidation Pressure

There are many methods for determining the pre-consolidation pressure (P_c) from the e -log p curve. The Silva's (1970) method was selected in this study for determination of pre-consolidation stress. The simplicity of this method is one of the reasons this method was used in this study. The pre-consolidation stress is empirically determined from the e -log p curve, where e is the void ratio, and p is the effective vertical stress. Using Silva's method, very similar preconsolidation stress values can be obtained by two different people because this method is not subjected to any

interpretations (Clementino, 2005). Unlike the Casagrande (1936) method in which different scales result in different pre-consolidation values, Silva's method is scale independent.

The following steps are the descriptions for obtaining pre-consolidation pressure by Silva's method.

1. Sketch a horizontal line (A-B) as seen in Figure 3-18 which passes the specimen's initial void ratio (e_0)
2. Draw a straight line (C-D) and extend until it intersects with (A-B)
3. Draw a vertical line from the intersection of A-B C-D lines until it intercepts with e -log p' curve at point E.
4. From point E, draw a horizontal line and extend to obtain 'point F' from its interception with line C-D
5. The associated value of point F on the horizontal axis is the pre-consolidation pressure

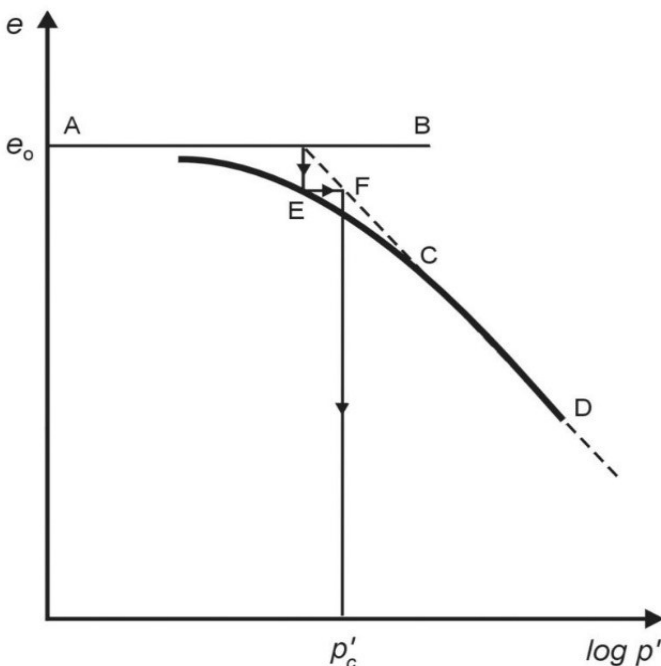


Figure 3-18: Silva's construction to determine pre-consolidation pressure (Clementino, 2005)

Yield stress (P_y') for the remoulded and cement-treated samples were also obtained using Siva's method.

It is recognized that the $e-\log(p)$ curve for a sensitive clay constitutes of three sections: over-consolidated region (Zone I), the soil collapse after preconsolidation pressure (Zone II), and after the soil has regained strength (Zone III). The combination of these three zones creates the sensitive clay well-known S-shaped compression curve. The compression indices of the three zones are referred to as, CC-I, CC-II, and CC-III consequently. The C_c from Zone I and Zone II are obtained in this study from the test results.

3.7 SUMMARY

This chapter presented the physical properties of the soil used in this study. Then, the equipment and sample preparation methods were discussed. Furthermore, the binder dosage, sample mixing procedure, curing time of DMM samples along with the salinity level of all the specimen were explained. Finally, the data processing for the major testing method, compressibility by CRS test, was described. The next chapter will present the results of compressibility tests by CRS testing device.

4. RESULT AND ANALYSIS OF CRS TESTS

4.1 IMPACT OF LEACHING ON UNDISTURBED CHAMPLAIN SEA CLAY

A total of four CRS tests were performed on undisturbed leached (UL) and undisturbed unleached (UL) samples. The testing specimens were obtained from a block of Laval sample from the depth of 38.8 m as discussed earlier. Two different strain rates: 1%/hr (loading) and 0.25%/hr (unloading) for Sample 1; 0.8%/hr (loading) and 0.2%/hr (unloading) for Sample 2 were used. The reason for the two different strain rates (20% slower rates for Sample 2) was to investigate any effect due to the loading rate. Usually, a faster strain rate would result in higher pore pressure during the consolidation test as seen in Figure 4-1 and Figure 4-2 of test results. A higher pore pressure ratio was recorded from Sample 1 due to the higher strain rate. The ratio of pore pressure during the test to the corresponding total vertical stress on the sample is called pore pressure ratio. It should be kept in mind that sometimes a very high pore pressure ratio can be seen at the initial stage of the CRS test. This is because at the beginning of the test the vertical stress is very small, so a small pore pressure on the transducer will result in a big value of pore pressure ratio. Similarly, high initial pore pressure is reported by Ahmadi *et al.* (2009 and 2011).

It can be expected that the excess pore water pressure dissipates quicker from the intact sample because the structure of voids and flow channels are undisturbed and interconnected. The structure of the voids in a clay sample will become narrower when the stress level on the sample starts to build up. Under stress higher than P_c' the structure of soil collapses and results in a significant change of the pore structure and flow channels. This effect was well observed in the test results as seen in Figure 4-1 and Figure 4-2. Pore pressure continued to build up until the stress level was reached the preconsolidation pressure, P_c' . In the undisturbed samples, the pore pressure ratio is reached to their peaks close to the effective stress ranging from 300-330 kPa where the preconsolidation pressure of the samples were recorded. However, depends on the strain rate and the accumulated pore pressure at the over-consolidated stage, when the stress level is passes the preconsolidation pressure, the pore pressure is either decreased or increased.

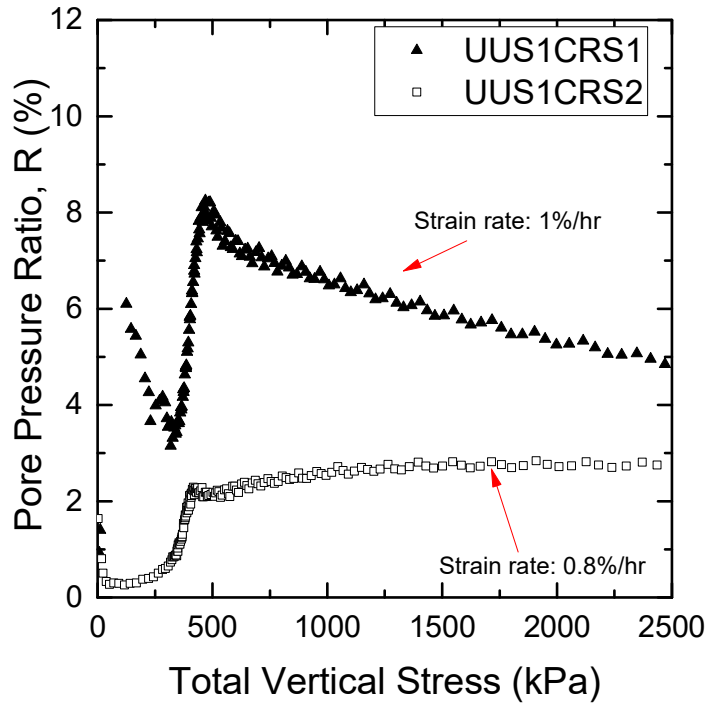


Figure 4-1: Pore pressure vs. effective stress UU samples at different strain rates

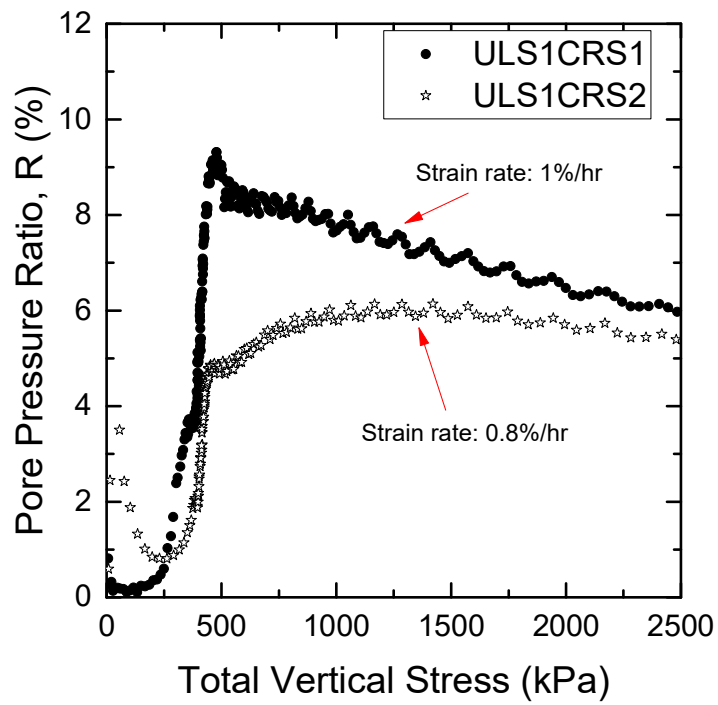


Figure 4-2: Pore pressure vs. effective stress UL samples at different strain rates

Void ratio against the effective stress of UU and UL samples are shown in Figure 4-3 and Figure 4-7. DDW was used to for UL samples while the CRS cell was filled with water collected from the leaching process after the salinity of the water was adjusted to the soil salinity level.

Similar initial void ratios ranging from 1.97 to 2.01 were obtained from all the UL and UU samples. Similarly, no change in initial void ratio due to leaching was reported in the results of consolidation tests conducted on two clay specimens (Baimahu clay and Kemen clay) by Hong et al. (2010). The preconsolidation stress of the samples is recorded in Table 4-1. No significant change in preconsolidation pressure of the sample can be seen. Except for the bigger compression indexes (Cc-II) were obtained from UL samples than that of their corresponding UU samples as seen in Table 4-1. The bigger Cc-II values in UL samples suggest that the strength of the clay structure was reduced due to leaching as the type of failure became more abrupt in the zone II of the consolidation curve. Under the current salinity level, except Cc-II values, minimal differences can be observed comparing the compressibility curves of UL and UU samples. Some of the small differences such as in P_c' values are expected to be seen due to the testing errors and sample disturbances.

No significant changes in the compressibility curves of the UU and UL samples further indicate that the different strain rates used in this study did not have significant effects on the compressibility of undisturbed samples. The pore pressure ratio stayed lower than 15% as per ASTM standard (ASTM, 2012) for both strain rates during the test as shown in Figure 4-1 and Figure 4-2.

Hydraulic conductivities are plotted against the void ratios of the samples throughout the consolidation process for the undisturbed samples shown in Figure 4-4 and Figure 4-8. It can be seen that the permeability was decreased with the decrease of the void ratio. The hydraulic conductivity can be divided into two stages. First, the hydraulic conductivity ranging from $8E-6$ to $9E-8$ m/s which was recorded during the over-consolidated state of the soil. At this stage, the hydraulic conductivity is significantly decreased. Second, the pore structure of the soil drastically changes when the stress level passes P_c' and result in further reduction of the hydraulic conductivity in the clay sample. In the second stage, the hydraulic conductivity were recorded

ranging from $9\text{E-}8$ to $3\text{E-}10$ m/. The slope of the plot from each test in the second stage of permeability was obtained from its best fit line and indicated with the symbol, C_k , in its corresponding plot.

Slightly lower permeabilities were expected from the UU samples than those of their corresponding UL samples due to the higher viscosity of saline CRS cell water. However, no significant changes of the permeability were observed in the test results. More tests are needed to confirm this finding.

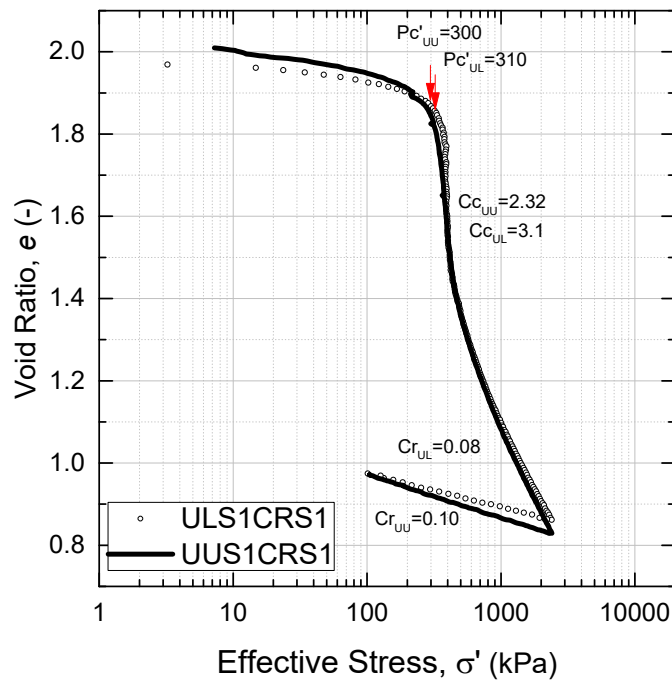


Figure 4-3: Influence of leaching on e -log p curve of undisturbed Sample 1

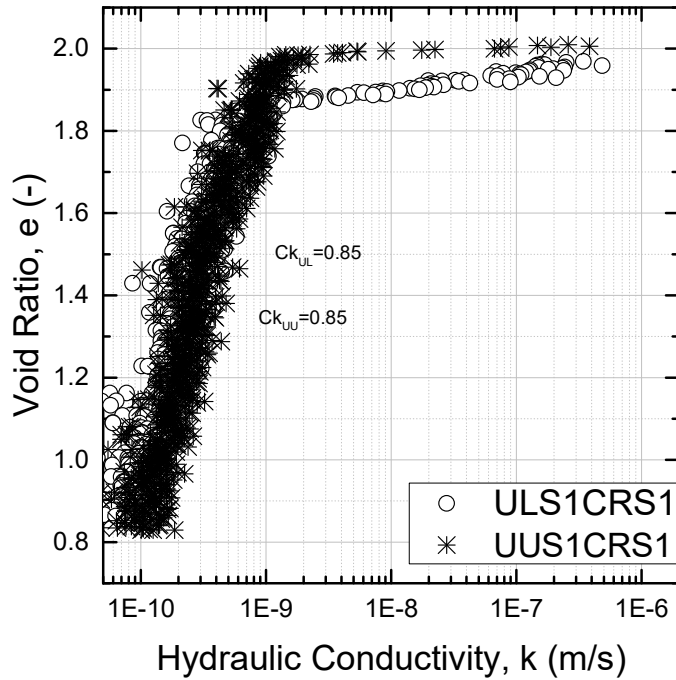


Figure 4-4: Influence of leaching on the permeability of undisturbed Sample 1

The coefficient of volume change, M_v , of the UL and UU samples are plotted against effective stress, shown in Figure 4-5 and Figure 4-9. Similarly, no significant differences can be seen comparing the results from UU and UL samples.

The recorded M_v values from all the undisturbed samples started from a value within the range of $1E-3$ to $1E-04$ -/kPa. Then, they were decreased until the stress level was close to P_c' . At stress closed to P_c' , the M_v values started to increase until the stress of about 400 kPa was applied. A sharp drop in M_v can be observed right after the effective stress passes 400 kPa and the values were continuously decreasing until the lowest M_v was recorded about $2E-05$ -/kPa at the end of the consolidation.

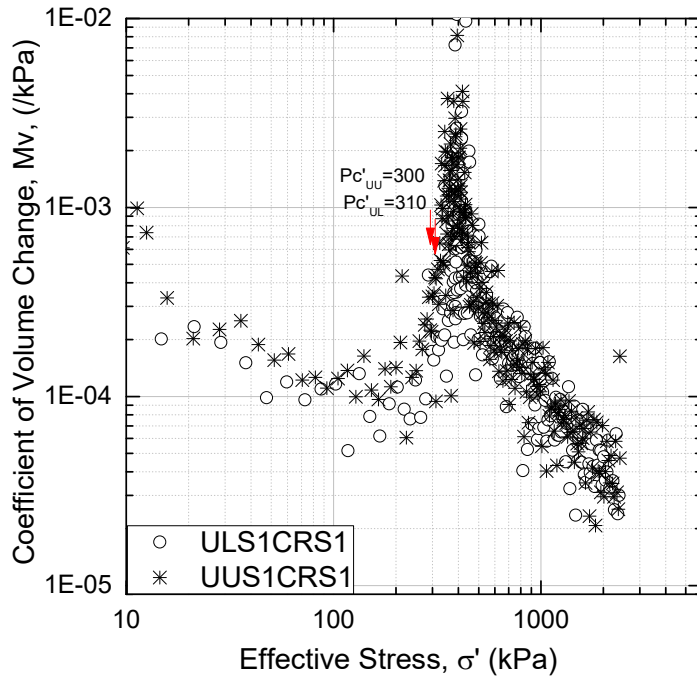


Figure 4-5: Influence of leaching on the coefficient of volume change of undisturbed Sample 1

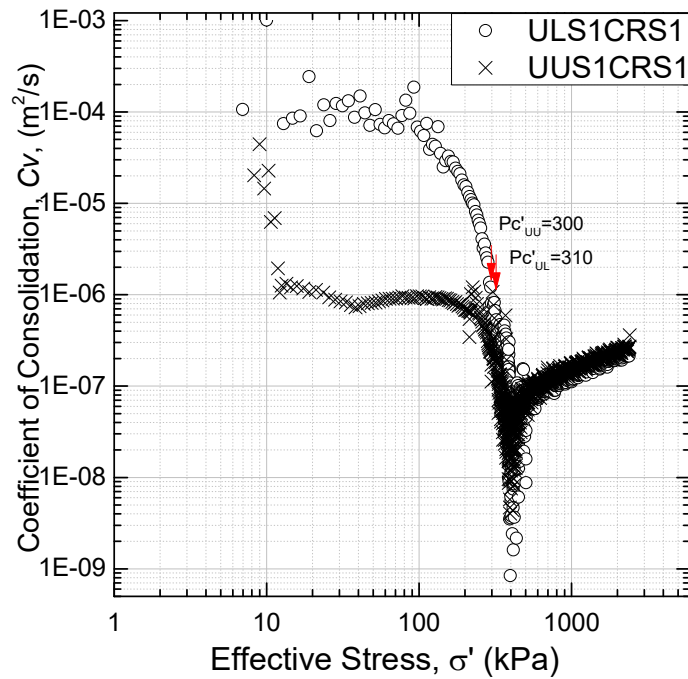


Figure 4-6: Influence of leaching on the coefficient of consolidation of undisturbed Sample 1

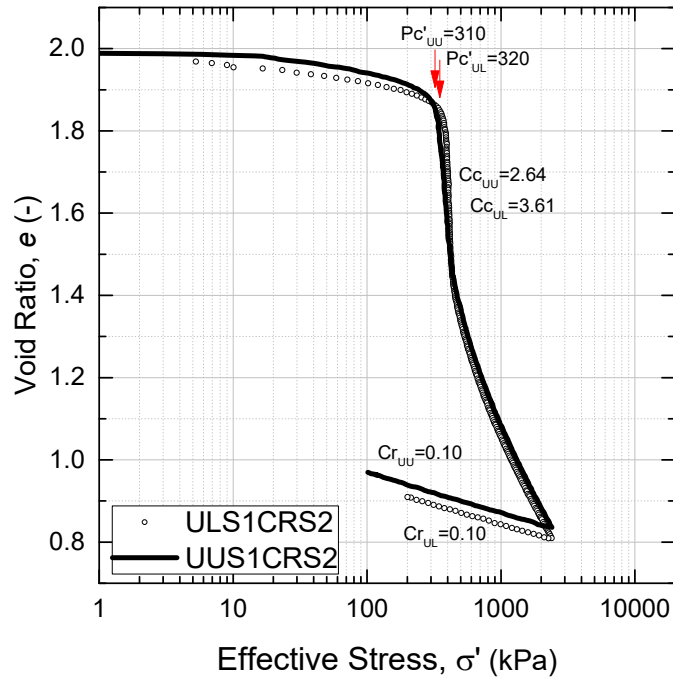


Figure 4-7: Influence of leaching on e-log p curve of undisturbed Sample 2

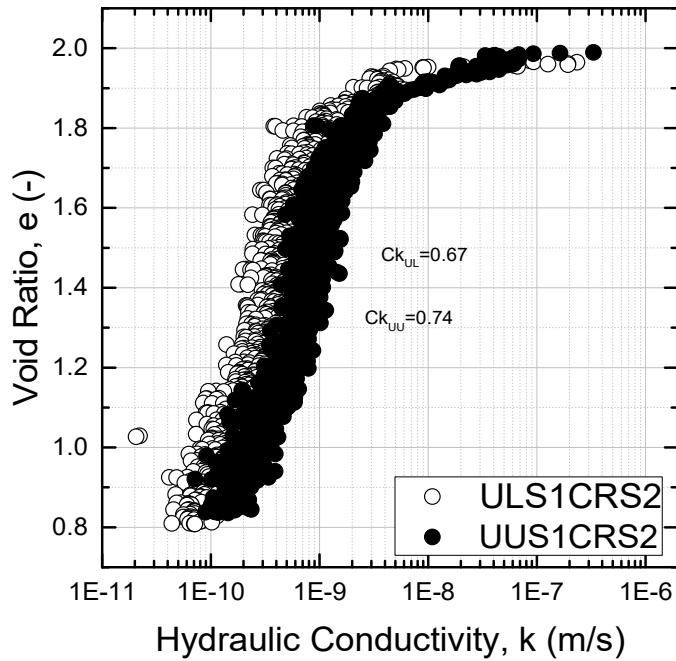


Figure 4-8: Influence of leaching on the permeability of undisturbed Sample 2

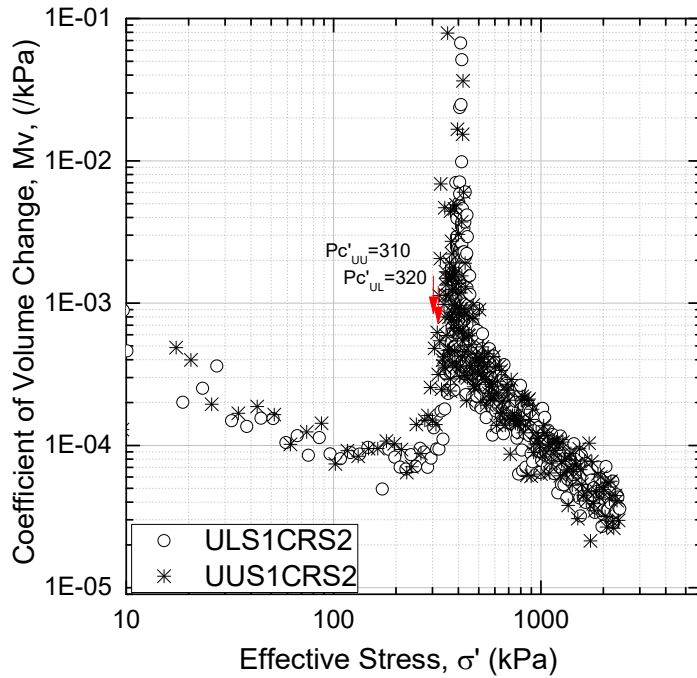


Figure 4-9: Influence of leaching on the coefficient of volume change of undisturbed Sample 2

The coefficient of consolidation, C_v , of the undisturbed samples is plotted in Figure 4-6 and Figure 4-10. C_v is related to the coefficient of volume change and hydraulic conductivity. A decrease in C_v values can be seen when the effective axial stress was increased in the over-consolidated state. In contrast, C_v was tended to increase in the normally consolidated range by increasing of the axial stress. The lowest C_v value was recorded about $1\text{E-}9 \text{ m}^2/\text{s}$ at 400 kPa from both of the tests on undisturbed leached samples. Similarly, but slightly higher C_v values about $5\text{E-}8 \text{ m}^2/\text{s}$ were achieved at the same stress level from the unleached samples. The higher value of C_v is believed to be due to its higher permeability values. Next, C_v values were sharply increased right after their lowest value around P_c' . The trend of increase became smaller when the axial stress passed 600 kPa. Significant changes in the C_v values at stress values close the preconsolidation pressure further adds evidence to the theory that flocs are breaking within the soil matrix and the soil structure changes when the stress is close to the preconsolidation pressure of soil.

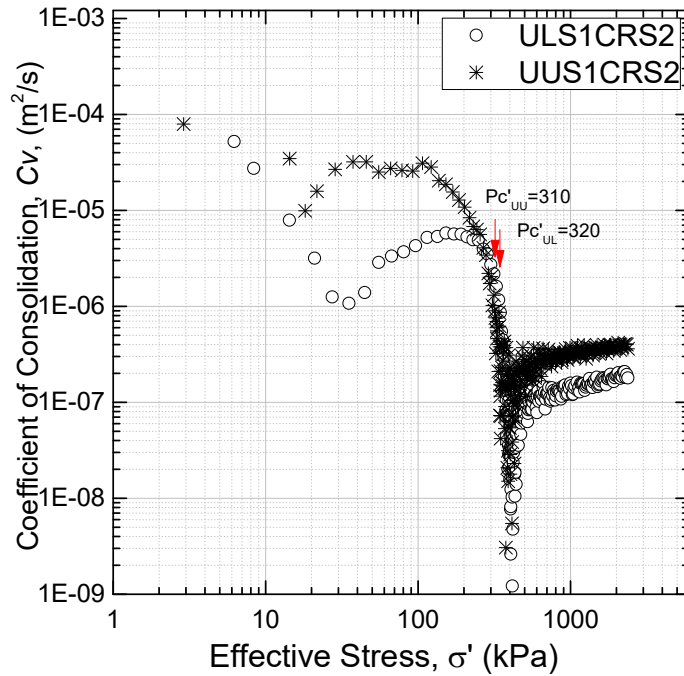


Figure 4-10: Influence of leaching on the coefficient of consolidation of undisturbed Sample 2

4.2 IMPACT OF LEACHING ON REMOULDED CHAMPLAIN SEA CLAY

Two remoulded samples were tested to compare the compressibility behaviour of remoulded Champlain Sea clay before and after leaching. The same loading rates ($\epsilon_{r1}=1\%/hr$ for loading and $0.25\%/hr$ for unloading) was used to conduct both tests. The results provide consistent information about the yield stress and other related compressibility parameters of remoulded leached (RL) and remoulded unleached (RU) samples.

Void ratio against the effective stress of (RL) and (RU) samples are shown in Figure 4-11. The same initial void ratio of 1.72 was obtained from both samples. The compressibility curve of RL sample come below the curve of the RU sample after a small vertical effective stress of 5 kPa at the beginning of the test. However, the same yielding stress (P_y') of 50 kPa was obtained from both samples consolidation curve using the Pacheco Silva method. The void ratios in both samples were decreased with a similar trend until the void ratio of 1.2 at the effective stress of 300 kPa was obtained. It appears that at this point some restructuration was happening in the RU sample as its

compressibility curve has changed its trend with a lower reduction in the void ratio. This may be the reason for the small difference between the final void ratio of the samples in Figure 4-11.

The compressibility curves of remoulded leached (RL) and undisturbed leached (UL) samples are plotted in Figure 4-12. Clearly, there are differences between the shape of the curves. The sudden failure seen in the compression curve of the undisturbed sample cannot be seen in the remoulded sample. Remoulding has erased any memory of the stress pass from it, so the remoulded clay behaved differently under the consolidation process. A smaller void ratio was obtained from the remoulded sample compared to that of its corresponding undisturbed sample. The reason for this can be due the compaction strokes applied to the remoulded sample while preparing them. That may also help to explain the relatively smaller compressibility that was obtained from remoulded samples compared to its corresponding undisturbed samples.

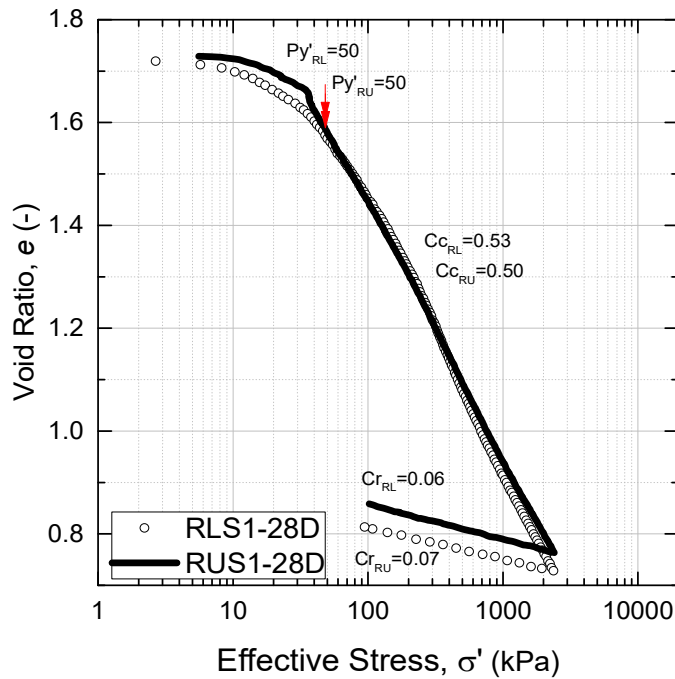


Figure 4-11: e-log p curves of RL and RU samples of Champlain Sea clay

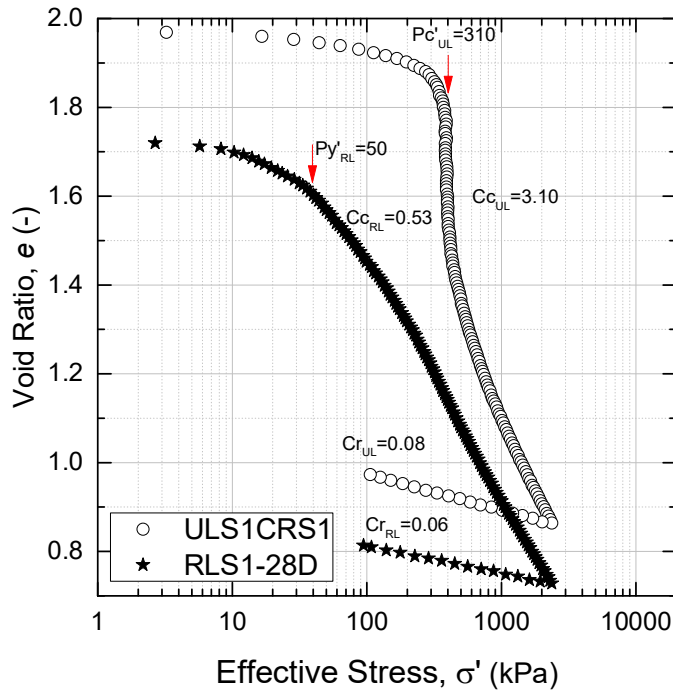


Figure 4-12: e-log p curves of UL and RL samples of Champlain Sea clay

Hydraulic conductivity against void ratio for both RU and RL samples throughout the consolidation test are plotted in Figure 4-13. Lower hydraulic conductivity was recorded from RU sample compared to the RL sample. One of the reasons for this could be the higher viscosity of saline water in the CRS cell while testing the RU sample compared to the DDW that was used for RL sample. However, the small difference of viscosity of the CRS cell water effect on the permeability results could not alter the results more than one order of magnitude as seen in Figure 4-13. There should have been some other effect of different salinity level on the samples that resulted in the differently recorded permeabilities. More tests are needed to be performed to confirm the results.

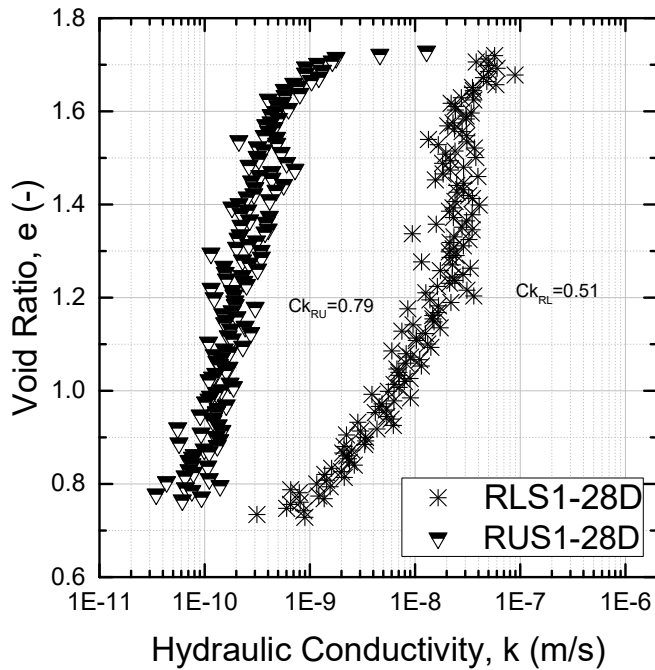


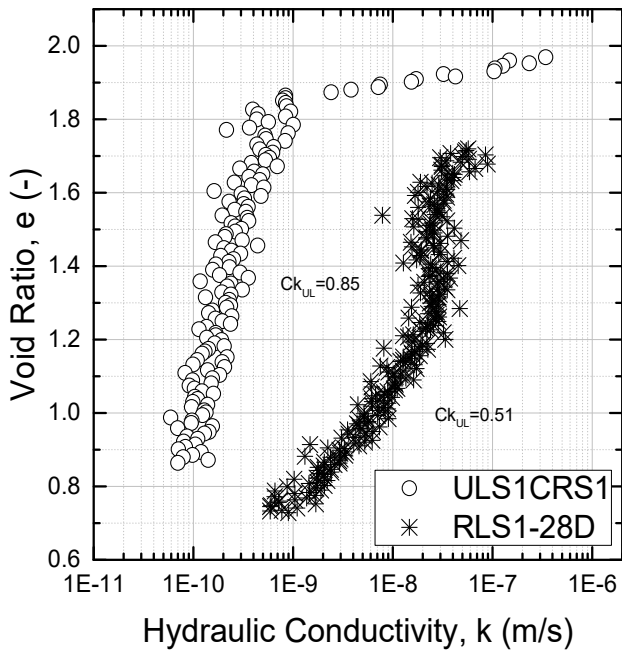
Figure 4-13: Variation of hydraulic conductivity versus change in void ratio of RL and RU samples

The variation of hydraulic conductivities against void ratio of UL and RL samples are plotted in Figure 4-14 a. The hydraulic conductivity of the RL sample was recorded lower than the UL sample at the beginning of the test. This may be due to the lower initial void ratio of the RL sample. However, despite the lower initial void ratio of the remoulded sample, the hydraulic conductivity of the UL sample became smaller throughout the test. This indicates that the leached clay particles in the remoulded state are placed on top of each other in a way that more flow channels and interconnected voids were remained open during the consolidation compared to that of the UL sample. Moreover, the salt level may define the way particles floc together and place on top of each other.

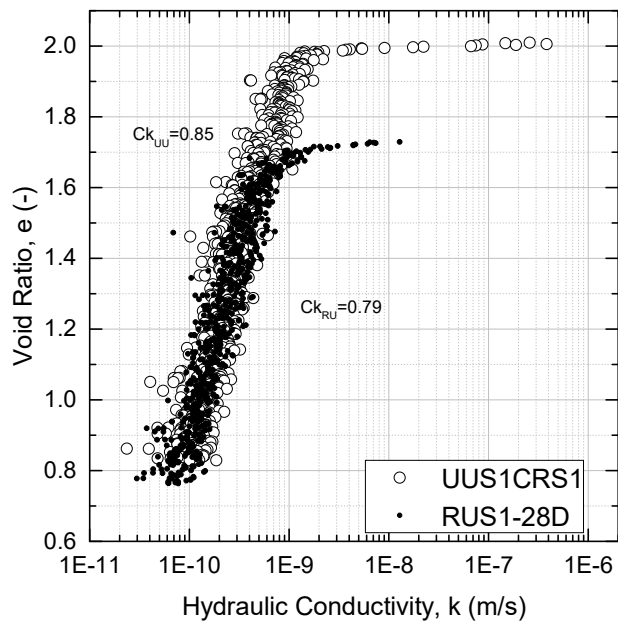
The variation of hydraulic conductive versus the void ratio of remoulded unleached (RU) and undisturbed unleached (UU) samples presented in

Figure 4-14 b further adds to the evidence. Initially, a lower permeability was recorded from RU sample due to its smaller initial void ratio compared to its corresponding UU samples. But then the hydraulic conductivities of both samples were converged at the void ratio of 1.7. This indicates

the particles in RU sample have not been affected as RL particles were affected due the lower double layer charges as the result of the lower salinity level.



a) leached samples



b) unleached samples

Figure 4-14: Variation in hydraulic conductivity versus change in void ratio of UU and RU samples

The coefficient of volume change against the effective stress of RL and RU samples are plotted as shown in Figure 4-15. No significant difference was observed between the test results. M_v started with values ranging from $8E-04$ to $1E-03$ /kPa for both samples. Then a small increase in M_v near the yielding stress, about 50 kPa was recorded. After that, M_v values were started to decrease to its lowest value about $1.5E-05$ /kPa in both samples at the end of the consolidation.

Comparing the M_v values obtained from UL and RL samples shown in Figure 4-16. Higher M_v values were recorded from RL sample at the beginning of the test until the effective stress was reached to P_y at approximately 300 kPa. At this point, the M_v of UL sample was sharply increased to its peak following by a sharp drop at the same point. Then the M_v values were started to decrease for both samples until the end of consolidation.

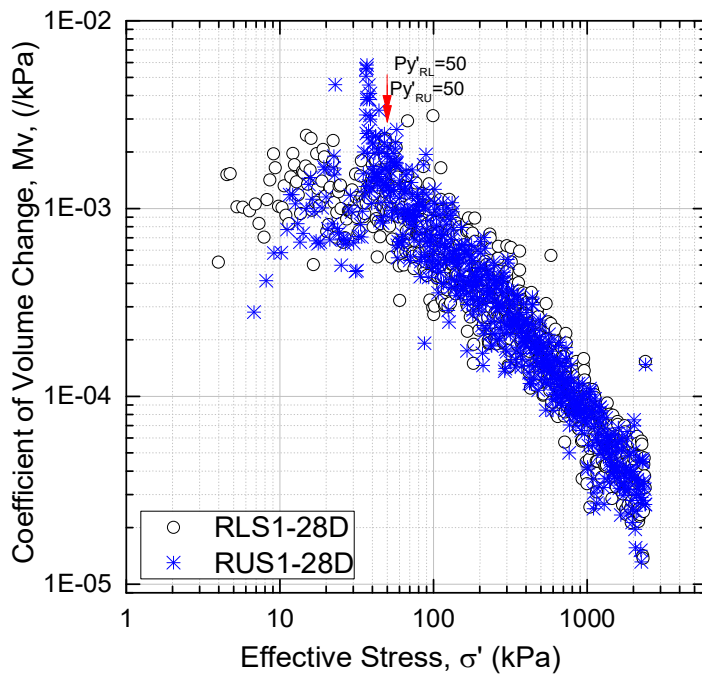


Figure 4-15: Variation of M_v versus log effective stress of RL and RU samples

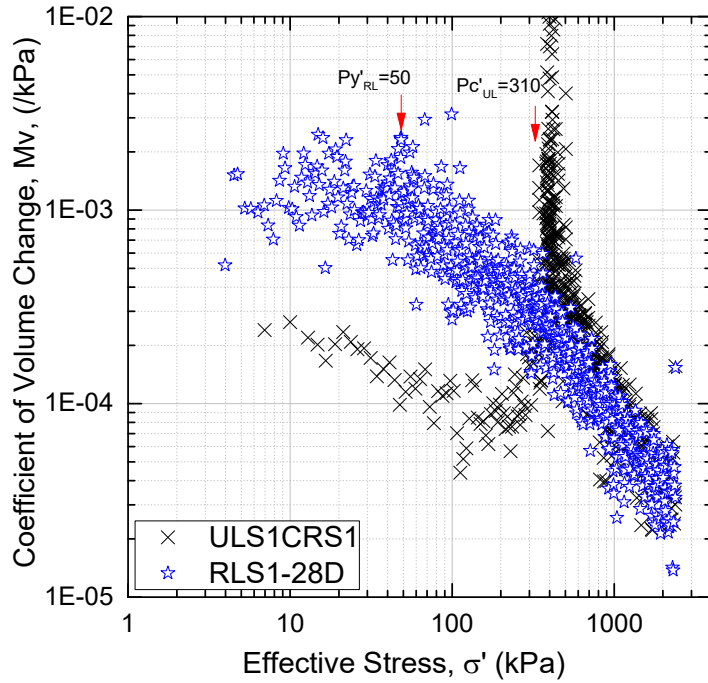


Figure 4-16: Variation of M_v versus log effective stress of UL and RL samples

The C_v values of RL and RU samples are plotted against the effective stress in Figure 4-17. Higher C_v values were recorded from the RL sample. The reason for this is believed to be the higher hydraulic conductivity in RL sample compared to its corresponding RU sample as discussed earlier. The lowest C_v values were recorded from both samples at the stress about their P_y' .

Similarly, C_v values of UU and RU samples are plotted against the effective stress in Figure 4-18. At the initial stage of the test, higher C_v values were recorded from the UU sample. However, the C_v values from both the tests were converged after the effective stress reached about 500 kPa. Then they followed the same trend with similar values until the end of consolidation.

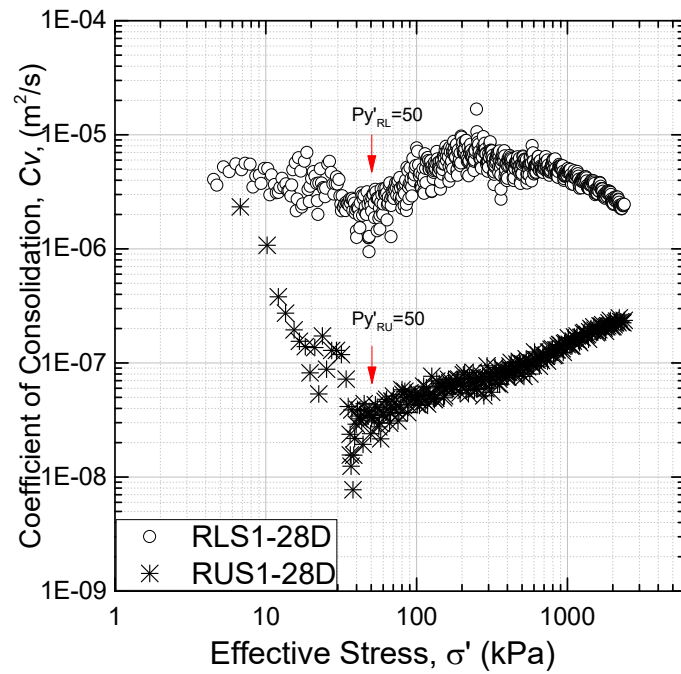


Figure 4-17: Variation of C_v versus log effective stress of RL and RU samples

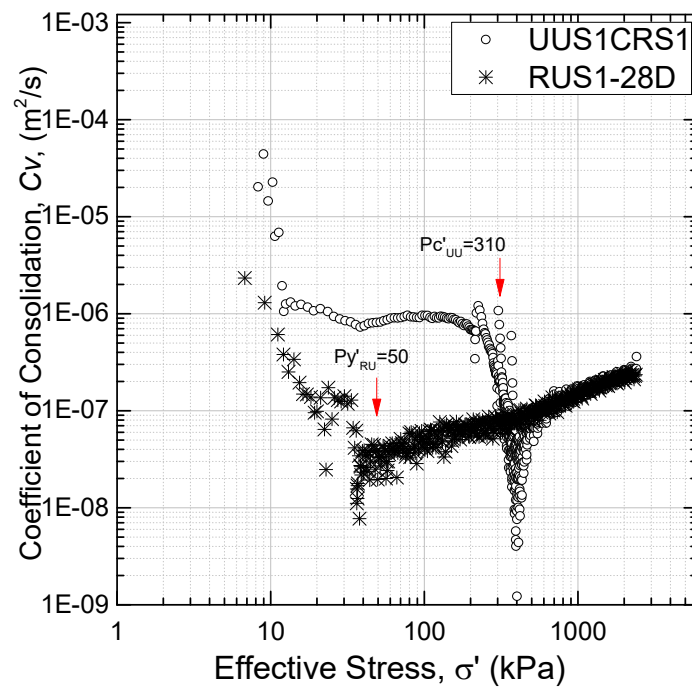


Figure 4-18: Variation of C_v versus log effective stress of UU and RU samples

4.3 COMPRESSIBILITY OF CEMENT-TREATED CHAMPLAIN SEA CLAY

A total of 6 CRS samples were prepared from the cement-treated leached and unleached samples. The cement dosage was selected at 50 kg/m^3 per wet volume of the total mix after treatment. The samples were cured at 2 days, 7 days, and 28 days. The main objective for preparing such samples was to investigate the impact of salinity level of natural clay on the compressibility of cement-treated Champlain Sea clay. The results show that DMM provided a consistent improvement in yield stress, stiffness, the coefficient of consolidation, and the permeability of Champlain Sea clay.

The nonlinear solution proposed by Wissa et al. (1971) was used to derive effective vertical stress, C_v , M_v , and hydraulic conductivity of specimen from the measurement of axial load, vertical displacement, cell (back) pressure, and the measurement of excess pore pressure at the base of soil.

The CRS results shown in Figure 4-19 to 4-22 were plotted to compare the compressibility behaviour of an untreated clay sample with a cement-treated sample. The most notable effect of the cement treatment was the increase in the yielding stress. The yielding stress increased almost four times from around 305 kPa in the untreated sample to about 1075 kPa in the treated sample after 28 days of curing.

As a result of the cementation induced, the change in the void ratio of the treated clay is about 400% smaller than the untreated sample under the same pressure range. This indicates a significant reduction in the compressibility of the cement-treated clay with the tested pressure limit of 2500 kPa.

Despite the lower initial void ratio, the initial hydraulic conductivity of cement treated samples were recorded slightly higher from both of the remoulded samples as seen in Figure 4-20. The change in the clay fabric due to cement reaction causes the increase in the initial hydraulic conductivity. When a clay sample is treated with cement, Ca^{2+} and OH^- are released. Due to this the pH and ionic strength of the treated sample will be increased. Thus, the double layer thickness of the phyllosilicate minerals presents in the clay reduces due to higher Ca^{2+} concentration and promote flocculation and aggregation of particles. Secondly, binding of clay particles together by the formation of C-S-H and C-A-H gels further contribute to aggregation and flocculation (Al-

Rawas, 2002; Rao & Rajasekaran, 1996; Tremblay, Leroueil, & Locat, 2001). More open fabrics and macropores will be formed as the result of these. This indicates that more cement content increases the size of flow channels. These hypotheses are also confirmed by Chew et al. (2004) through observation of the microstructure of cement treated clay by scanning electron microscopy (SEM). SEM observation was illustrated that the cement produces a flocculated structure that results in the size of the opening between the soil particles clusters to increase.

The change in M_v with the effective stress of a UU sample and the cement treated sample cured for 28 days is plotted in Figure 4-21. Initially in both samples M_v was decreasing with increasing the effective stress, increased rapidly to its peak at stress level near the P_c' , and right after the peak, a sharp drop in M_v values can be seen. Overall, the M_v from the cement-treated sample was recorded lower than that of the UU sample throughout the test. The lower M_v in cement-treated samples can be a good indication of the reduction of compressibility due to cement treatment.

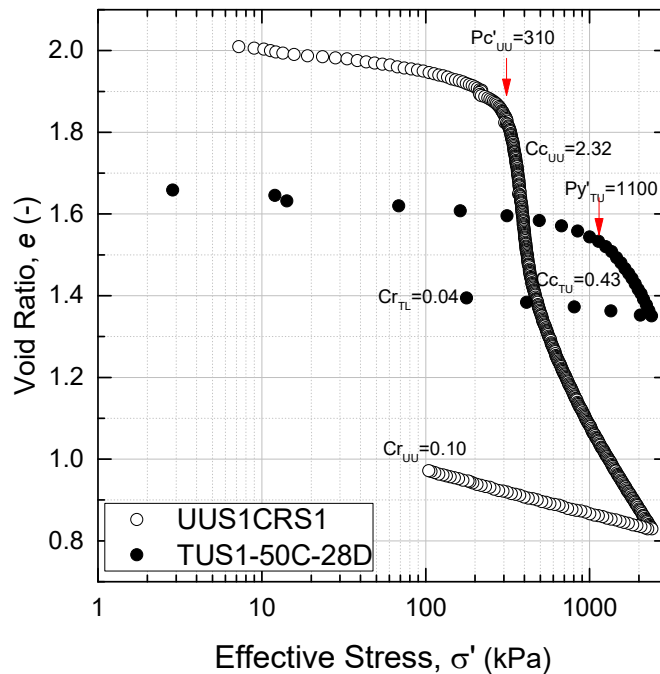


Figure 4-19: e-log p curve of UU and TU samples

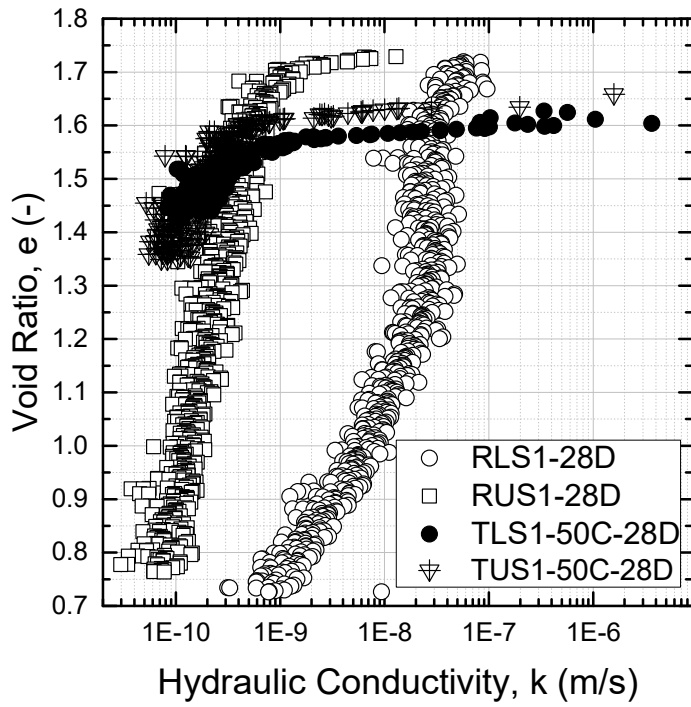


Figure 4-20: Hydraulic conductivity of cement-treated and remoulded clay

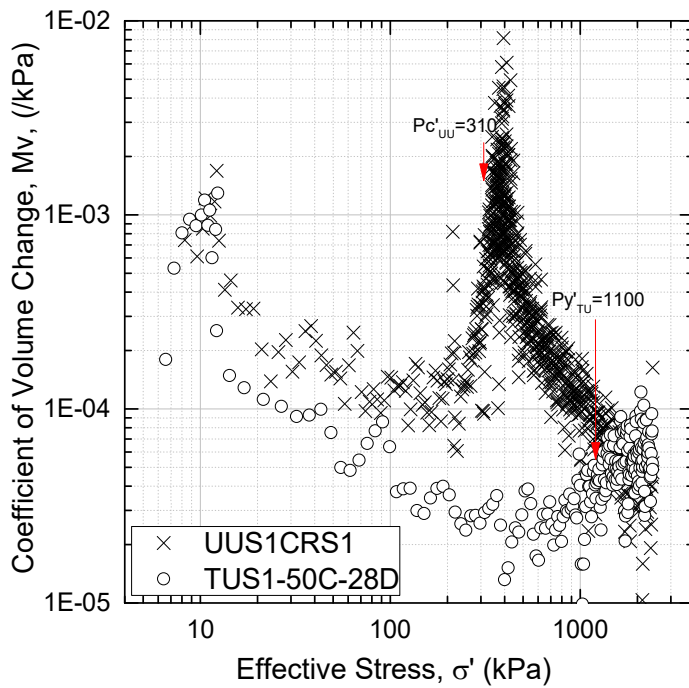


Figure 4-21: Variation of M_v versus log effective stress of UU and the TU sample

The change in the coefficient of consolidation against effective stress is plotted in Figure 4-22. Generally, C_v was recorded higher from the cement-treated samples compared to their corresponding untreated samples. The higher C_v in the cement-treated sample is due to a combined effect of the increase in hydraulic conductivity and the decrease in compressibility. This observation agrees with the result obtained from other soils treated with lime and cement reported in the literature (Brom, 1999; Cortellazzo & Cola, 1999; Kassim, 1999).

V-shape curves were obtained from the plot of C_v versus the effective stress of untreated samples. The initial values of C_v were started from a high value in all the UL samples, then they were dropped to the lowest point near P_c' but again were increased by increasing of the effective stress. However, in the cement-treated leached samples (TL), the minimum value of C_v was not recorded anywhere closed to P_y' . From the beginning of the test, the C_v was tended to decrease until the end of the test. More tests are needed to confirm this finding.

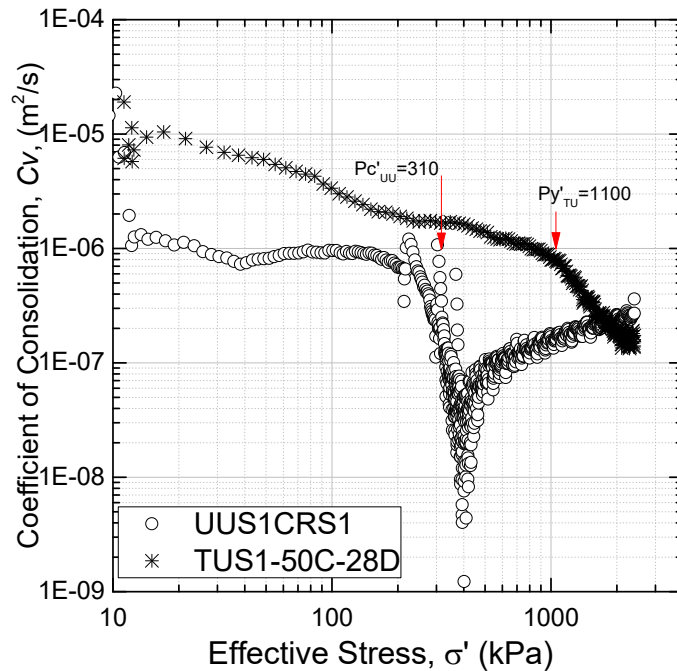


Figure 4-22: Variation of C_v versus log effective stress of UU and TU samples

4.4 IMPACT OF CEMENT TREATMENT ON CHAMPLAIN SEA CLAY AT DIFFERENT SALINITY LEVELS

This section addresses the impact of cement treatment on Champlain Sea clay samples at different salinity levels. The results of CRS tests on treated leached and unleached clay samples with the same cement dosage of 50 kg/m^3 and curing time are presented in Figure 4-23 through Figure 4-33. Each plot consists of the group of tests conducted on samples with the same mix and test conditions except for the curing time.

The void ratio against the effective vertical stress of all treated samples is presented in Figure 4-23 and Figure 4-24. The initial void ratios of all the samples were measured within the range of 1.65 to 1.68, which are smaller than the initial void ratio of the intact clay. The smaller initial void ratio in the samples is because the effect of cement treatment on the structure of the clay and the applied compaction when the samples were prepared.

A significant increase in the yielding stress can be seen from the cement treated samples. For example, the yielding stress was increased almost three folds from 300 kPa in undisturbed samples to approximately 850 kPa in the TU sample cured for just 2 days. The yield stress was further increased to 1050 kPa and 1100 kPa with curing time of 7 days and 28 days, consecutively.

It is as expected that the cement treating of leached samples (TL) resulted in a higher yield stress as seen in Table 4-1. A valid reason for this is not yet confirmed. To the author's knowledge, there is not any other investigation on the impact of salinity on the performance of DMM for sensitive clay. Similarly, in some investigations on the effect of sea/saline water on durability and performance of concrete some reductions of strength due to salt crystallization and salt scaling are reported from studies on concrete performance that were prepared with saline water. Moreover, among the findings by Guo et al. (2018), using seawater for mixing and curing has increased the strength of concrete at the early stage of curing, but ultimately the strength has decreased. They reported that the later lower strength is due to the attack of magnesium sulphate (MgSO_4) by crystallization, and sulphate attack by potassium sulphates (K_2SO_4). Similar effects may have contributed to obtaining the lower P_y ' stresses from the TU samples in this study due to higher salt level.

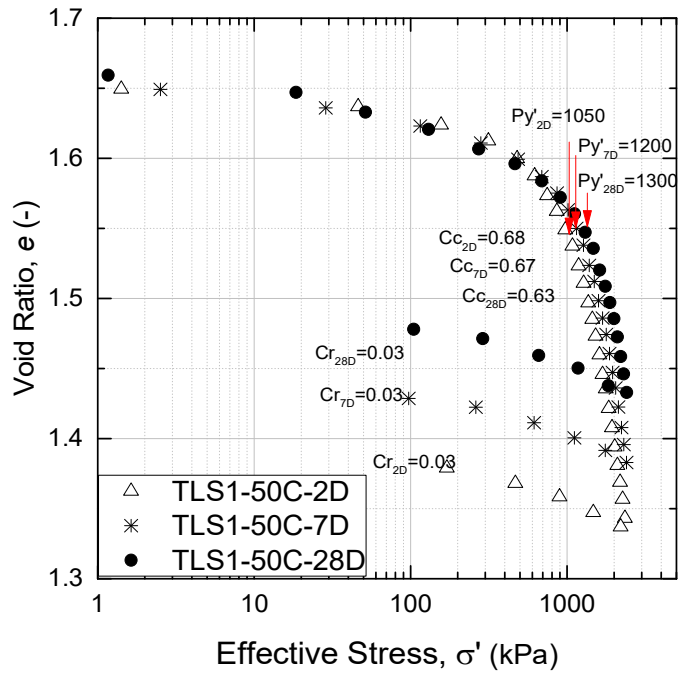


Figure 4-23: Variation of the e-log p curve of treated leached (TL) samples due to curing

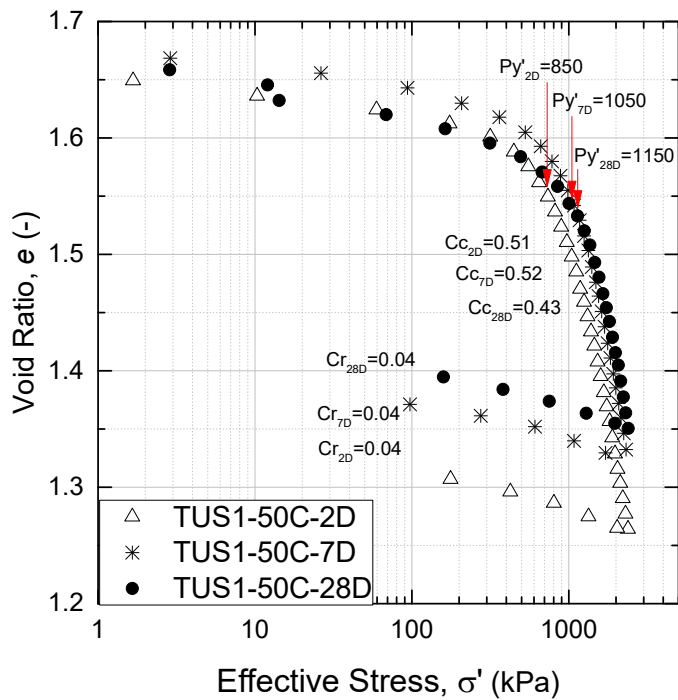


Figure 4-24: e-log p curve of TU samples due to curing period

The change in hydraulic conductivity against the void ratio of TL samples is plotted in Figure 4-25. Higher hydraulic conductivities that in remoulded samples were obtained from cement-treated samples. The increase in hydraulic conductivity in cement-treated samples is due to an increase in the size of the macropores and a change in the fabric of the clay because of the cement reaction. The pH and ionic strength of a clay sample increase as the result of the cement reaction that releases Ca_2^+ and OH. A higher Ca_2^+ concentration reduces the double layer thickness of the phyllosilicate minerals in the clay and promotes flocculation and aggregation of its particles. It should be noted that recording an accurate initial hydraulic conductivity from CRS test is a challenging task and most often factors, like a small residual stress in pressure sensors, seating error, unsaturated bottom pore stone, and unsaturated sensors will affect the results, so inconsistent and invalid pore pressure data may be recorded at the beginning of the tests. However, the results became consistent after the vertical stress accumulated higher than 5-10 kPa. Effect of curing on hydraulic conductivity can be detected at first glance at the hydraulic conductivity curves of TL samples shown in Figure 4-25. Samples with longer curing periods have lower hydraulic conductivities compared to their corresponding samples with shorter curing time. For example, at the void ratio around 1.58, the permeability was recorded to be about $1\text{E-}7$ m/s from 2 days cured sample, while the permeability was reduced to $1\text{E-}8$ m/s for the sample after 7 days and $1\text{E-}9$ m/s after 28 days curing. In other words, hydraulic conductivity spanned more than two orders of magnitude as the result of the curing period ranging from 2 to 28 days. The lower hydraulic conductivity may be due to the formation of C-S-H during the curing period that further bonded the clay particles, closed the gaps between them, and hindered the flow of water through voids.

The results of hydraulic conductivity vs. void ratio of the TU samples are plotted in Figure 4-26. As it was expected the hydraulic conductivities of TU samples were lower than those of corresponding TL samples at both curing times of 2-day and 7-day due to the higher viscosity of saline cell water during the test, but similar hydraulic conductivities were recorded from both TL and TU samples at 28-day curing time. Almost the same values of initial permeability, $k = 7\text{E-}6$ m/s and final permeability, $k = 1\text{E-}10$ m/s were recorded from all three TU samples. No change in k values of the samples means curing period did not affect on hydraulic conductivities of TU samples.

The pore pressure ratios against the total vertical stress of TL and TU samples are plotted in Figure 4-27, and Figure 4-28. Similar to the hydraulic conductivities of the samples, the pore pressure ratio of TU and TL samples were recorded with the different trend. The pore pressure ratio in TL samples was started to accumulate from zero value in all the tests and reached to their maximum amount of 0.1%, 0.5% and 3% in samples cured 2-day, 7-day, and 28-day, consecutively. It can be observed from the pore pressure ratio of TL samples that some changes had happened in the structure of clay during the tests when the total vertical stress was increased to about 750 kPa. At this stress point, the pore pressure ratio started kicking upward in all the samples and reached to its maximum value at the end of the test. However, the pore pressure in the TU samples shown in Figure 4-27 was recorded completely different. The pore pressure started from zero and rapidly increased to its peak in all the samples when the effective stress was below 250 kPa. These high values of the pore pressure at the initial stage of the tests can be due to a small residual pore pressure on transducer divided by the small total stress at the beginning of the test. Another hypothesis is that initially the pores and flow channels in the sample are disconnected so that the pore pressure built up at the bottom of the sample at the early stage of the test. Once the pore pressure increases to a higher value, results in connecting the flow channels from the bottom of the sample to the top of it, thus, the pore pressure releases from the bottom of the samples. After the recorded peak, the pore pressure gradually dropped until the effective stress was about 1000 kPa. After this point, the decrease in pore pressure ratio of the 2-day cured samples was almost flattened out, but the values were started to increase for the 7-day, and 28-day cured samples. In contrast to the divergence value of pore pressure from TL samples at the end of the test, the three graphs of TU samples converged together at about 5% pore pressure ratio. Overall, higher values of pore pressure were recorded from TU samples during the tests. This may be due to the saline water with a higher viscosity that was used as the cell water for TU samples.

Generally speaking, it can be concluded that the cement treatment affected the structure of leached and unleached Champlain Sea clay differently by comparing the yielding stress, hydraulic conductivities and pore pressure values of all TL and TU samples.

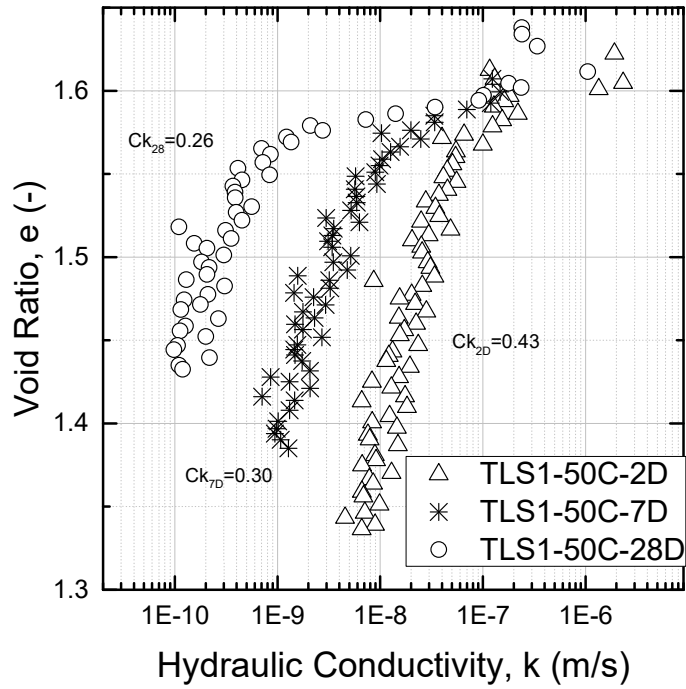


Figure 4-25: Change in e - $\log k$ curves of TL samples

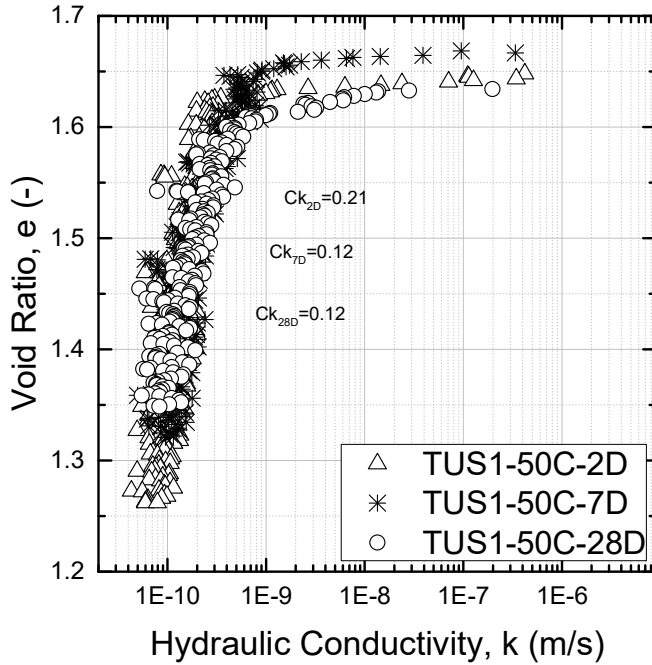


Figure 4-26: Change in e - $\log k$ curves of TU samples

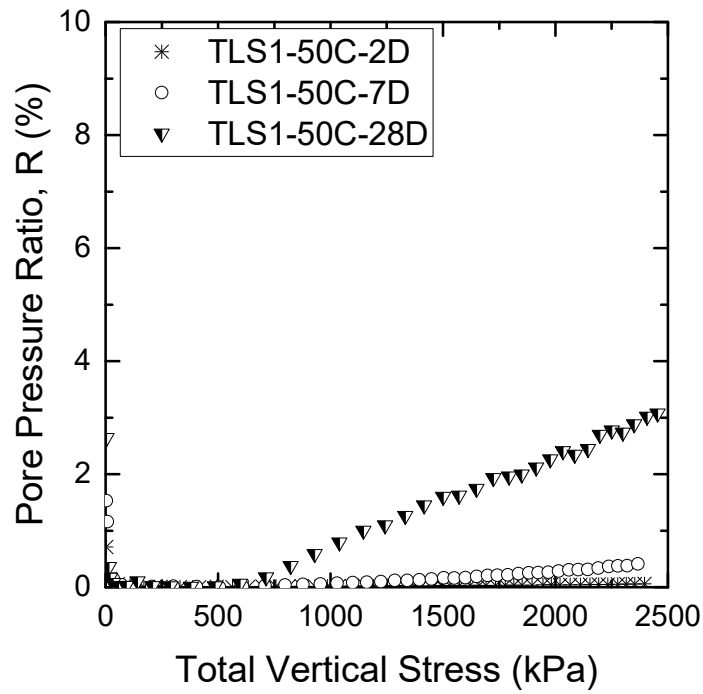


Figure 4-27: Change in pore pressure ratio vs total effective stress of TL samples

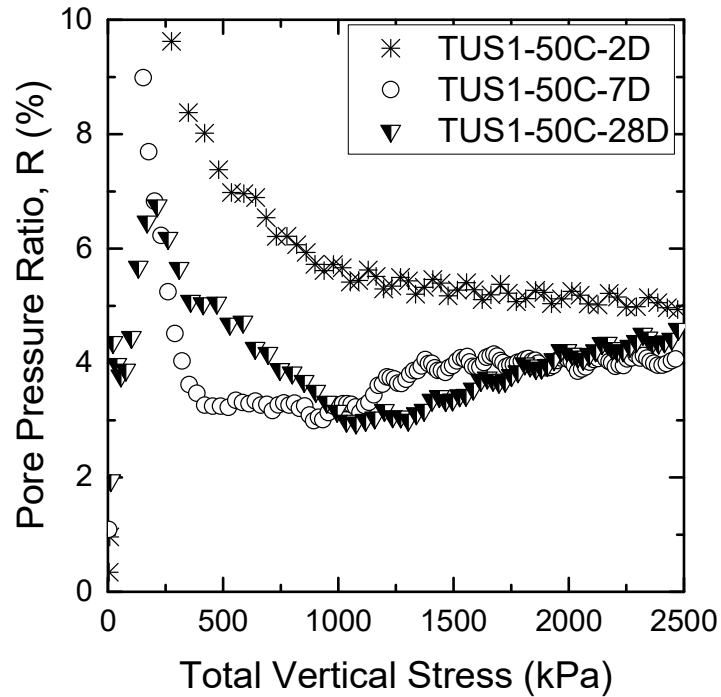


Figure 4-28: Change in pore pressure ratio against the total effective stress of TU samples

The coefficients of volume change (M_v) against the effective stress of all treated samples are shown in Figure 4-29 and Figure 4-30. The values of M_v from all treated samples were about $1\text{E-}03$ -/kPa at the initial stage of the test, then decreased to the minimum values at a stress level ranging 300-700 kPa. After that, started to increase with the increase of the applied vertical effective stress until 1000 kPa. At some point which is believed to be the yielding point of the samples, M_v started to decrease once more until the end of the test. The later decrease in M_v is not entirely apparent in Figure 4-29 and 4-30 because the test results overlap. Figure 4-31 is plotted to illustrate the trend of M_v values in treated samples better. Overall, a small shift of the M_v values to higher stresses can be seen from the results of samples with a longer curing period. The shift in the M_v values indicates that the samples with longer curing period became less compressible.

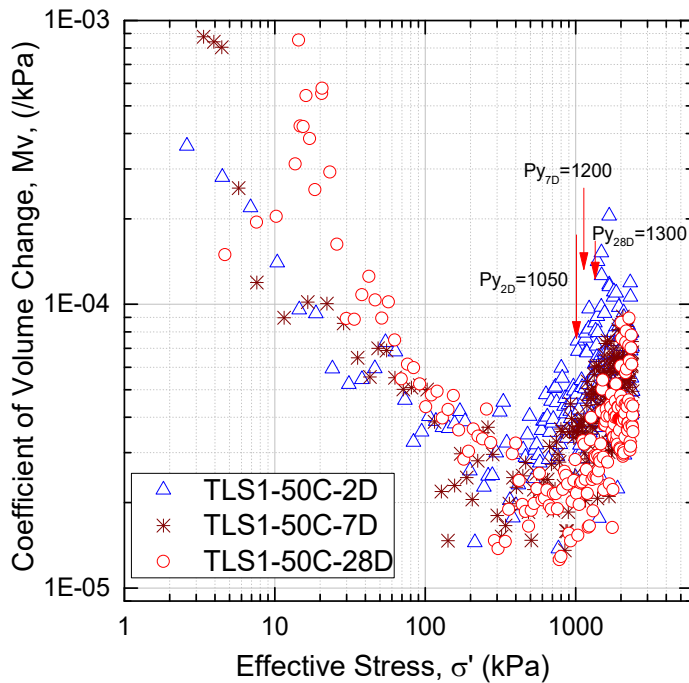


Figure 4-29: Variation of M_v vs effective stress of TL samples

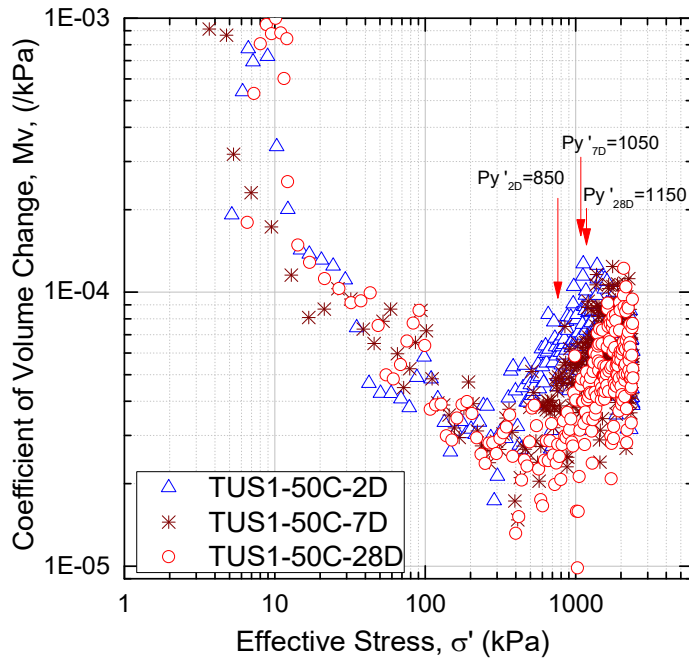


Figure 4-30: Variation of M_v vs effective stress of TU samples

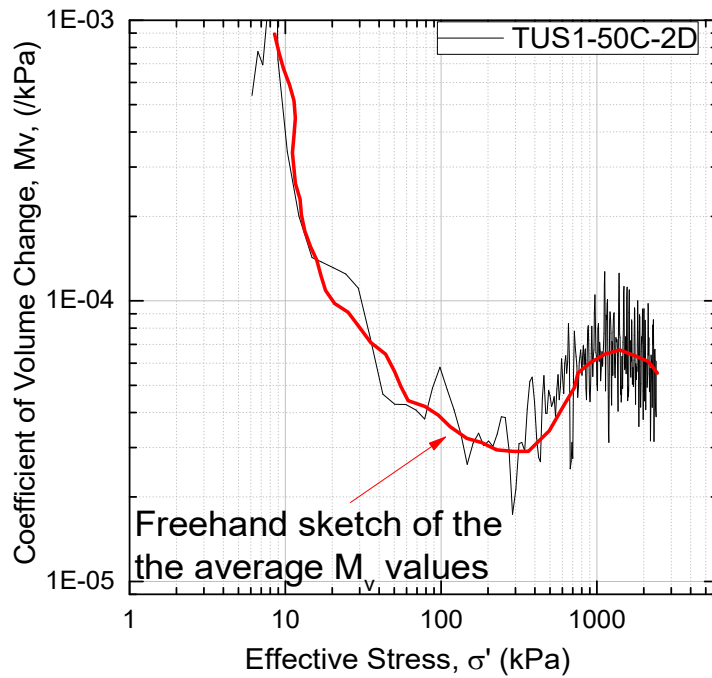


Figure 4-31: Trend of M_v change vs effective stress from 2 day-cured TU sample

The coefficients of consolidation versus the effective stress of all TL and TU samples are plotted in Figure 4-32 and Figure 4-33. The C_v values of TL samples had the same trend. In each TL sample, C_v started from an initial value of about $5E-05 \text{ m}^2/\text{s}$, kept increasing until its peak at a stress level ranging 300-700 kPa was recorded and then continually decreased until the end of the consolidation. Among the TL samples, the lowest C_v was recorded about $2E-7 \text{ m}^2/\text{s}$ from the sample with the longest curing period. The reason for this is the decrease in the permeability of TL samples due to prolonged curing time as discussed earlier. From the TU samples, the maximum C_v was recorded about $3E-5 \text{ m}^2/\text{s}$ at the beginning of the test following with a sharp drop at effective stress ranging 8 to 10 kPa. Then, the C_v value began to decrease gradually in all samples until the end of consolidation. However, in the 2-day and 7-day cured samples a rise in C_v values can be seen when the stress level was between 100 to 350 kPa and then started to drop throughout the remainder of the test. All the C_v curves of TU samples were converged at the end of the consolidation, and the smallest C_v value was recorded around $1E-7 \text{ m}^2/\text{s}$ from all the samples. Overall, in all the TU sample, the C_v values have decreased by increasing the curing time.

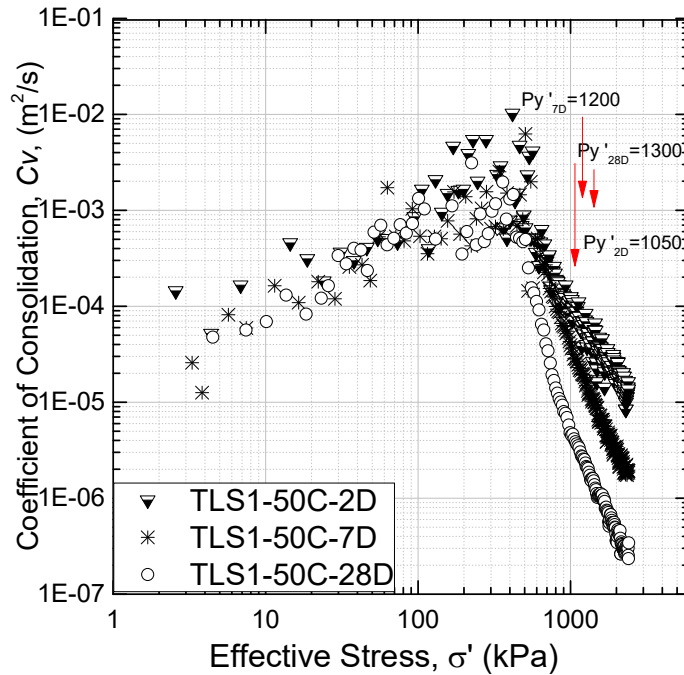


Figure 4-32: Variation of C_v -log p curves of TL samples

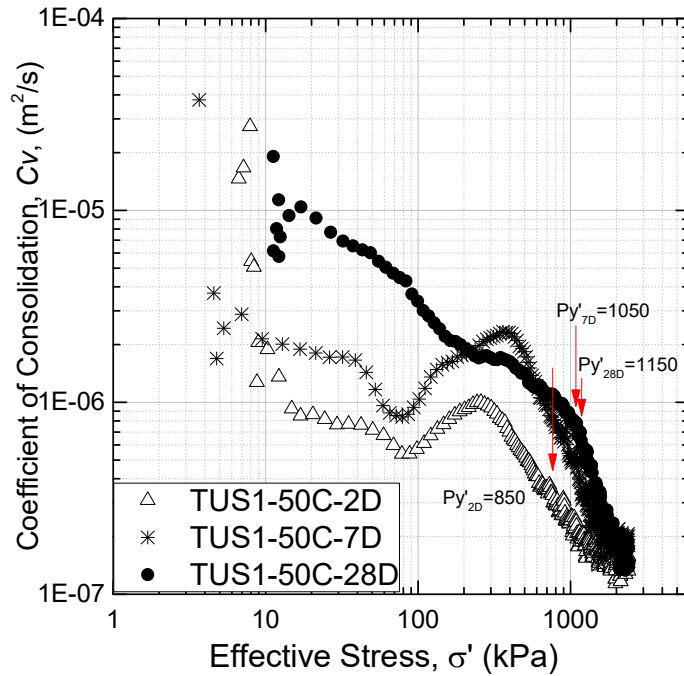


Figure 4-33: Change of C_v -log p curves of TU samples

4.5 SUMMARY

This section presented and compared the effect of pore water salinity level on compressibility behaviour of undisturbed, remoulded and cement-treated Champlain Sea clay samples. The result showed that cement treating of Champlain Sea clay can significantly improve the compressibility parameters of the clay. Furthermore, salinity level affected the cement improvement as the compressibility of cement treated leached (TL) Champlain sea clay shown a better compressibility result compared to its corresponding samples of treated unleached (TU) samples. All the parameters obtained from the CRS tests are summarized in Table 4-1.

Table 4-1: List of CRS tests conducted on various soil condition of Champlain Sea clay samples

Sample tag	Salinity level (g/L)	Cement dosage (kg/m ³)	Curing period (day)	P _c ' or P _y ' (kPa)	Comp. index (C _{c-II}) (-)	Comp. index (C _{c-III}) (-)	Rebound index (C _r) (-)	Ck (-)/m/s	Initial Condition		At P _c ' or P _y ' Stress				At Max Stress			
									e (-)	K (m/s)	e (-)	K (m/s)	Cv (m ² /s)	Mv (/kPa)	e (-)	K (m/s)	Cv (m ² /s)	Mv (/kPa)
ULS1CRS1	0.79	0	0	310	3.10	0.69	0.08	0.85	1.91	1E-6	1.79	9E-10	2E-9	2E-4	0.81	7E-11	2E-7	3E-5
ULS1CRS2	0.79	0	0	320	3.61	0.73	0.10	0.67	1.94	2E-7	1.8	1E-9	1E-9	2E-4	0.80	7E-11	2E-7	3E-5
UUS1CRS1	19.81	0	0	300	2.32	0.73	0.10	0.85	2.01	2E-7	1.8	1E-9	7E-8	2E-4	0.81	7E-11	3E-7	3E-5
UUS1CRS2	19.81	0	0	310	2.64	0.74	0.10	0.74	1.99	2E-7	1.8	2E-9	1E-7	3E-4	0.83	2E-10	4E-7	3E-5
RLS1-28D	0.79	0	28	50	0.53	N/A	0.06	0.51	1.72	1E-7	1.58	3E-8	1E-6	2E-3	0.71	7E-10	2E-6	2E-5
RUS1-28D	19.81	0	28	50	0.50	N/A	0.07	0.79	1.73	2E-8	1.59	7E-10	4E-8	2E-3	0.78	6E-10	3E-7	2E-5
TUS1-50C-2D	19.81	50	2	850	0.51	N/A	0.04	0.21	1.65	2E-6	1.57	7E-8	2E-4	5E-5	1.34	6E-9	1E-5	1E-4
TUS1-50C-7D	19.81	50	7	1050	0.52	N/A	0.04	0.12	1.67	4E-7	1.56	1E-8	3E-5	3E-5	1.38	8E-10	2E-6	2E-5
TUS1-50C-28D	19.81	50	28	1100	0.43	N/A	0.04	0.12	1.66	2E-6	1.55	6E-10	3E-6	2E-5	1.44	1E-10	2E-7	4E-5
TLS1-50C-2D	0.79	50	2	1050	0.68	N/A	0.03	0.43	1.65	4E-7	1.48	2E-10	2E-7	7E-5	1.26	6E-11	1E-7	3E-5
TLS1-50C-7D	0.79	50	7	1200	0.67	N/A	0.03	0.30	1.65	2E-7	1.55	2E-10	3E-7	5E-5	1.32	8E-11	2E-7	4E-5
TLS1-50C-28D	0.79	50	28	1300	0.63	N/A	0.03	0.26	1.66	2E-7	1.52	2E-10	4E-7	4E-5	1.35	5E-11	2E-7	2E-5

5. SUMMARY AND CONCLUSION

5.1 INTRODUCTION

The compressibility behaviour of untreated and cement treated Champlain Sea clay due to changes in its pore fluid chemistry was investigated in this experimental study. A leaching apparatus was designed and built for this study. The salinity level of undisturbed Champlain Sea clay was lowered from its initial of 12.68 g/kg to about 0.5 g/kg of salt mass to dry soil mass. A series of constant rate of strain (CRS) consolidation tests were performed on leached Champlain Sea clay samples under undisturbed, remoulded, and cement treated conditions, and the results were compared with their corresponding unleached samples.

5.2 MAIN CONCLUSIONS

Within the study range of salinity levels, the following conclusions can be drawn based on the test results:

1. Leaching did not affect the void ratio of the undisturbed samples of Champlain Sea clay. Similar void ratios ranging from 1.97 to 2.01 were recorded from all the undisturbed samples.
2. No significant change in preconsolidation pressure of the UL and UU samples can be found. However, bigger compression indexes (C_{c-II}) were obtained from UL samples. The bigger C_{c-II} values in UL samples suggest that the strength of the clay structure was reduced due to leaching as the type of failure became more abrupt in the zone II of the consolidation curve.
3. From the RU and RL tests, P_y' values were recorded the same, but lesser compressibility was recorded from RU sample. It appears that at stress about 300 kPa some restructuration was happening in the RU specimen as its compressibility curve has changed its trend with a lower reduction in the void ratio. The higher compressibility in RL samples is believed to be due to the effect of leaching on the remoulded Champlain Sea clay.

4. The coefficient of permeability was recorded lower in RU samples compared to its corresponding RL condition. In the remoulded Champlain Sea clay, the salt level may define the way particles floc together. Lower salinity level may cause more flow channels and interconnected voids which leads to the higher recorded permeability values.
5. The compressibility of Champlain Sea clay is significantly reduced due to the cementation induced in clay samples by cement treating. The change of the void ratio of the treated clay with 50 kg/m^3 is recorded about 400% smaller than that of the untreated sample under the same pressure range.
6. Cement treating of leached samples resulted in a better compressibility improvement. Thus, lower pore water salinity level results in better cement improvement of Champlain Sea clay.
7. The most notable effect of the cement treatment is the increase in the yielding pressure. The yielding pressure was improved almost four times from around 300 kPa in the untreated sample to about 1075 kPa in the treated sample after 28 days of curing.
8. The change of C_v with the effective stress resembled a V-shape curve for untreated samples with its lowest value at stress close to the preconsolidation pressure of the sample. However, in the cement-treated samples, the curves of C_v vs effective stress did not have the same pattern, and the lowest C_v is recorded at the end of the consolidation from all treated samples.
9. The permeability of cement treated samples increased compared to its remoulded condition. The increase in permeability is believed to be due to an increase in the size of the macropores and a change of the fabric of the clay because of the cement reaction.
10. Prolonged curing affected the permeability of TL samples. However, no effect of curing could be seen on the permeability of TU samples.

5.3 RECOMMENDATION FOR FUTURE WORK

Throughout this research samples of Champlain Sea clay with two different salinity levels of 19.81 g/L and 0.79 g/L were investigated. More tests with a wider range of salinity levels are needed to be performed to obtain a better picture of the leaching effect on the compressibility characteristics of Champlain Sea clay.

Due to the load cell capacity restriction of the CRS machine used in this study, test results wouldn't be obtainable if the clay was treated with higher cement dosages than 50 kg/m³. Higher range of cement content is needed to be investigated with stronger CRS machine.

It is believed that the different salinity level will alter the structure and binding of Champlain Sea clay particles. The result of SEM analysis of the samples will be fascinating and will provide a better picture and a closer view of the changes.

Remoulded samples were cured for 28 days in the CRS rings to allow the clay particles to bind together under the effect of charges between particles. However, after curing, some reduction of the clay volume in the CRS cell was observed as the particles were moved closer and formed a sample with higher density than that of fresh remoulded clay. To prevent the effect of volume loss in the testing specimen. It will be better to provide the testing specimen from a bigger chunk remoulded clay after completion of curing period.

This study just focussed on the effect of leaching on compressibility characteristics of Champlain Sea clay. Conducting shear strength associated tests are needed to be performed in future studies.

APPENDICES

Appendix A:

Sample of CRS test record sheet and void ratio calculation

File Name:	Undisturbed Unleached sample	Date mixed:	N/A	
Sample Des.	UUS1CRS2	Start of test:	April 3rd, 18	
Tested by:	A.A			
Mass of ring + glass + grease + Soil + etc (g)		Ring Data		
Before curing		Ring No.	#1	
After curing		Dia (mm)	63.5	
Water loss	0	Height (mm)	25.4	
		Mass (g)	215.55	
Mass of sample in + ring (g)		Mass of Sample (g)	Porous stone	
Before test	344.55	129	Height (mm)	6.33
After test	319.46	103.91	Mass (g)	93.81
Height of soil (mm)	1	2	3	Ave
Just Sample (before test)	25.4	25.38	25.34	25.37
Sample (After test)	17.4	17.36	17.39	17.38
Sample (After test)+2 porous stone				
Change in height (mm)	7.99			
Loading Information		Rate (%)	Pressure (psf)	
1	L	0.8	50000	
2	U	0.2	2000	
Saturation Information				
Back Pressure (psi)	50	Start of Saturation	2:12 Apr 3rd	
Ramp time (min)	60	End of Saturation	2:12 Apr 4th	
Seating Stress (Psf)	128			
Water Content				
Before Test		Trial 1	Trial 2	Trial 3
Dish No.		BG3-S2	BG1-S4	BG4-S4
Mass of dish (g)		14.02	13.9	14.24
Mass of wet soil + dish (g)		24.4	32.88	24.49
Mass of dry soil + dish (g)		20.32	25.24	20.38
Mass of water, Mw (g)		4.08	7.64	4.11
Mass of dry soil, Ms (g)		6.3	11.34	6.14
Water content, W (%)		64.76	67.37	66.94
Average water content		66.36		
After Test		Trial 1	Trial 2	Trial 3
Dish No.		#4		
Mass of dish (g)		528.09		
Mass of wet soil + dish (g)		631.72		
Mass of dry soil + dish (g)		603.66		
Mass of water, Mw (g)		28.06		
Mass of dry soil, Ms (g)		75.57		
Water content, W (%)		37.13		
Average water content		37.13		
Comment:				

Calculation of void ratio Sample: UUS1CRS2		
Area of ring	cm ²	31.66921744
Mass of solid	g	75.77
Mass of water	g	28.14
Volume of water	cm ³	28.18655168
Total volume	cm ³	55.05165632
Volume of solid	cm ³	26.86510465
H _{solid}	cm	0.848303394
H _{water}	cm	1.689029939
e		1.99

Appendix B:

Sample of mix design sheet from cement treated samples

Mix Design for Treated Unleached (TU) samples		
Mix Design per FHWA-HRT-13-046		
Symbol	Long name	
Input		
Nm	Number of mold to be used	6
Hm (m)	Height of mold (meter)	0.0254
Dm (m)	Dia of mold (meter)	0.0635
w:b	Water to binder ratio	0.7
γ soil	Total unit weight of soil (kg/m ³)	1615
ω	Water content (/100)	0.5865
G _s	Specific gravity of soil	2.65
G _b	Specific gravity of binder	3.15
α in-place	Binder dosage; Factor per total volume of mix (kg/m ³)	50
Calculations		
α	Binder dosage; Factor per volume of wet soil (kg/m ³)	52
α_w (%)	Binder content in percentage of soil solid	5
V _{mix} (m ³)	(# of molds)(volume of mold)	0.00048
γ_d soil	Dry unit weight of soil (kg/m ³)	1018
S	Soil saturation	0.969
VR	Volume ratio expressed in terms of binder factor in-place for any S	0.053
V _s	Volume of the dry soil (m ³)	0.0002
V _{soil}	Volume of wet soil (m ³)	0.0005
W _s	Weight of soil (wet) (kg)	0.74
W _{soil}	Weight of soil (dry) (kg)	0.47
W _b	Weight of the binder (kg)	0.024
W _{w,slurry}	Weight of water in the slurry for wet mixing (kg) (water added) (kg)	0.017
V _b	Volume of the binder (m ³)	0.000008
γ_d , slurry	Dry unit weight of the slurry (W _b /V _{slurry})	983
V _{w,slurry}	Volume of water in the slurry for wet mixing (m ³)	0.00002
V _{w,mix}	Volume of water in the mixture	0.000290
V _{w,s}	Volume of water in the soil (m ³)	0.000274
W _{w,mix}	Weight of water in the mixture (m ³)	0.29
V _{slurry}	Volume of slurry before mixing (V _b + V _{w,slurry}) (m ³)	0.000024
V _{mix}	Volume of the mixture (V _s + V _b + V _{w,mix}) (m ³)	0.00048
W _{mix}	Weight of the mixture (W _s + W _b + W _{w,mix}) (m ³)	0.7808
Results		
w:b	Water to binder ratio	0.7
wT:b	Total water-to-binder ratio of mix (wT:b)	12.25
VR	Volume ratio expressed in terms of binder factor in-place for any S	0.05
α in-place	Binder dosage; Factor per total volume of mix (kg/m ³)	50
α	Binder dosage; Factor per volume of wet soil (kg/m ³)	52
α_w (%)	Binder content in percentage of soil solid	5
W _{soil}	Weight of the soil to be used (wet) (kg)	0.741
W _b	Weight of the binder (kg)	0.024
W _{w,slurry}	Weight of water in the slurry for wet mixing (kg)	0.017
Total ω (%)	Mix total water content (%)	59.20

	A	B	C
1	Mix Design for Treated Unleached (TU) samples		
2	Mix Design per FHWA-HRT-13-046		
3	Symbol	Long name	
4	Input		
5	Nm	Number of mold to be used	6
6	Hm (m)	Height of mold (meter)	0.0254
7	Dm (m)	Dia of mold (meter)	= 0.0635
8	w:b	Water to binder ratio	0.7
9	γ_{soil}	Total unit weight of soil (kg/m ³)	1615
10	ω	Water content (/100)	0.5865
11	Gs	Specific gravity of soil	2.65
12	Gb	Specific gravity of binder	3.15
13	a _{in-place}	Binder dosage; Factor per total volume of mix (kg/m ³)	50
14	Calculations		
15	a	Binder dosage; Factor per volume of wet soil (kg/m ³)	= C20 * C28
16	a _w (%)	Binder content in percentage of soil solid	= C28 / C18 * C20 * 100
17	V _{mix} (m ³)	(# of molds)(volume of mold)	= PI0 * (C7/2) * 2 * C6 * C5
18	γ_d soil	Dry unit weight of soil (kg/m ³)	= C9 / (1 + C10)
19	S	Soil saturation	= C10 * C11 * C18 / (C11 * 1000 - C18)
20	VR	Volume ratio expressed in terms of binder factor in-place for any	= C19 * (1 + C10 * C11) / (C19 + C10 * C11) * C13 / (C28 - C13)
21	V _s	Volume of the dry soil (m ³)	= (C23 / C9) - ((C23 - (C23 / (1 + C10))) / 1000)
22	V _{soil}	Volume of wet soil (m ³)	= C23 / C9
23	W _s	Weight of soil (wet) (kg)	= (1 * C17 * C9) / (1 + C20)
24	W _{soil}	Weight of soil (dry) (kg)	= C23 / (1 + C10)
25	W _b	Weight of the binder (kg)	= (C20 * C17 * C28) / (1 + C20)
26	W _{w,slurry}	Weight of water in the slurry for wet mixing (kg) (water added) (kg)	= C8 * C25
27	V _b	Volume of the binder (m ³)	= C25 / (C12 * 1000)
28	γ_d , slurry	Dry unit weight of the slurry (W _b /V _{slurry})	= C12 * 1000 / (1 + C8 * C12)
29	V _{w,slurry}	Volume of water in the slurry for wet mixing (m ³)	= C26 / 1000
30	V _{w,mix}	Volume of water in the mixture	= (C22 - C21) + C29
31	V _{w,s}	Volume of water in the soil (m ³)	= C22 - C21
32	W _{w,mix}	Weight of water in the mixture (m ³)	= (C23 - C24) + C26
33	V _{slurry}	Volume of slurry before mixing (V _b + V _{w,slurry}) (m ³)	= C27 + C29
34	V _{mix}	Volume of the mixture (V _s + V _b + V _{w,mix}) (m ³)	= C21 + C27 + C30
35	W _{mix}	Weight of the mixture (W _s + W _b + W _{w,mix}) (m ³)	= C23 + C25 + C26
36	Results		
37	w:b	Water to binder ratio	= C26 / C25
38	wT:b	Total water-to-binder ratio of mix (wT:b)	= (C10 * C18 / (C20 * C28)) + C37
39	VR	Volume ratio expressed in terms of binder factor in-place for a	= C9 * C25 / (C28 * C23)
40	a _{in-place}	Binder dosage; Factor per total volume of mix (kg/m ³)	= (C19 + C10 * C11) * C39 * C28 / (C19 * (1 + C10 * C11) + (C19 + C10 * C11) * C39)
41	a	Binder dosage; Factor per volume of wet soil (kg/m ³)	= C39 * C28
42	a _w (%)	Binder content in percentage of soil solid	= C28 * C39 / C18 * 100
43	W _{soil}	Weight of the soil to be used (wet) (kg)	= C23
44	W _b	Weight of the binder (kg)	= C25
45	W _{w,slurry}	Weight of water in the slurry for wet mixing (kg)	= C37 * C44
46	Total ω (%)	Mix total water content (%)	= ((C23 - C24) + C45) / (C24 + C44) * 100

REFERENCES

- Ahmadi, H., Hoorfar, A. H., Rahimi, H., & Soroush, A. (2009). Hydraulic characteristics and pore water flow rule in constant rate of strain consolidation. *American Journal of Applied Sciences*, 6(7), 1429–1435.
- Ahmadi, H., Rahimi, H., & Soroush, A. (2011). Investigation on the characteristics of pore water flow during CRS consolidation test. *Geotech Geol Eng.* <http://doi.org/10.1007/s10706-011-9431-z>
- Al-Rawas, A. A. (2002). Microfabric and mineralogical studies on the stabilization of an expansive soil using cement by-pass dust and some types of slags. *Canadian Geotechnical Journal*, 39(5), 1150–1167. <http://doi.org/10.1139/t02-046>
- ASTM. (2012). D4186/D4186M-12. Standard test method for one-dimensional consolidation properties of saturated cohesive soils using controlled-strain loading. *American Journal of Engineering and Applied Sciences.*, 2458000(D4186/D4186M), 1–18. <http://doi.org/10.1520/D4186>
- ASTM. (2016). Standard test methods for laboratory miniature vane shear test for saturated fine-grained clayey soil. *American Society for Testing and Materials*, (D4648M). http://doi.org/10.1520/D4648_D4648M-16
- ASTM. (2017). Standard Test Methods for Liquid Limit, Plastic Limit, and Plasticity Index of Soils. *American Society for Testing and Materials*, (D4318). <http://doi.org/DOI: 10.1520/D4318-17>
- Bentley, S., & Smalley, I. (1979). Mineralogy of a Leda/Champlain clay from Gloucester (Ottawa, Ontario). *Engineering Geology*, 14(14: 209-217), 209–217.
- Bjerrum, L. (1954). Geotechnical properties of Norwegian Marine clays. *Geotechnique*, 4(2), 49–69. <http://doi.org/10.1680/geot.1954.4.2.49>
- Bjerrum, L. (1967). Engineering geology of Norwegian normally-consolidated marine clays as related to settlements of buildings. *Géotechnique*, 17(2), 83–118. <http://doi.org/10.1680/geot.1967.17.2.83>
- Bouassida, M., & Porbaha, A. (2004). Ultimate bearing capacity of soft clays reinforced by a group of columns. *Soil and Foundations Japanese Geotechnical Society*, 44(3), 91–101.
- Brand, E., & Brenner, R. (1981). *Soft clay engineering*. Elsevier Scientific Pub. Co.
- Brom, B. (1999). Design of lime, lime/cement and cement columns. *Dry Mix Method for Deep Soil Stabilization*, 125–153.
- Bruce, D. A., Dimillio, A., & Ellen, M. (1998). Deep mixing method: A global perspective. *Deep Foundations Institute*, 177–202.
- Bruce, Mary, E., Berg, R. B., Collin, J. G., Filz, G. M., Terashi, M., & Yang, D. S. (2013). *Federal Highway Administration Design Manual: Deep Mixing for Embankment and Foundation Support (FHWA-HRT-1)*. U.S. Department of Transportation.

- Casey, B. (2014). *The consolidation and strength behavior of mechanically compressed fine-grained sediments*. Massachusetts Institute of Technology.
- CGS. (2006). *Canadian Foundation Engineering Manual*. Vancouver, BC: Canadian Geotechnical Society.
- Chew, S., Kamruzzaman, A., & Lee, F. (2004). Physicochemical and engineering behavior of cement treated clays. *Journal of Geotechnical and Geoenvironmental Engineering*, 130(7), 696–706. [http://doi.org/10.1061/\(ASCE\)1090-0241\(2004\)130:7\(696\)](http://doi.org/10.1061/(ASCE)1090-0241(2004)130:7(696))
- Choquette, M., Berube, M. A., & Locat, J. (1987). Mineralogical and microtextural changes associated with lime stabilization of marine clays from eastern Canada. *Applied Clay Science*, 2, 215–232. [http://doi.org/10.1016/0169-1317\(87\)90001-1](http://doi.org/10.1016/0169-1317(87)90001-1)
- Clementino, R. V. (2005). Discussion of an oedometer test study on the preconsolidation stress of glaciomarine clays. *Canadian Geotechnical Journal*, 40, 857–872. <http://doi.org/10.1139/T05-010>
- Cortellazzo, G., & Cola, S. (1999). Geotechnical characteristics of two Italian peats stabilized with binders. *Dry Mix Methods for Deep Soil Stabilization*, 93–100.
- Crawford, C. (1968). Quick clays of eastern Canada. *Eng. Geol.*, 2(4), 239–265.
- Desaulniers and, D., & Cherry, J. (1989). Origin and movement of groundwater and major ions in a thick deposit of Champlain Sea clay near Montreal. *Can. Geotech. J.*, 26, 80–89.
- Duchesne, A., & Dolbec, M. (2016). *Waba Dam Arnprior, Ontario Geotechnical Investigation*. Quebec.
- Eden, W., & Crawford, C. (1957). Geotechnical properties of Leda clay in the Ottawa area. *National Research Council Canada-NRC No. 4383221*, 22–27.
- Filz, G. M., Hodges, D. K., Weatherby, D. E., & Marr, W. A. (2005). Standardized definitions and laboratory procedures for soil-cement specimens applicable to the wet method of deep mixing. *Innovations in Grouting and Soil Improvement Innovations*, 1–15.
- Gao, Y.-B., & Ge, X.-N. (2016). On the sensitivity of soft clay obtained by the field vane test. *Geotechnical Testing Journal*, 39(2), 1–9. <http://doi.org/10.1520/GTJ20150046>
- Gillott, J. (1969). Fabric of Leda clay investigated by optical, electron- optical, and x-ray diffraction methods. *Engineering Geology*, 4, 133–153.
- Gillott, J. (1970). Mineralogy of Leda clay. *The Canadian Mineralogist*, 797–811.
- Gillott, J. (1979). Fabric, composition and properties of sensitive soils from Canada, Alaska and Norway. *Engineering Geology*, 14, 149–172.
- Guo, Q., Chen, L., Zhao, H., Admilson, J., & Zhang, W. (2018). The effect of mixing and curing sea water on concrete strength at different ages. *MATEC Web of Conferences*, 142, 1–6. <http://doi.org/10.1051/mateconf/201814202004>
- Hendershot, W., & Carson, M. (1978). Changes in the plasticity of a sample of Champlain clay after selective chemical dissolution to remove amorphous material. *Can. Geotech. J.*, 15, 609–

- Jia, R. (2010). *Consolidation behavior of Ariake clay under constant rate of strain (PhD dissertation)*. Saga University, Japan.
- Kassim, K. (1999). Constant rate of strain consolidation equipment and procedure for stabilized soils. *Geotechnical Testing Journal*, 22(1), 13–21.
- Kim, Y.-T., & Do, T.-H. (2010). Effect of leaching on the compressibility of Busan clay. *KSCE Journal of Civil Engineering*, 14(4), 291–297. <http://doi.org/10.1007/s12205-010-0291-5>
- Kitazume, M., & Terashi, M. (2013). *The deep mixing method*. Taylor & Francis Group. CRC Press. <http://doi.org/doi:10.1201/b13873-7>
- Leroueil, S., Tavenas, F., Samson, L., & Morin, P. (1983). Preconsolidation pressure of Champlain clays. Part 11. Laboratory determination. *Can. Geotech. J.*, 20, 803–816.
- Li, S. (2017). *Experimental investigation of using deep mixing method to stabilize problematic soils in Ontario (Masters thesis)*. Ryerson University.
- Liu, J., Shi, C., Afroz, M., & Kirstein, A. (2017). *Numerical Investigation of Long-Term Settlement of Waba Dam*.
- Locat, J., Berube, M., & Choquette, M. (1990). Laboratory investigations on the lime stabilization of sensitive clays: shear strength development. *Can. Geotech. J.*, 27, 294–304.
- Locat, J., Lefebvre, G., Ballivy, R., & Ballivy, G. (1984). Mineralogy, chemistry, and physical properties interrelationships of some sensitive clays from Eastern Canada. *Can. Geotech. J.*, 21(3), 530–540. <http://doi.org/10.1139/t84-055>
- Loiselle, A., Massiera, M., & Sainani, U. (1970). A study of the cementation bonds of the sensitive clays of the Outardes river region. *Canadian Geotechnical Journal*, 8, 479–498.
- Lorenzo, G. A., & Bergado, D. T. (2004). Fundamental parameters of cement-admixed clay—new approach. *J. Geotech. Geoenviron. Eng.*, 130(10), 1042–1050. [http://doi.org/10.1061/\(ASCE\)1090-0241\(2004\)130:10\(1042\)](http://doi.org/10.1061/(ASCE)1090-0241(2004)130:10(1042))
- Lorenzo, G. A., & Bergado, D. T. (2006). Fundamental characteristics of cement-admixed clay in deep mixing. *Journal of Materials in Civil Engineering*. <http://doi.org/10.1061/ASCE0899-1561200618:2161>
- Mitchell, R. (1970). On the yielding and mechanical strength of Leda clays. *Can. Geotech. J.*, 7, 297–312.
- Miura, N., Horpibulsuk, S., & Nagaraj, T. S. (2002). Engineering behavior of cement stabilized clay at high water content. *Soils and Foundations*, 41(5), 33–45. <http://doi.org/10.1248/cpb.37.3229>
- Moore, J., Brown, J., & Rashid, M. (1977). The effect of leaching on engineering behaviour of a marine sediment. *Geotechnique*, 27(4), 517–531. <http://doi.org/10.1680/geot.1977.27.4.517>
- Moum, J., & Rosenqvist, I. (1961). The mechanical properties of montmorillonitic and illitic clays related to the electrolytes of the pore water. *Proceedings of the 5th International Conference*,

5, 263–268.

- Nabil, I. (1993). Laboratory and field leaching tests on coastal salt-bearing soils. *Journal of Geotechnical Engineering*, 119(3), 453–470.
- Nagaraj, T., Murthy, B., Vatsala, A., & Joshi, R. (1990). Analysis of compressibility of sensitive soils. *Journal of Geotechnical Engineering*, 116(1), 105–118.
- Penner, E. (1965). A study of sensitivity in Leda clay. *Canadian Journal of Earth Sciences*, 2(8592), 425–441. <http://doi.org/10.1139/e65-037>
- Penner, E., & Burn, K. (1978). Review of engineering behaviour of marine clays in Eastern Canada. *Canadian Geotechnical Journal*, 15, 269–282.
- Puppala, A. ., Nazarian, S., Yuan, D., & Hoyos, L. (2007). *Deep Soil Mixing Technology for Mitigation of Pavement Roughness*. Austin, Texas.
- Quigley, R. (1980). Geology, mineralogy, and geochemistry of Canadian soft soils: a geotechnical perspective. *Can. Geotech. J.*, 17, 261–285.
- Quigley, R., Gwyn, Q., White, O., Rowe, R., Haynes, J., & Bohdanowicz, A. (1983). Leda clay from deep boreholes at Hawkesbury, Ontario. Part I: Geology and geotechnique. *Can. Geotech. J.*, 20(2), 288–298. <http://doi.org/10.1139/t83-032>
- Quigley, R., & Thompson, C. (1966). The Fabric of anisotropically consolidated sensitive marine clay. *Can. Geotech. J.*, 3(2), 61–73.
- Rankka, K., Andersson-Skold, Y., Hulten, C., Larsson, R., Leroux Torleif, V., & In, D. (2004). *Quick clay in Sweden*.
- Rao, S., & Rajasekaran, G. (1996). Reaction products formed in lime-stabilized marine clays. *Journal of Geotechnical Engineering*, 122(5), 329–336. [http://doi.org/10.1061/\(ASCE\)0733-9410\(1996\)122:5\(329\)](http://doi.org/10.1061/(ASCE)0733-9410(1996)122:5(329))
- Rasmussen, K. (2012). *An investigation of monotonic and cyclic behaviour of Leda clay (Masters thesis)*. University of Western Ontario.
- Rosenqvist, I. (1946). Om leirers kvikkaghtighet. Statens Vegvesen. Veglaboratoriet. Meddelande Nr 4. Oslo. *Google Scholar*.
- Rosenqvist, I. (1966). Norwegian research into the properties of quick clay-- A review. *Engineering Geology*, 6(1), 445–450.
- Shen, S.-L., Han, J., & Du, Y.-J. (2008). Deep mixing induced property changes in surrounding sensitive marine clays. *Journal of Geotechnical and Geoenvironmental Engineering*, 136(6), 845–854. <http://doi.org/10.1061/ASCE1090-02412008134:6845>
- Skempton, A., & Northey, R. (1952). The Sensitivity of Clays. *Géotechnique*, 3(1), 30–53. <http://doi.org/10.1680/geot.1952.3.1.30>
- Soderblom, R. (1966). Chemical aspects of quick-clay formation. *Eng. Geol.*, 1(6), 415–431.
- Song, M.-M., Zeng, L.-L., & Hong, Z. (2017). Pore fluid salinity effects on physicochemical-compressive behaviour of reconstituted marine clays. *Applied Clay Science*.

<http://doi.org/10.1016/j.clay.2017.06.015>

- Sridharan, A., & Prakash, K. (1999). Mechanisms controlling the undrained shear strength behaviour of clays. *Can. Geotech. J.*, 36, 1030–1038.
- Taha, A. M. (2010). *Interface shear behavior of sensitive marine clays -Leda clay (Masters thesis)*. University of Ottawa.
- Terashi, M. (1997). Deep mixing method- Brief state of the art. *Proc. of the 14th International Conference on Soil Mechanics and Foundation Engineering*, 2475–2478.
- Torrance, J. (1974). A laboratory investigation of the effect of leaching on the compressibility and shear strength of Norwegian marine clays. *Géotechnique*, 24(2), 155–173. <http://doi.org/10.1680/geot.1974.24.2.155>
- Torrance, J. (1975). On the role of chemistry in the development and behavior of the sensitive Marine clays of Canada and Scandinavia. *Can. Geotech. J.*, 12, 326–335.
- Torrance, J. (1979). Post-depositional changes in the pore-water chemistry of the sensitive marine clays of the Ottawa area, eastern Canada. *Engineering Geology*, 14(2–3), 135–147. [http://doi.org/10.1016/0013-7952\(79\)90081-4](http://doi.org/10.1016/0013-7952(79)90081-4)
- Torrance, J. (1984). A comparison of marine clays from Ariake Bay, Japan and the South Nation river landslide site, Canada. *Soil and Foundations Japanese Geotechnical Society*, 24(2), 75–81.
- Trautwein. (2001). *Sigma-1 CRS- Instruction Manual* (ver 1.01.0). Houston, TX: Trautwein Soil Testing Equipment Company.
- Tremblay, H., Leroueil, S., & Locat, J. (2001). Mechanical improvement and vertical yield stress prediction of clayey soils from eastern Canada treated with lime or cement. *Canadian Geotechnical Journal*, 38(3), 567–579. <http://doi.org/10.1139/t00-119>
- Yong, R., Elmonayeri, D., & Chong, T. (1985). The effect of leaching on the integrity of a natural clay. *Engineering Geology*, 21, 279–299.
- Yong, R., Sethi, A., & Larochelle, P. (1979). Significance of amorphous material relative to sensitivity in some Champlain clays. *Can. Geotech. J.*, 16, 511–520.